UNIVERSITY OF CALIFORNIA,
IRVINE

Expanding Signaling-Molecule Wavefront Model for Cell Polarization and Proliferation in the *Drosophila* Wing Primordium

DISSERTATION

submitted in partial satisfaction of the requirements
for the degree of

DOCTOR OF PHILOSOPHY

in Physics

by

Juliana Caroline Wortman

Dissertation Committee:
Professor Clare C. Yu, Chair
Professor Arthur D. Lander
Professor Zuzanna S. Siwy

2014

Table of Contents

List of Figures

Acknowledgments

First, I wish to thank Professor Clare Yu, who supervised my work. This project would not have been possible without her patience and dedication. Over the years, she has vastly helped to clarify and improve both my research and my writing. It has been a privilege to work with her.

I wish to thank Professor Arthur Lander, whose expertise allowed me to focus on the key questions to address in my research. I also wish to thank Professor Elliot Botvinick for his enthusiasm in discussions, the new perspectives on my topic, and the opportunities to collaborate with his group.

Similarly, I would like to thank Professors Zuzanna Siwy and Thorsten Ritz for serving on my committees and for their helpful comments.

Last but not least, I am deeply grateful to my family and friends for their boundless love and support.

This work was supported in part by NIH grant P50-GM076516.

Curriculum Vitae

Juliana Caroline Wortman

Education

- Ph.D., Physics. University of California, Irvine, 2014
- M.S., Physics. University of California, Irvine, 2007
- B.S., Physics. Harvey Mudd College, Claremont, CA, 2005

Research Experience

Graduate Research Assistant, biophysics, University of California, Irvine, 2006-present

- Dynamics of morphogen signaling in developing tissues
- Mechanical limits to axonal transport
- Role of mechanical stresses in cancer progression

Teaching Experience

Teaching Assistant, University of California, Irvine

- Mathematics 2A-B, Calculus. Discussion and tutoring.
- Physics 2, Mathematical Methods in Physics. Discussion and tutoring.
- Physics 3A-C, Basic Physics. Discussion and laboratory.
- Physics 7C-E, Classical Physics. Discussion and laboratory.
- Physics 19, Great Ideas of Physics. Discussion.
- Physics 52A, Fundamentals of Experimental Physics. Laboratory.

Fellowships

- UC Regents' Fellowship, 2005

Publications

- Furlani, E.P., Sahoo, Y., Ng, K.C., Wortman, J.C., and Monk, T.E. A model for predicting magnetic particle capture in a microfluidic bioseparator. *Biomedical Microdevices*, 9:451-463, 2007.
- Wortman, J.C., Shrestha, U.M., Barry, D.M., Garcia, M.L., Gross, S.P., and Yu, C.C. Axonal transport: How high microtubule density can compensate for boundary effects in small-caliber axons. *Biophysical Journal*, 106:813-823, 2014.
- (in preparation) Wortman, J.C., Nahmad, M., Lander, A.D., Yu, C.C., Expanding signaling-molecule wavefront model for cell polarization in the *Drosophila* wing primordium.

Invited Presentations

- Maggots, peer pressure, and a sense of direction: cell growth through lopsided forces in the developing fly. Presented at Growth and Form: Pattern Formation in Biology at the Aspen Center for Physics, Aspen, CO, January 2012.
- Regulation of growth in the *Drosophila* wing disc through mechanical interactions. Presented at Dynamics of Development at the Kavli Institute for Theoretical Physics, Santa Barbara, CA, August 2011.
- Monte Carlo simulations of *Drosophila* wing disc. Presented at Morphodynamics of Plants, Animals, and Beyond at the Kavli Institute for Theoretical Physics, Santa Barbara, CA, September 2009.

Abstract of the Dissertation

Expanding Signaling-Molecule Wavefront Model for Cell Polarization and Proliferation in the *Drosophila* Wing Primordium

By

Juliana Caroline Wortman

Doctor of Philosophy in Physics

University of California, Irvine, 2014

Professor Clare C. Yu, Chair

The spatial patterns of cell proliferation and polarization in developing organisms depend on, yet differ from, the profiles of related signaling molecules. A classic case is the *Drosophila* wing primordium, a developing tissue whose cells demonstrate a consistent polarization despite depending on proteins with fairly uniform concentration profiles. Although the profiles of the Fat (Ft) pathway components Four-jointed (Fj) and Dachsous (Ds) are typically viewed as smoothly graded with uniform slope stretching across the wing pouch, this is not the case. Rather, the protocadherin Ds is expressed at high levels outside the wing pouch and low, roughly uniform levels within it, with a steep transition region at the border of the wing pouch. The Golgi kinase Fj has a complementary profile with uniformly high expression levels within the pouch, low levels in the periphery of the wing disc, and a steep concentration gradient in the transition region. However, the Fj and Ds profiles are not static; Ds-expressing cells are gradually recruited into the Fj-expressing wing pouch. We present a computational model that incorporates these profiles and their dynamics. Ft and Ds are protocadherins that form heterodimers between adjacent cells with a binding affinity that depends on Fj. In our model the asymmetry of the Ft-Ds bond distribution around the periphery of a cell defines the polarization. This asymmetry is greatest in the transition region. The transition region expands radially outwards with

time, leaving in its wake polarized cells that retain their asymmetric bond distributions and direction of polarization, even after cell division. Similarly, the cells of the pouch proliferate roughly uniformly despite nonuniform profiles of proteins involved in growth signaling, such as Decapentaplegic (Dpp) and Wingless (Wg). In our model, cells grow and proliferate in response to the asymmetry of their Ft-Ds bond distributions as well as to the local morphogen (Dpp and Wg) concentration which increases with time. Since the morphogen profile decays exponentially with radial distance, Dpp and Ft-Ds-Fj signaling form counterbalancing gradients that result in fairly uniform cell proliferation. The overall result is a pattern of cell polarization and proliferation that is consistent with experimental observations.

Chapter 1: Introduction

In this chapter, we introduce the related questions of polarization and growth of the *Drosophila* wing imaginal disc, including various models and signaling pathways. We begin with a general description of the development of the wing disc, its use as a model system, and outstanding questions regarding its growth and polarization. Next, we review existing models of wing disc development, including their results, assumptions, and limitations. In particular, we concentrate on models of two signaling mechanisms: signaling via Fat-Dachsous (Ft-Ds) bond distribution and via the Decapentaplegic (Dpp) concentration profile. Finally, we examine each of the signaling molecules used in our model, to ensure each component is accurately represented.

1.1 The wing imaginal disc

The *Drosophila* wing is a widely used model system for studying organ development, since it grows quickly, it is easy to isolate in a larval fly and observe on an adult fly, and the wing's size and pattern (such as the location of veins and the alignment of hairs) are well characterized. The size and pattern of the prospective wing are largely determined well in advance of metamorphosis, during the larval phase.

1.1.1 Disc development

The cells of the prospective wing proliferate rapidly during the larval phase. This phase of *Drosophila* development lasts roughly four days and is divided into three phases, called instars, that are separated by molting of the skin. During the larval phase, many adult appendages, including the wings, are present in the form of internal structures called imaginal discs. The wing disc consists of a single sheet of epithelial cells, as shown in Figure 1.1, which are columnar near the center of the disc and taper into squamous cells at

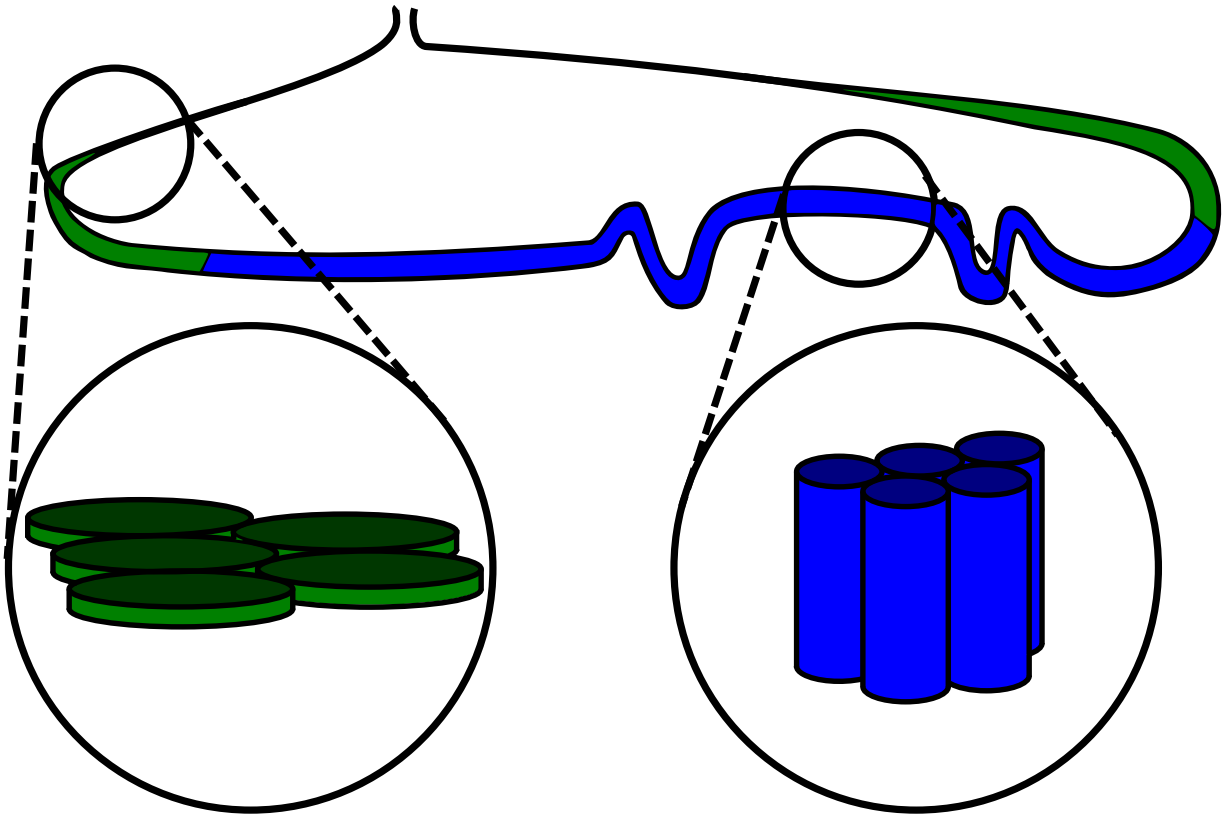

Figure 1.1: Cross-section of the wing disc late in the larval phase. The disc consists of a single layer of cells. The apical surface of each cell faces the interior, or lumen, of the disc, and the basal surface of each cell faces outward. The cells at the periphery of the disc (green, left inset) are squamous, with a large apical cross-section and relatively little lateral surface area. Closer to the center of the disc (blue, right inset), the cells become columnar, with a greater apical-basal distance, a smaller apical cross-section, and more lateral surface area. The wing pouch (zoomed blue area) is ringed by folds in the tissue and goes on to form the wing blade proper; surrounding tissues form the base of the wing and the hinge attaching it to the thorax.

the disc's periphery [1]. The apical side of these epithelial cells faces the inside, or lumen, of the folded tissue, and the basal side faces out. The center of the disc, which goes on to form the wing blade, is also called the wing pouch or wing primordium. The tissue is folded, particularly around the edge of the wing pouch. However, since it contains only one layer of cells throughout, it is generally treated as two-dimensional for the purpose of modeling cell-cell interactions.

During metamorphosis, the discs evert through the body wall to become external appendages (Figure 1.2). In the case of the wing disc, the regions that were originally around the periphery of the disc become various structures at the base of the wing, while the central part of the disc becomes the wing blade. For this reason, the central part of the disc is also referred to as the distal part (because it becomes the end of the wing), and the outer part is the proximal part (because it forms the wing's base). The radial direction in the disc is then also called the proximal-distal axis. The adult wing consists of two layers of cells, forming the dorsal and ventral surfaces.

In the *Drosophila* larva, the wing disc grows from approximately 50 to 50,000 cells over the course of four days, corresponding to about 10 cell cycles [2]. The prospective wing blade (or wing primordium) becomes distinct from the rest of the disc during the second instar [3], and its patterning becomes more pronounced during the third instar, which lasts roughly the last two days of the larval phase. At the beginning of the third instar, the disc has about 1000 cells [4]. Cell proliferation is roughly exponential during the entire second instar and part of the third instar, then slows during the last day or so before entering the pupal phase [5, 6]. During exponential growth, the cell cycle time is roughly 6 hours [5]; when averaged over the whole larval phase, the cell cycle time is about 8.5 hours [7]. These cells form a single-layered epithelium [8]. In most of the disc—particularly in the wing primordium—cells are columnar, with a width on the order of microns and an apical-basal height on the order of tens of microns [1]. We primarily consider the columnar cells of the wing primordium in our model.

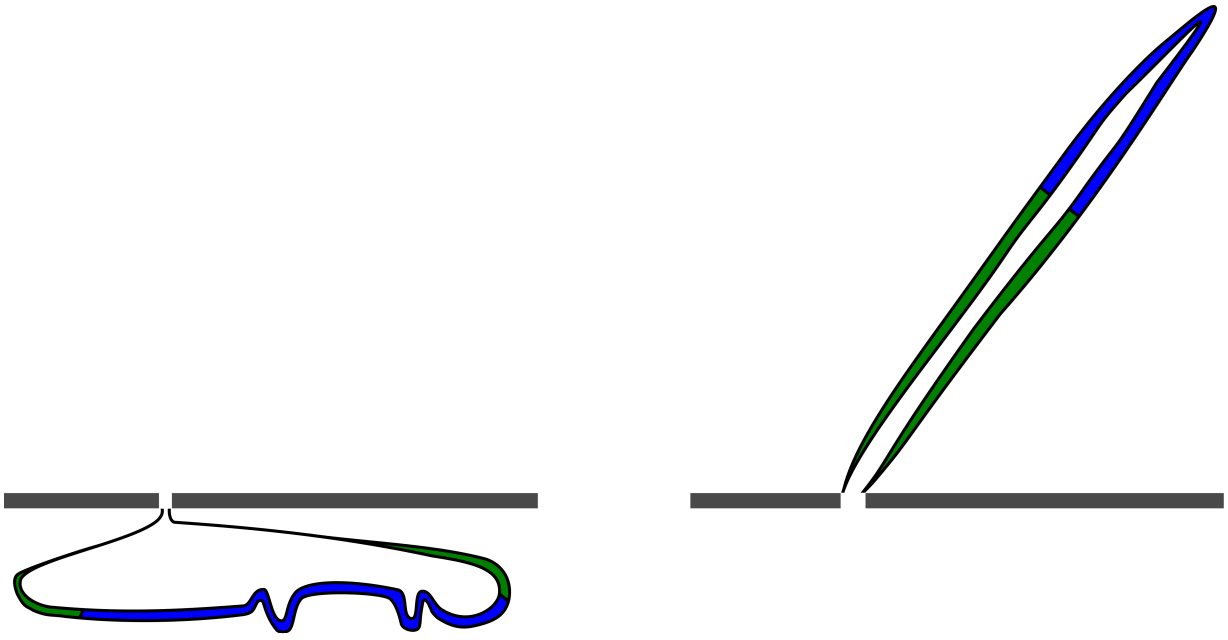

Figure 1.2: Eversion of the wing disc during metamorphosis. The blue and green tissue represents the wing disc, as in Figure 1.1. The gray line represents the fly's body wall; the disc is inside (below the line) before metamorphosis and outside (above the line) afterward. During metamorphosis, the disc turns inside-out as it is pushed through the body wall. The central part of the disc (blue) forms the end, or distal region, of the adult wing. The outer parts of the disc (green) form the wing's base, or proximal region. Note that the adult wing has two layers of cells, while the wing disc has one.

1.1.2 Outstanding questions

Although the overall behavior of the developing wing disc is well characterized, the underlying mechanisms are not as well understood. Many studies of the wing disc focus broadly on two features: local (i.e., cell-scale) polarization and global (i.e., tissue-scale) growth. Cells throughout the disc proliferate such that the overall size of the disc increases exponentially with time. Each cell in the wing primordium also interacts with its neighbors to become polarized along the disc's proximal-distal (i.e., radial) axis. As we will show, these two processes are both related to the Fat (Ft) pathway, which incorporates the protocadherins Ft and Dachsous (Ds), along with the Golgi kinase Four-jointed (Fj).

Individual cells within the disc exhibit polarization within the plane of the tissue. In particular, cells in the wing pouch are polarized along the proximal-distal (i.e., radial) axis. The myosin Dachs, whose localization is affected by Ft pathway activity, normally localizes to the distal part of each cell, i.e., the part closest to the disc's center, throughout the wing pouch [9]. Direct observation of Ft and Ds shows that cells throughout the wing pouch tend to have more Ds on their distal surface and more Ft on their proximal surface (the side facing the disc's edge) [10, 11]. This asymmetry, along with the fact that Ft and Ds bind to one another, suggests that adjacent cells have different amounts of Ft or Ds available to form bonds. Thus, the amount of asymmetry in the distribution of these bonds may constitute a measure of the local concentration gradients of Ft pathway components. (Here, we will use the word "gradient" to refer to the spatial slope or steepness of the concentration profile.)

However, there is scant evidence to suggest that the concentrations of Ft, Fj, or Ds are evenly graded—i.e., have a constant slope—throughout the wing pouch. Rather, Fj is expressed at high levels in the wing primordium, while Ds is expressed at high levels in the periphery, with a steep transition region at the edge of the wing primordium [12–18]. The Fj and Ds concentration profiles resemble sigmoid curves that are flat in the wing pouch

and periphery and steep at the boundary of the wing pouch. (Ft is expressed comparatively uniformly throughout the disc [19].) But if cell polarization depends on the local slope of the Fj and Ds concentrations, we would expect to see strong polarization only at the boundary of the wing pouch, when instead polarization is observed throughout the wing pouch. How do the cells inside the wing pouch become polarized when they and their neighbors all have similar amounts of Ft, Ds, and Fj?

Furthermore, cell proliferation in the disc is approximately uniform, even though the concentration profiles of proteins related to growth are not. DNA synthesis and apoptosis pathway activity show no obvious spatial pattern across the disc, so cells presumably proliferate and die at fairly spatially uniform rates [2, 20, 21]. Similarly, clones (clusters of cells descended from a single progenitor) labeled at the same time have similar sizes regardless of their position within the disc [22]. However, various signaling molecules that are known to affect cell growth and proliferation, such as Ft pathway components and the growth factor Decapentaplegic (Dpp), are not present in uniform concentrations across the disc. If the growth rate were simply proportional to the concentration of one of these signals, we would not expect to see uniform cell proliferation. A model of growth due to a spatially graded signal, then, cannot depend only on the local, instantaneous concentration of that signal.

We are left with two related questions: How does a pattern of cell polarization arise from (locally) uniform signals, and how does uniform disc growth arise from (globally) graded signals? Next, we review existing models of growth and polarization that have examined these questions, and demonstrate the need to consider a cell's history in addition to its instantaneous behavior when developing such a model. We begin with a summary of the possible relationships between the Dpp profile and growth, with a particular focus on the spatial gradient of Dpp. We then examine the potential role of the Ft pathway in sensing the steepness of Dpp and its likely function as an intermediate step between the Dpp gradient and the observed growth and polarization in the wing pouch.

1.2 The Dpp profile and growth

We now examine past models of morphogen-mediated growth in the disc, beginning with a general description of morphogens, and examine the activity of Dpp as a classical morphogen. The connection between Dpp signaling and cell proliferation is of particular interest because the Dpp concentration profile is spatially graded while proliferation is comparatively spatially uniform. However, the rate of cell proliferation does depend on Dpp signaling in some capacity, since cells with increased Dpp signaling proliferate faster than normal [23–25]. These results seem paradoxical: how can uniform growth result from a nonuniform growth signal? To address this question, several past models have focused on aspects of the Dpp profile other than its instantaneous concentration, such as its spatial steepness, its possible interaction with other signals, and its temporal rate of change.

1.2.1 Dpp as a classical morphogen

For a tissue to develop with a predictable pattern, its individual cells need to receive signals that determine their eventual roles, locations, and orientations within the tissue. This information can take the form of the concentration of some signaling molecule, called a morphogen, produced in one part of the tissue and dispersing throughout, reacting with other molecules [26]. Cells could then respond to this signal—for example, by differentiating into other cell types, changing their proliferation rates, or expressing certain genes—depending on their local concentration of this molecule [27]. In this view, called the French flag model, a cell's local concentration of the morphogen would be its source of positional information, and each cell's responses to the differing concentrations would form a regular spatial pattern (Figure 2.1).

The protein Decapentaplegic (Dpp) in the *Drosophila* wing disc is one example of a morphogen that behaves in this fashion. It is expressed in a stripe running between the anterior and posterior compartments of the disc [28, 29], and spreads to the anterior and

posterior sides of the disc, forming a roughly one-dimensional concentration profile [30] that decays roughly exponentially with distance to the source [31, 32]. Dpp has been shown to activate the expression of other genes, including *optomotor-blind (omb)* and *spalt (sal)*, in a manner dependent on its concentration, as in the classic French flag model [33]. Furthermore, Dpp is involved in the patterning of the adult wing. Discs that ectopically express Dpp in a clone can give rise to two wing blades rather than one. The winglet resulting from the clone does not consist solely of Dpp-expressing cells, but rather has the Dpp-expressing clone running along the proximal-distal axis of the wing, forming a stripe between its anterior and posterior halves [29]. Thus, Dpp appears to organize surrounding cells as it establishes the wing's axes, indicating a role in patterning and polarization.

1.2.2 Dpp signaling and growth

In addition to its patterning properties, Dpp signaling is also linked to cell proliferation. However, Dpp signaling is nonuniform while cell proliferation occurs relatively uniformly in the wing disc. Under the French flag model, this might suggest that there are simply two cell phenotypes: normal growth and non-growth. In this case, the threshold of Dpp signaling necessary to cause the growth phenotype would be very low, low enough that every cell in the disc would have enough Dpp signaling to grow at the standard rate. However, the proliferation rate exhibits at least some dependence on the level of Dpp signaling. Discs with elevated Dpp expression—either from expressing Dpp ubiquitously, or by overexpressing it in its normal domain—will grow larger than wild-type discs [23–25]. Similarly, discs that lack the Dpp receptor Thickveins (Tkv), and therefore experience no Dpp signaling, undergrow [23].

These results might also suggest that the entire disc grows at a single rate based on some global average of Dpp signaling. However, we also know that cells respond autonomously to their local level of Dpp, rather than taking a broad spatial average. Ectopic Dpp signaling

(whether through ectopic expression of Dpp itself or of a constitutively active form of its receptor Tkv) in specific areas of the disc leads to ectopic cell proliferation in the same areas [29, 34, 35]. Thus, cells are responding to their own individual levels of Dpp signaling. Once again, though, cells cannot simply proliferate at a rate proportional to their local amount of Dpp signaling, since this would lead to proliferation that is graded rather than uniform. Some other aspect of the Dpp signaling profile, or some combination of mechanisms, must be involved in controlling proliferation.

1.2.3 Mechanical feedback

One way in which uniform proliferation might arise from a nonuniform growth factor is via a second signal—this time, a growth inhibitor—with a similar profile to the growth factor. In this model, cells with high levels of the growth factor would also have high levels of the growth inhibitor, and cells with low levels of the growth factor would have low levels of the growth inhibitor. The net result would be fairly uniform growth, because the two signals would roughly cancel each other out. If the growth of cells also increased the activity of the inhibitor, forming a negative feedback loop, the system could then be self-regulating and stop growing when it reaches a certain size.

Mechanical compression is a reasonable candidate for this growth-inhibiting signal. Although the wing disc consists of a single layer of cells, this layer does not lie in a flat plane. Cross-sectional images of the disc reveal folds running circumferentially around the edge of the wing primordium [36], suggesting that the disc is under compression in the radial direction, causing it to buckle. Direct studies of mechanical stresses in the disc have confirmed that compression is greatest at the disc's center [37, 38]. Furthermore, cell divisions are not randomly oriented; clones tend to elongate along the proximal-distal (i.e., radial) axis [39], which would give rise to radial compression in the growing disc in the absence of substantial cell rearrangement. Because local mechanical forces can in turn affect

the orientation of cell division [40], there may be a feedback loop relating cell proliferation, mechanical compression, and mitotic angle.

Shraiman [41] and Hufnagel et al. [42] proposed a model in which mechanical forces and autonomous Dpp signaling act jointly to control cell proliferation and the disc's eventual size. In this model, a cell's growth rate increases with its level of signaling from some secreted growth factor (analogous to Dpp) and decreases with its degree of mechanical compression from its neighbors. If a cell grows faster than its neighbors, it becomes compressed by the surrounding cells, which slows its growth. The effects of growth factor signaling and mechanical compression, then, can counteract one another and lead to uniform cell growth. If this growth factor is most strongly concentrated in the center of the disc and forms a radial concentration gradient, the cells near the center of the disc receive the most signal from this growth factor, but also tend to be more strongly compressed by their neighbors. Cells near the edge of the disc, however, receive the least signal but are under less radial compression, consistent with experimental results.

This model has some appealing features: it predicts that cells will proliferate uniformly because of these similar profiles of growth factor and mechanical compression. It predicts that compression will be greatest in the center of the disc. It also predicts that the disc will eventually reach a steady-state size once the cells in the center of the disc are too compressed to grow and the cells on the edge have too little growth factor to grow. However, these predictions rely on the assumption that the growth factor profile—both its amplitude (i.e., its maximum concentration) and its length scale—will not vary substantially over time. A steady increase in the amplitude or decay length of the growth factor profile would cause cells to experience more growth signaling without a concomitant increase in compression, causing the disc to continue growing without reaching a steady-state size.

Aegerter-Wilmsen et al. [43] proposed a similar mechanical model in which the disc is made up of concentric rings. This model also involves a growth factor analogous to Dpp whose concentration is greatest in the disc's center and least at the disc's edge. Similarly,

the growth rate of each ring is determined both by its growth factor concentration and by mechanical forces. Again, radial compression tends to slow the growth rate of a ring, leading to a steady state in which the profiles of growth factor and mechanical compression are similar. A ring will also grow faster in this model when stretched, which occurs when its next innermost ring is growing faster than it is.

This model makes a number of accurate predictions. For example, it gives rise to increased cell proliferation around clones with increased Dpp signaling, because it would be an eventual consequence of Dpp-induced growth in the same clone. (Clones with artificially high Dpp signaling can exhibit faster proliferation near their edges [44].) In this case, cells near the edge of the clone are stretched circumferentially as a result of the clone's elevated growth rate and then grow faster in response to that tension. However, growth within the clone followed later by growth at the edge of the same clone has not been observed experimentally. Furthermore, this model, much like the one mentioned previously, assumes that the concentration profile of the growth factor (both its amplitude and its spatial scale) does not change substantially as the disc grows, and this assumption is what allows the disc to reach a steady-state size. The assumption that the Dpp profile is fairly static warrants further examination.

1.2.4 Dpp dynamics

As the size of the disc varies over time, so do the expression domains and concentrations of its signaling molecules. In particular, both the Dpp concentration and Dpp signaling activity in any given cell in the disc appear to increase over time [45]. The amplitude of the Dpp concentration profile (i.e., the maximum concentration of Dpp) undergoes a clear increase as the disc grows. It is less clear whether the spatial scale of the profile remains constant or scales with the overall size of the disc.

Past experiments have given conflicting results regarding whether the Dpp signaling profile scales with disc size. Recall that Spalt (Sal) expression depends on Dpp signaling in a manner consistent with the French-flag model [33]. In discs where one compartment grows faster than the other, the width of the Sal expression domain in that compartment increases to match it [46], suggesting that the Dpp gradient becomes shallower to compensate for the compartment's size, thus moving the threshold Dpp concentration necessary for Sal expression further from the Dpp source. So the Dpp profile appears to adjust separately to the size of each compartment, indicating that expression levels of proteins in the receiving tissue can alter the local Dpp concentration. For instance, the Dpp receptor Tkv is not expressed uniformly; it is present in higher concentrations in the lateral regions of the disc than in the medial region. It may be that uptake of Dpp by Tkv is also a factor in shaping the Dpp profile, potentially adjusting the spatial scale of the Dpp profile as the disc grows [30, 47]. Similarly, other factors like Magu (also called Pentagone) may control the degradation rate of Dpp, allowing the Dpp profile to scale as the disc grows [48, 49].

However, other studies have suggested that the Dpp profile does not in fact scale with disc size. When normalized for amplitude but not for position, Dpp concentration profiles from discs at different stages of development look very similar, implying that the Dpp scale is roughly constant over time [42]. Multiple studies [31, 32] suggest that the decay length of the Dpp profile (i.e., the distance over which the concentration decreases by a factor of e) is consistently about 15-20 μm during the third instar. These observations are not completely incompatible with a scaling Dpp profile, however; it may be the case that the mechanism allowing the Dpp profile to scale becomes less effective as the disc grows, meaning that the scale of the Dpp profile does not change as fast during the third instar as it does earlier in the larval phase.

Wartlick et al. [45] measured the concentration of Dpp throughout the wing disc over several cell cycles and claimed that both the amplitude and the decay length of the Dpp profile increased over time; in particular, the decay length remained proportional to the

radius of the disc as it grew. Because both the Dpp concentration in a given cell and the total number of cells in the disc increased roughly exponentially, they found that each cell cycle corresponded to a 40% increase in the average Dpp concentration. Thus, they claimed that the uniformity of growth in the disc was a result of the uniformity of the relative rate of change (that is, the rate of change divided by the total amount) of Dpp.

Although the study presents ample evidence that the amount of Dpp signaling in any given cell increases over time, the evidence given for the decay length increasing is ambiguous; it may instead be the case that the decay length stops increasing after reaching roughly 20 μm. The assertion that every cell in the disc experiences the same relative increase in Dpp signaling is dependent on the decay length scaling with disc size. In this case, each cell would need to stay the same number of decay lengths away from the Dpp source, so that only the amplitude of the Dpp profile would change for a given cell. Regardless of its findings on decay length, though, the study does show evidence that the Dpp concentration in any given cell has a tendency to increase over time.

The effect of Dpp signaling on a cell's growth rate, then, is a complex one. Although cells lacking Dpp signaling undergrow and cells with excess Dpp signaling overgrow, the overall growth rate in the disc is much more spatially uniform than the Dpp profile. In addition, the Dpp signaling in each cell increases over time, while the growth rate does not. It is clear that the growth rate of a cell responds to something other than, or in addition to, its local level of Dpp signaling. As shown above, the temporal rate of change of Dpp signaling may be related to the rate of growth. The spatial steepness of the Dpp profile (i.e., the Dpp gradient) may also be a factor.

1.2.5 The steepness hypothesis

Another model [50] suggests that cells might grow faster when the local morphogen profile is steeper. Rogulja and Irvine [44] proposed that two different aspects of the Dpp

profile affected cell proliferation: its local concentration and its local steepness (or gradient). They investigated the relationship between the Dpp gradient and growth by causing clones of cells to produce constitutively active Tkv in different regions of the disc. These clones were more likely to exhibit autonomous growth (i.e., growth within the clone itself) when located in the lateral regions of the disc (which contain the least endogenous Dpp). In other words, cells belonging to these clones tended to proliferate faster than cells outside the clones in these regions, presumably due to their increased Dpp signaling, in agreement with existing results.

However, clones expressing activated Tkv in the medial region of the disc (the region with the most endogenous Dpp) were more likely to exhibit *nonautonomous* growth (i.e., growth at the clone's edge). Cells near the boundaries of these clones—both inside and outside the clones themselves—often proliferated faster than cells near the clones' centers or far from the clones [44]. The cells immediately outside these clones did not experience elevated Dpp signaling, since neither they nor their neighbors were expressing extra Dpp, but proliferated faster regardless. In contrast, cells near the clones' centers–in the clones but several cells away from the clone boundary–frequently were unaffected, proliferating no faster than wild-type cells far from the clones. This result suggested that a cell's growth rate can respond to the spatial steepness of the Dpp profile, not just to the local amount of Dpp signaling.

Thus, Rogulja and Irvine's conclusions were threefold. First, two separate mechanisms are responsible for the autonomous and nonautonomous responses to Dpp signaling. Second, these two mechanisms tend to dominate in different parts of the disc: the autonomous response is stronger in the lateral regions of the disc (the anterior and posterior extremes, where the least Dpp is present), and the nonautonomous response is stronger in the medial region (the region near the anterior-posterior boundary, where the most Dpp is present). Third, the superposition or sum of these two different responses leads to the relatively uniform cell proliferation seen in wild-type discs. The exact natures of these two mechanisms

(especially the nonautonomous mechanism) and the reason why they would dominate in different parts of the disc, however, was less clear.

1.3 Ft-Ds binding, cell polarization, and proliferation

The nonautonomous response to Dpp signaling described above suggests that cells have a way of sensing the local steepness of the Dpp profile. The spatial scale of the Dpp profile compared with that of a single cell, combined with variations in cell size and shape as well as stochasticity in receptor-ligand binding, means that Dpp steepness is likely not measured by simply comparing the Dpp concentrations on either side of a cell [1, 31, 32, 45].

However, a cell can sample a larger area by interacting with its neighbors. If a cell has a way of detecting the relative amounts of Dpp activity in adjacent cells, it would then be able to sense the steepness of the profile (by measuring the variation in Dpp signaling among all of its neighbors) as well as the direction of the Dpp source (by locating the neighbor with the most Dpp signaling). In this way, a graded morphogen could also give rise to a consistent polarization within the plane of the tissue, since cells could localize certain proteins toward neighbors with more or less morphogen signaling. If the growth rate of a cell depends on the local steepness of the morphogen, as results suggest [44], then the proliferation and polarization of the cells—in other words, the growth and patterning of the disc—are linked. This brings us to models of cell polarization.

1.3.1 Experiments linking the Ft pathway with proliferation

Indeed, evidence suggests that a mechanism downstream of Dpp signaling is involved both in cell proliferation and cell polarity. Rogulja et al. [9] explored the link between the Fat (Ft) signaling pathway and the nonautonomous effects of Dpp signaling on cell proliferation. The Ft pathway (Figure 1.3) includes the transmembrane proteins Ft and Dachsous (Ds) [12, 51] and the Golgi kinase Four-jointed (Fj) [16, 52], which phosphorylates

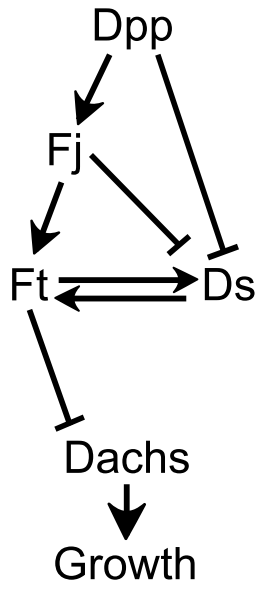

Figure 1.3: The Fat (Ft) pathway. Increased Dpp activity is associated with more Fj and less Ds expression. Ft and Ds form bonds with one another between adjacent cells. Phosphorylation by Fj makes Ft more likely and Ds less likely to form bonds. Dachs localizes to cell-cell interfaces where less bound Ft is present. Increased Dachs localization is associated with faster cell proliferation.

them, as well as the unconventional myosin Dachs. Cells with artificially elevated Dpp signaling express more Fj and less Ds [9], suggesting that Dpp affects Fj and Ds expression in the way described by the French-flag model. In contrast, Ft is expressed comparatively uniformly throughout the disc [19]. A Ft protein on one cell binds to a Ds protein on an adjacent cell [53, 54], suggesting that cells might interact with their neighbors via Ft-Ds binding. Fj activity affects the ability of Ft and Ds to form bonds. Experimentally, cells co-expressing Ft and Fj more readily bind extracellular Ds than do cells expressing only Ft. However, Ds is much less likely to bind to Ft when co-expressed with Fj than it is when expressed alone [55, 56]. This suggests that Fj makes Ft more likely to bind and Ds less likely to bind.

Cells proliferate faster when the local gradient of Fj or Ds is steeper. Clones of cells that are mutant for Fj, or that overexpress Fj or Ds, exhibit nonautonomous cell proliferation; i.e., cells near the edges of these clones proliferate faster [9, 57], much like clones with

elevated Dpp signaling. These results suggest that steep discontinuities in Fj and Ds are responsible for the nonautonomous proliferation around clones with Dpp signaling [44], since Dpp signaling affects Fj and Ds expression. For example, clones with constitutively active Tkv (i.e., artificially high Dpp signaling) have high Fj and low Ds expression [9], leading to very steep Fj and Ds gradients at the clone's edge. These boundaries of Fj and Ds expression, then, may be what drives proliferation around these clones.

Cells in the disc may then measure the steepness of the Dpp profile indirectly, through measuring the steepness of the Fj and Ds profiles. The results showing that Ft and Ds are transmembrane proteins, that they form bonds between adjacent cells, and that Fj is a Golgi kinase that acts on them, together suggest a mechanism by which cells might measure the local steepness of the Fj and Ds expression profiles. In particular, they suggest that cells respond to the arrangement of their Ft-Ds bonds by proliferating faster when these bonds are more asymmetrically distributed.

1.3.2 A common model for the Ft pathway

Here we summarize a frequently-used conceptual model (Figure 1.4) describing how cells might sense the local steepness of the Fj and Ds profiles, and, by extension, the Dpp gradient. Each cell has a set of Ft-Ds bonds with each of its neighbors. A Ft-Ds bond consists of a Ft on one cell bound to a Ds on an adjacent cell. Fj acts on both Ft and Ds by affecting their binding affinities, making Ft more likely and/or Ds less likely to bind. If Fj and Ds are present in fairly uniform concentrations near a cell (i.e., the spatial scale on which the concentration varies is large compared to the width of a cell), then that cell and its neighbors will all have roughly the same amount of Ft and Ds available to bind, and each cell's Ft-Ds bonds will be fairly symmetrically distributed among its neighbors. However, if Fj or Ds are steeply graded, then adjacent cells will have appreciably different amounts of Ft or Ds available to bind, due to differences in Ds expression and Ft-Ds

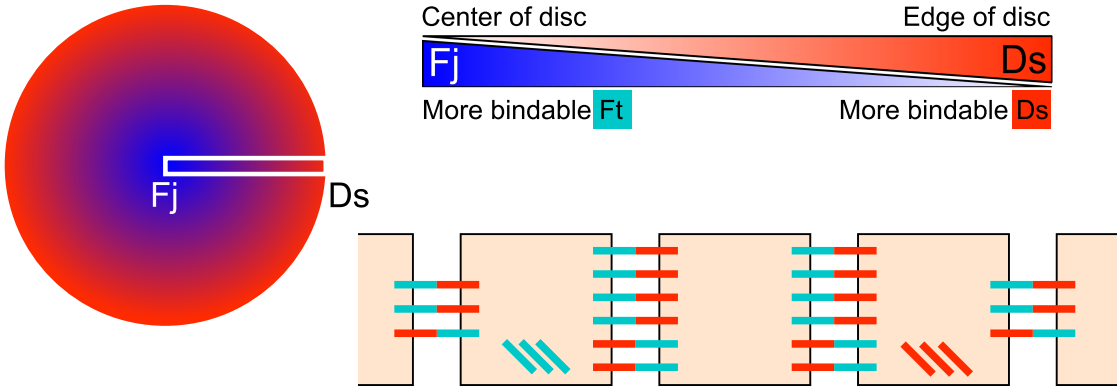

Figure 1.4: Common model of Ft-Ds bond asymmetry in the disc. The disc (shown at left) contains complementary concentration profiles of Fj (dark blue) and Ds (orange). We consider the radial stripe of cells outlined by the white rectangle on the disc. Individual cells are shown at the bottom as beige squares. Fj is expressed at higher levels in the disc's center (left side of stripe) and Ds is expressed at higher levels at the disc's edge (right side of stripe). Fj makes Ft more likely and Ds less likely to bind, so the concentrations of bindable Ft (light blue) and bindable Ds are also spatially graded. A Ft protein on one cell binds to a Ds protein on an adjacent cell. Because adjacent cells have different amounts of bindable Ft and Ds, cells will tend to have asymmetrically distributed bonds, as well as leftover free (i.e., unbound) Ft and Ds, shown here near the bottom surfaces of cells. In general, cells will have more bound Ft on their proximal side (the surface facing the edge of the disc; here, the right surface) and more bound Ds on their distal side (the surface facing the center of the disc; here, the left surface). This is because a cell's proximal (outer) neighbor is likely to have the most available Ds of all the cell's neighbors, and its distal (inner) neighbor is likely to have the most available Ft. If the Fj and Ds profiles are linear, i.e., they have spatially uniform slope, then all cells should exhibit a similar degree of asymmetry in the distribution of their Ft-Ds bonds.

binding affinity. In this case, a cell's Ft-Ds bonds will be unevenly distributed among its neighbors. A cell, then, can measure the local steepness—the spatial derivative—of the Fj and Ds profiles via the asymmetry of its Ft-Ds bond distribution. This mechanism could also constitute an indirect measure of the steepness of the Dpp profile, since Dpp signaling determines Fj and Ds expression. If the Fj and Ds profiles have a fairly consistent steepness throughout the disc, then all cells will have similarly asymmetrically distributed Ft-Ds bonds. If a cell's growth rate is tied to this asymmetry (as experiments suggest), then a uniform steepness (i.e., a linear profile) of Fj and Ds expression should give rise to a uniform pattern of polarization. Furthermore, since the asymmetry of the Ft-Ds bond distribution is associated with a faster growth rate, uniform Fj and Ds gradients should also lead to uniform proliferation.

1.3.3 Limitations of the common model

This model gives a plausible explanation for why cell proliferation is roughly uniform, and how cell polarization might arise via the Ft pathway. However, it makes a number of questionable assumptions that must be addressed before implementing it as a simulation.

If a cell's proliferation rate is driven by the degree of asymmetry in its Ft-Ds bonds, then cells should proliferate faster where Fj or Ds are steeply spatially graded. Thus, if the Fj and Ds profiles each have a uniform steepness throughout the disc, then all cells in the disc should have a similar degree of asymmetry in their Ft-Ds bonds, leading to uniform growth. However, neither the Fj nor the Ds profile is known to have a uniform steepness. Fj is expressed primarily in the wing primordium (the central region of the disc), while Ds is expressed largely in the hinge region (the disc's edge) [9, 12, 14, 18, 58]. Both proteins exhibit a steep concentration gradient near the border of the wing primordium, but are present comparatively uniformly otherwise—most of the wing pouch has high levels of Fj and low levels of Ds, while the periphery of the disc has more Ds and less Fj. If proliferation

is caused primarily by the gradients of Fj and Ds, we would therefore expect to see a ring of fast cell proliferation at the border of the wing primordium. Similarly, we would expect cells near the center of the wing pouch to have fairly symmetrically distributed bonds, resulting in less Dachs localization and slower proliferation. Thus, this mechanism is also insufficient to explain why the cells of the disc proliferate uniformly and exhibit proximal-distal polarization.

The model also describes an instantaneous "snapshot" of cells in the disc, and does not account for changes in Dpp, Fj, or Ds expression. However, evidence suggests that the amplitude (and possibly also the spatial scale) of the Dpp concentration profile increases as the disc grows [45]. This would suggest that the Fj and Ds profiles are also dynamic, since Fj and Ds expression are dependent on Dpp signaling. Indeed, the profiles of Fj and Ds expression are not static. Rather, cells just outside the wing primordium become "recruited" into the primordium over time, decreasing their Ds expression rate and increasing their Fj expression rate [58]. In other words, the size of the Fj-expressing wing primordium does not simply scale with the size of the entire disc, but rather grows to encompass an increasing fraction of it. This means that the region where the Fj and Ds profiles are steeply graded moves outward over time, sweeping over many cells. It may be more realistic, then, to treat this region as a propagating wave front of protein expression, rather than a stationary feature.

Another consequence of modeling only a snapshot of the disc is that each cell is treated as if its set of neighbors never changes. Although cells in the disc do not appear to actively rearrange themselves [59], each cell's set of neighbors is not static. As a cell (or its neighbors) grows and divides, it will gain and lose neighbors. These changes in a cell's neighbors must also affect a cell's distribution of Ft-Ds bonds, since the bonds are formed between adjacent cells. The possible effects of these changes in neighbors on a cell's bond distribution (and, therefore, its direction of polarization and growth rate) are worth investigating.

Similarly, modeling an effectively one-dimensional line of cells makes the assumption that each cell has exactly the same number of neighbors: two, one on either side. In the wing disc, cells have a rough average of six neighbors, but can have as few as four or as many as eight [59]. This means that a realistic model would often juxtapose cells with different numbers of neighbors, and cells with different numbers of neighbors presumably partition their Ft and Ds differently. Whether realistic variations in neighbor number have a substantial effect on Ft-Ds bond distribution and the resulting growth and polarization warrants further study.

The rationale for our model, then, is as follows. A cell might, in some sense, sense the local steepness of the Dpp signaling profile through the formation of Ft-Ds bonds with its neighbors. However, the expression patterns of Fj and Ds, which determine the availability of Ft and Ds for binding, do not directly parallel the expression pattern of Dpp. Rather, the Fj and Ds profiles are relatively flat in most of the wing pouch and steeply graded at the border of the wing primordium. We know, however, that cells throughout the wing pouch have asymmetrically distributed Ft-Ds bonds, not just cells at the edge of the pouch [10,11]. A cell's distribution of Ft-Ds bonds, then, is at best an indirect measure of the instantaneous Fj and Ds gradients. Thus, this problem necessitates a model that does not equate a cell's Ft-Ds bond distribution asymmetry with the instantaneous Fj and Ds concentration gradients near that cell. Furthermore, cells in the disc grow and divide, causing a cell's set of neighbors to change over time. This means that we cannot assume that a cell keeps the same neighbors, the same number of neighbors, or the same set of Ft-Ds bonds, as the disc grows. Our model must also incorporate cell proliferation and account for changes in each cell's set of neighbors when forming Ft-Ds bonds.

1.4 Signaling molecules

Based on these observations, a model of the Ft pathway and its effects on growth and patterning should include the entire disc, because the expression patterns of Dpp, Fj, and Ds vary on a disc-wide scale. It should account for individual cells and allow them to divide, because growth and polarization are affected by interactions between each cell and its neighbors. Furthermore, it should track the phosphorylation and binding states of individual Ft and Ds proteins, because Ft-Ds bonds can form and dissolve over time, and a cell's amount of Ft, Ds, and Fj can vary over time. The model should track and update each cell's set of neighbors, since neighbors will change as cells proliferate, and changes in a cell's set of neighbors will in turn affect its set of Ft-Ds bonds. Finally, it should be a two-dimensional model of the entire wing pouch rather than a one-dimensional radial stripe of cells, since cells in the disc have neighbors on all sides, and not all cells have the same number of neighbors.

Our model needs to incorporate a graded morphogen profile roughly analogous to Dpp that spans the disc and changes over time in a realistic fashion. It should also have individual cells that express Ft, Ds, and Fj; form Ft-Ds bonds with their neighbors; and proliferate based on their levels of morphogen signaling and Ft-Ds bond distribution asymmetry. This means that the model should include the morphogens Dpp and Wg, the protocadherins Ft and Ds, the Golgi kinase Fj, and the myosin Dachs. Here, we examine these proteins, their interactions, and their respective roles in wing disc growth and polarization in more detail to justify the way we represent them in the model.

1.4.1 Decapentaplegic

Decapentaplegic (Dpp) is critical for the development of the fly; null mutations in the *dpp* gene are lethal during the embryonic stage [60]. Dpp helps give rise to dorsal-ventral patterning in the fly embryo [61]. It is also found in each of the developing imaginal discs

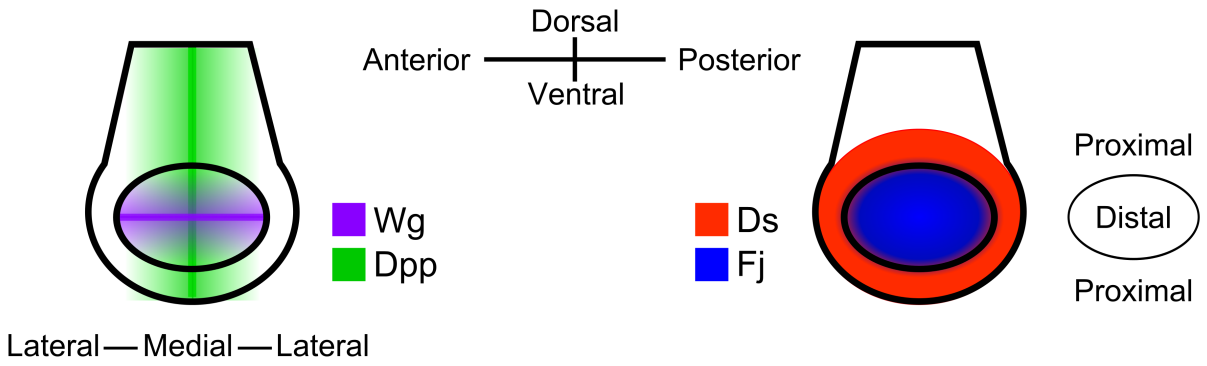

Figure 1.5: Approximate expression patterns of Decapentaplegic (Dpp, green), Wingless (Wg, purple), Dachsous (Ds, orange), and Four-jointed (Fj, blue) in the wing disc. The smaller oval represents the (distal) prospective wing blade, while the surrounding area is the (proximal) wing base and hinge region. Dpp is expressed in a stripe near the anterior-posterior compartment boundary and forms a concentration gradient along the anterior-posterior axis. Similarly, Wg is expressed between the dorsal and ventral halves of the disc and forms a gradient parallel to the dorsal-ventral axis. Ds is expressed primarily around the edge of the disc outside the prospective wing blade, while Fj is expressed within the prospective wing blade. Ds and Fj have steep concentration gradients near the border of the wing primordium, and plateaus at the center and edge of the disc.

and is necessary for the growth of at least fifteen of them, hence the name [62]. In the wing disc, Dpp is expressed only in a narrow band of cells alongside the anterior-posterior compartment boundary (Figure 1.5), but is found in a roughly one-dimensional graded concentration profile throughout the disc [30, 46]. Discs that express null mutant *dpp* alleles will dramatically undergrow, and will fail to activate pathways known to be downstream of Dpp signaling [63, 64]. Dpp signaling (along with Wg signaling, as discussed below) is associated with cell shape and adhesion; clones of cells with reduced Dpp or Wg signaling are shorter than their wild-type counterparts and can be extruded from the disc [65–68]. Furthermore, wing discs that overexpress Dpp, whether in its usual domain or ubiquitously, will overgrow [23, 24, 69].

The main receptor of Dpp is Thickveins (Tkv), so experiments on Dpp signaling often involve altering Tkv activity. Tkv is expressed at higher levels in the lateral regions of the disc where less Dpp is present and expressed at lower levels in the medial region

where more Dpp is present [47]. Both constitutively active and loss-of-function mutants of Tkv are used experimentally to control levels of Dpp signaling. Tkv activity, normally associated with Dpp-Tkv binding, leads to the phosphorylation of Mothers against Dpp (Mad). Phosphorylated Mad is also frequently used as an indicator of Dpp activity, and its presence is typically associated with an autonomous increase in cell proliferation due to Dpp signaling [44].

While Dpp clearly has an autonomous effect on growth (i.e., the growth rate of a cell depends on its own level of Dpp signaling), it also appears to have a separate nonautonomous effect. Clones of cells with increased levels of Dpp signaling can induce proliferation nonautonomously, i.e., near the clone's edge rather than inside the clone itself [44]. This effect may result from the Ft pathway; differences in Dpp signaling in adjacent cells at the clone's border lead to differences in Fj and Ds expression, which in turn lead to unevenly distributed Ft-Ds bonds [9]. Both the autonomous and nonautonomous effects gradually wear off over the course of roughly 50 hours [44].

In addition to its role as a growth factor, Dpp appears to fit the classical definition of a morphogen. The genes *optomotor-blind (omb)* and *spalt (sal)* are expressed in stripes spanning the anterior-posterior compartment boundary, and their expression domains widen to encompass the entire disc in the case of ubiquitous Dpp signaling [33]. This suggests that *omb* and *sal* are each expressed when the Dpp concentration is above a certain threshold quantity. Similarly, increased Dpp signaling is associated with elevated Fj expression and lowered Ds expression [9]. Since Dpp is expressed only in a thin stripe of cells, moves outward over time, and is degraded throughout the tissue, it forms a graded concentration profile. Because the degradation rate is typically assumed to be spatially uniform, the Dpp profile is often described as a one-dimensional exponential decay:

$$C(x) = C_0 e^{-x/\lambda} \tag{1.1}$$

This concentration profile $C(x)$ can then be fully characterized using three quantities: the spatial coordinate x (the distance from the morphogen source), the maximum concentration (or amplitude) C_0, and the decay length (i.e., the length over which the concentration decreases by a factor of e) λ. Over time, the Dpp-expressing cells proliferate, and the amplitude C_0 of the gradient increases, since more Dpp is being expressed [45]. A number of factors may affect the decay length. For example, the concentration of Thickveins (Tkv), a Dpp receptor, varies across the disc; Tkv is expressed more strongly in the lateral regions of the disc and less in the medial region [47]. Since the binding of Dpp to Tkv prevents Dpp from moving through the disc, the concentration of Dpp should fall more steeply when more unbound Tkv is available.

The decay length of Dpp should also depend on its degradation rate; the faster it is degraded, the shorter the distance it should be able to travel before degradation. Wartlick et al. [45] claim that the decay length scales with the size of the disc, staying roughly 1/9 of the distance from the Dpp source to the disc's edge. They suggest that this scaling is caused by a decrease in the Dpp degradation rate over time that widens the Dpp profile. This degradation rate may be related to Dpp-Tkv binding, or it may be affected by some other factor. For example, in an expansion-repression system, a second molecule called the expander tends to increase the decay length of a morphogen, perhaps by inhibiting the morphogen's degradation. The morphogen in turn represses the expander's expression. This feedback loop allows the morphogen gradient to scale with the size of a tissue [70]. Experiments have shown that Magu (Pentagone) may act as such an expander. In Magu mutant discs, the profile of Dpp activity has the same scale regardless of the overall size of the disc, while discs that express Magu uniformly have overexpanded Dpp gradients [48, 49]. These results suggest that Magu is responsible for regulating the decay length of the Dpp profile, allowing it to scale to the size of the disc.

However, other results suggest that the Dpp profile does not scale with the size of the disc for the entire larval phase. Rather, the decay length may reach a plateau of about

20 μmduring the third instar [45]. Kicheva et al. [31] measured a decay length of roughly 20 μm for the Dpp profile in several different mature discs. Similarly, the Dpp profiles in different discs, when normalized for the amplitude C_0, are similar regardless of tissue size [42]. Given these results, our model should not exhibit a steep dependence on the decay length of Dpp (or the quantity analogous to Dpp), or whether it scales with tissue size or remains constant.

In summary, cells in our model should grow in response to Dpp signaling via both autonomous and nonautonomous mechanisms. In other words, the growth rate of a cell should depend on its own level of Dpp signaling, as well as on the spatial gradient of Dpp signaling. Cells should express Fj and Ds in a manner dependent on their levels of Dpp signaling, as in the French flag model; they can then respond to the slope of the Dpp profile by comparing their levels of Fj and Ds with those of their neighbors. The amplitude of the Dpp profile should increase over time, so that all cells experience a gradual increase in their local Dpp concentration. Finally, the decay length of the Dpp profile should scale as the disc grows; however, the system should not exhibit a steep dependence on this quantity.

1.4.2 Wingless

A similar protein, Wingless (Wg), is also necessary for wing disc growth. It is expressed in a stripe between the dorsal and ventral parts of the disc (Figure 1.5), as well as around the border of the wing pouch. Like Dpp, it forms a graded concentration profile in the wing pouch, though with a smaller decay length [31,71], and is considered to act as a morphogen, acting at a distance from its source to affect gene expression [72,73]. Dpp and Wg signaling also appear to have similar effects on polarization via the Ft pathway [9]. Wingless signaling (along with Dpp signaling) is necessary for the recruitment of Ds-expressing cells into the Fj-expressing wing primordium [58,74]. This mechanism gives rise to a "wave front" that

moves outward as the wing primordium grows to encompass an increasing fraction of the disc.

Since Dpp and Wingless have similar roles in regulating growth and patterning, we conflate them into a single morphogen for the purposes of our model. Since they are expressed in perpendicular stripes running through the center of the disc, the total concentration of Dpp and Wg is greatest in the disc's center and decreases with radial distance. To replicate this behavior while maintaining simplicity, we use a radially symmetric profile for our composite morphogen. The morphogen concentration, then, will be greatest at the center of the disc and decay exponentially with radial distance, and it will affect the expression rates of proteins in the Ft pathway.

1.4.3 Fat and Dachsous

Fat (Ft) and Dachsous (Ds) are atypical cadherins that form bonds between adjacent cells. Cadherins, so named because they are involved in intercellular adhesion and require calcium ions to function, are found in many types of tissue. They are transmembrane proteins typically containing an intercellular and extracellular domain. The intracellular domain is generally attached to the cytoskeleton, while the extracellular domain binds to the extracellular domains of other cadherins, either on the same cell or on an adjacent one. These sets of cadherin bonds between adjacent cells are known as adherens junctions. A cadherin's extracellular domain contains several identical segments called cadherin repeats; between these repeats are binding sites for calcium ions [75]. Most types of cadherins form homodimers (matched pairs on the same cell), which then bind to cadherin homodimers on adjacent cells [76, 77]. Cells in the wing disc are attached primarily via DE-cadherin (*Drosophila* epithelial cadherin, also called Shotgun [78]), which is expressed throughout the disc [66].

Some types of cadherins are involved in morphogenesis by controlling cell adhesion and transducing signals between adjacent cells. For example, Ft and Ds are protocadherins [12, 51] found in various regions of the developing fly, including imaginal discs. They are involved in cell polarity in the adult wing, eye, and abdomen [79–81]. In general, their function appears to involve spatial coordination between adjacent cells. In the case of the wing disc, they are involved in establishing the proximal-distal axis (i.e., the axis running from the base to the end of the wing). Like other cadherins, they are also transmembrane proteins involved in intercellular adhesion, but contain many more cadherin repeats than DE-cadherin. A Ft on one cell binds to a Ds on an adjacent cell. Cells that fail to express Ft will have most of their Ds localized to sides abutting a wild-type (i.e., Ft-expressing) neighbor [53], rather than sides abutting other *ft-* cells. Furthermore, no Ft-Ft or Ds-Ds binding is observed between adjacent cells [54]. This suggests that, unlike other cadherins, Ft and Ds only bind heterophilically (i.e., to one another). Ds is observed primarily near the apical surface of each cell, suggesting that Ft-Ds interactions occur in roughly a single plane [15, 82].

While Ft is expressed at somewhat higher levels near the dorsal-ventral boundary of the disc, its expression is not steeply spatially graded [17, 19]. Ds is expressed primarily outside the wing primordium, in the prospective hinge region [14, 17]. There is a clear border of Ds expression at the edge of the wing pouch; much less Ds is expressed inside than outside (Figure 1.5). In addition, Dpp signaling appears to affect Ds expression; clones of cells expressing an activated form of the Dpp receptor Tkv express less Ds than the surrounding wild-type cells [9].

Both Ft and Ds are involved in disc growth in addition to proximal-distal patterning. *ft* mutant discs overgrow dramatically, while *ds* mutant discs can overgrow to a lesser degree [15, 51, 83–86]. Adult wings that are mutant for Ds may not overgrow substantially, but are typically shorter and wider than wild-type wings, depending on the specific allele [12, 87, 88]. Wing discs that uniformly express Ds at high levels undergrow [9].

However, *clones* of cells that overexpress Ds exhibit nonautonomous growth at their boundaries [9], much like clones of cells with elevated Dpp signaling. This suggests that spatially flat expression of Ds is associated with slower growth, and spatially graded expression of Ds is associated with faster growth.

Ft also appears to be involved in signaling that is independent of its binding. A number of experiments have shown that the intracellular and extracellular domains of Ft have separate signaling functions [86, 89–91]. Matakatsu and Blair [86] performed a number of experiments using modified forms of Ft that lacked either the intracellular or the extracellular domain. Notably, discs that expressed only Ft lacking an intracellular domain overgrew to an even greater extent than *ft* null mutant discs [86]. Note that it is the extracellular domain that binds to Ds, which suggests that the disc expressing this form of Ft should still have been able to form Ft-Ds binds, unlike a *ft*- disc.

In contrast, discs that expressed a form of Ft lacking an extracellular domain grew to be considerably *smaller* than *ft* mutant discs, even though neither disc should be capable of forming any Ft-Ds bonds. Furthermore, *ft ds* double mutant discs overgrow more than either the *ft* or the *ds* single mutants [86], and Ft-overexpressing clones proliferate more slowly than wild-type ones [92], suggesting that the presence of Ft or Ds affects the rate of disc growth even in the absence of Ft-Ds bonds.

These results have several implications for the model. The Ds expression profile in our model should consist of two plateaus—a high one in the periphery and a low one in the wing pouch—with a narrow, steeply graded transition region in between. The Ft expression profile should be spatially flat, at least in comparison. The growth rate should be dependent on the presence and arrangement of Ft-Ds bonds. A disc without bonds should overgrow dramatically, and cells with asymmetrically distributed bonds should grow faster than cells with evenly distributed bonds. Finally, free (i.e., unbound) Ft and Ds, not only Ft-Ds bonds, should have some effect on the growth rate. In particular, the more free Ft and Ds a cell has, the slower it should grow.

1.4.4 Four-jointed

Four-jointed (Fj) is another major component of the Ft signaling pathway, affecting Ft-Ds binding. It is a Golgi kinase that phosphorylates the cadherin domains of Ft and Ds [16, 52]. This phosphorylation of Ft and Ds by Fj appears to affect their binding probabilities in different ways. In particular, phosphorylation by Fj makes Ds less likely to bind to Ft [55] and also may make Ft more likely to bind to Ds [56].

Fj, like Ds, appears to be related to proximal-distal patterning in appendage growth. It is so named because in *fj* mutants, the tarsus—the most distal part of the leg—has four segments rather than the usual five [13, 18, 93, 94]. Fj has a seemingly paradoxical role in wing disc growth: *fj* mutant discs undergrow, but so do discs uniformly overexpressing Fj [9, 13, 16, 18, 94]. These results suggest that the effect Fj has on growth is not due to its overall concentration. Rather, it appears that the spatial pattern of Fj expression, rather than its absolute concentration, is key for normal wing growth.

Indeed, Fj expression is typically not uniform. Fj is expressed primarily in the wing primordium, which is in the center of the wild-type disc [14], and its concentration is steeply graded near the border of the wing primordium (Figure 1.5). In other words, it is expressed largely in the distal, but not the proximal, region of the wing. Its expression pattern is then roughly complementary to that of Ds, with a high plateau at the disc's center, low levels in the periphery, and a steep transition region at the border of the wing pouch. The expression pattern of Fj also appears to change over time. Increased Dpp signaling is associated with an increase in Fj expression [9], and individual cells in the disc appear to experience an increase in Dpp signaling over time [45]. This would suggest that the Fj-expressing portion of the disc expands over time. Indeed, the border of the prospective wing blade moves outward through the disc over time, recruiting cells into the wing primordium [58]. Since cells inside the wing primordium express Fj at high levels, the Fj expression domain grows over time to encompass an increasing fraction of the disc.

This pattern of Fj expression has implications for Ft-Ds binding, which in turn affects a cell's growth rate. If the expression patterns of Ds and Fj are steeply graded compared to the size of a cell in a particular region, cells in this region should have asymmetrically distributed Ft-Ds bonds. This is because adjacent cells will have significantly different amounts of Ds and Fj, and thus different amounts of Ft and Ds available for binding. Indeed, experiments have shown that a cell grows faster when its local slopes of Fj and Ds are steeper. Clones of cells that overexpress either Fj or Ds exhibit more cell proliferation near their edges, and this increased proliferation includes cells both inside and outside the clone [9]. Furthermore, this effect is most pronounced when Fj-expressing clones are induced near the disc's periphery (containing the least endogenous Fj) and when Ds-expressing clones are induced near the disc's center (containing the least endogenous Ds). This suggests that steeper spatial differences of Fj or Ds expression lead to a more asymmetric bond distribution, which in turn leads to faster cell proliferation.

We can now predict the pattern in which Ft-Ds bonds will form in the wild-type disc. Consider a cell near the wing primordium boundary, where Fj and Ds expression are both steeply spatially graded. This cell's outer or proximal neighbors (i.e., neighbors that are closer to the disc's edge) will tend to have more Ds, while the cell's distal or inner neighbors (i.e., neighbors nearer the disc's center) will have more Fj. This means that the cell is more likely to bind its Ft to its outer neighbors (which have more Ds available, and that Ds is more likely to bind since it is largely unphosphorylated by Fj). Similarly, the cell is more likely to bind its Ds to its inner neighbors (whose Ft is more likely to bind since more of it is phosphorylated by Fj). Images of the wild-type disc do indeed show that cells bind more Ft to their outer neighbors and more Ds to their inner neighbors [10].

However, the spatial gradients of Fj and Ds are unlikely to be the only factors in determining bond distribution and proliferation rate. The concentration profiles of Fj and Ds do not have uniform steepness throughout the wild-type disc; rather, there is a narrow transition region at the border of the wing primordium that separates the Fj-expressing

cells in the wing primordium from the Ds-expressing cells in the periphery. The Fj and Ds profiles are steeply graded in this region, and comparatively flat within the wing primordium and periphery. If cells simply responded to the local, instantaneous steepness of Fj and Ds concentration, we would expect an annulus of fast proliferation at this border and slower proliferation at the center and edge, not the relatively uniform proliferation that is observed. Cells must be responding to some additional factor.

Suppose, as existing models suggest, the growth rate of a cell responds to the degree of asymmetry in its Ft-Ds bond distribution rather than directly to the instantaneous slope of Fj and Ds. If Ft-Ds bonds persist for some time after they are formed, then the bond distribution can reflect a cell's cumulative history of Fj and Ds expression, not just the instantaneous expression rates. Recall that the boundary of the wing primordium, where Fj and Ds are most steeply graded, sweeps outward over time. In this case, a large fraction of the cells in the disc will have the front sweep over them and then remain in the Fj-expressing wing pouch afterward. The Ft-Ds bonds around a given cell will become more asymmetrically distributed when the cell is at the wing primordium boundary, and persist after the cell has entered the wing primordium. With this mechanism, cells within the wing pouch, not just those at the boundary, can have asymmetrically distributed bonds, as observed experimentally. Furthermore, if bond distribution is asymmetric throughout the pouch, this mechanism could explain why cell proliferation is uniform, since more asymmetric bond distribution is associated with faster proliferation. Because a cell's distribution of Ft-Ds bonds depends on its history of Fj and Ds expression rather than its instantaneous state, our model needs to track individual Ft-Ds bonds, rather than simply measuring the local slopes of the Fj and Ds concentrations.

These results inform the way Fj is represented in the model. Fj should be expressed at high levels in the wing pouch and low levels in the periphery, in a complementary pattern to Ds. The phosphorylation rates of Ft and Ds in each cell should depend on that cell's amount of Fj, and the ability of Ft and Ds to form bonds should depend on whether they

are phosphorylated. We also hypothesize that the arrangement of Ft-Ds bonds around a cell persists after the local expression rates of Fj and Ds have changed. Our model, then, needs to incorporate Ft-Ds binding explicitly, rather than simply measuring the local slopes of the Fj and Ds concentration profiles. This suggests that each cell should have its own pools of Ft, Ds, and Fj. Each of these proteins should be expressed and degraded at each time step. Furthermore, Ft and Ds should be split into phosphorylated and unphosphorylated pools, and only phosphorylated Ft and unphosphorylated Ds should be able to form bonds. Finally, since bonds form between adjacent cells, the model should be able to track which cells are adjacent and how many Ft-Ds bonds connect each pair of neighboring cells.

1.4.5 Dachs

The polarization of cells in the disc—in particular, their arrangement of Ft-Ds bonds—is often determined by examining each cell's pattern of Dachs (D) localization. Dachs is an unconventional myosin, a motor protein, whose activity is affected by the Ft pathway. In wild-type wing discs, Dachs tends to localize to the part of each cell closest to the disc's center [9, 95]. More generally, it localizes to the same side of the cell as bound Ds and the opposite side as bound Ft [10, 95, 96]. Cells that are mutant for *ft* have Dachs on all sides rather than localized to one side [9], suggesting that the distribution of Ft-Ds bonds affects Dachs localization. This asymmetric localization of Dachs is more pronounced in cells at the edge of the wing primordium than at the center [11], but is visible in cells throughout the wing primordium [9]. Since Dachs is asymmetrically localized even in cells that are far from the boundary of the wing primordium, this also suggests that cells have asymmetrically distributed Ft-Ds bonds when they are not near the Fj/Ds expression front. Indeed, Ft and Ds are asymmetrically localized on cells throughout the pouch [10, 11].

Dachs is necessary for the overgrowth phenotype in *ft* mutants [14], suggesting that it is part of the mechanism that links the distribution of Ft-Ds bonds to cell growth. The

localization of Dachs as a result of Ft pathway activity affects the activity of Warts (Wts), a kinase that deactivates Yorkie (Yki) through phosphorylation [97]. Both Dachs and Yki are necessary for normal growth, and their localization within the cell is affected to some degree by the Ft pathway [95, 98].

Dachs, as a motor protein, also appears to be involved in mechanotransduction (i.e., the sensing of mechanical signals by a cell); it affects the overall shape of the disc by determining the orientation of cell divisions. In particular, it exerts a contractile force on cell-cell junctions [99]. Furthermore, Yes-associated protein (YAP), which is homologous to Yki, is associated with contact inhibition, interactions between the cell and the extracellular matrix, and mechanotransduction [100, 101]. The Ft pathway, then, may be involved in sensing mechanical signals between cells, and in how cells grow in response to those signals.

To compare the results of our model to experimental results involving Dachs localization, we can implement quantities corresponding to both the degree and the position of Dachs localization in each cell. In our model, we assign a vector to each cell, with its magnitude and direction corresponding to those of Dachs localization. In particular, the vector's direction points toward the side of a cell with the fewest bound Ft proteins, and its magnitude represents how asymmetrically distributed the cell's bonds are. For the sake of simplicity, Dachs localization will not affect the growth rate in our model, even though Dachs mutants undergrow.

1.5 Summary

Here, then, is how existing results regarding signaling pathways inform our model of growth and patterning in the wing disc. The disc should consist of a single, roughly circular, two-dimensional layer of cells that grow and divide. It should represent Dpp and Wg as a single radially symmetric concentration profile that decays exponentially with distance from the center. The amplitude of this concentration profile should increase with time,

causing a gradual increase in morphogen signaling in every cell. Cells should have their own pools of Ft, Ds, and Fj; keep track of their neighboring cells; be able to form Ft-Ds bonds with these neighbors; and record how many bonds they have with each neighbor. The availability of Ft and Ds for binding should change over time due to changes in Fj and Ds expression. Because the availability of Ft and Ds can change over time, the number and distribution of bonds on each cell should be able to evolve with time as well.

Since we are interested in cell polarization in the form of Dachs localization, each cell should also have a vector representing Dachs localization that is affected by its bond distribution. Since we are also interested in what makes the spatial pattern of cell proliferation uniform, each cell should calculate its growth rate independently. This growth rate should depend on the local morphogen concentration, the asymmetry of the Ft-Ds bonds around the cell, and the number of free Ft and Ds the cell has left over.

1.6 Overview

We present a model of polarization and growth in the *Drosophila* wing imaginal disc. This model takes into account the binding between Ft and Ds on adjacent cells, as well as signaling by a morphogen analogous to Dpp. As such, it treats cells as individual units that can grow and divide, allowing for the rearrangement of cells as they proliferate. It also tracks the number of Ft-Ds bonds on each cell-cell interface through multiple cell cycles. We show that this model as a whole—and the movement of the Fj/Ds expression boundary in particular—is consistent with a number of experimental results regarding the growth and patterning of the wing disc.

In Chapter 2, we explain the motivation for implementing a model of this kind. We introduce the related problems of cell polarization from uniform signals and uniform cell proliferation from nonuniform growth signals. We then explain why existing models of morphogen signaling and Ft-Ds binding are insufficient to explain the results seen

experimentally. In particular, we examine a widely used conceptual model of cell polarization via Ft-Ds binding, along with the assumptions on which this model is based. Finally, we describe the properties of our model that make it well suited to simulate polarization and growth in the disc.

In Chapter 3, we present the model in detail. We first describe how cells keep track of and interact with their set of neighbors. We note that a cell's set of neighbors will change as they grow and divide, and show how the simulation handles this rearrangement. The expression and interaction of the various signaling molecules in the model is explained, including the morphogen profile; the expression of Ft, Ds, and Fj; and the binding of Ft and Ds between adjacent cells. We show how these quantities evolve over time as cells grow and divide and as the expression patterns change. We also analyze the factors known to affect the growth rate of cells in the disc, particularly the asymmetry in a cell's Ft-Ds bond distribution, and combine them into the single expression used in the model. Finally, we describe the types of input and output that the simulation uses.

Chapter 4 presents results related to cell polarization. First, we describe what happens in an ordinary run of the simulation representing a wild-type disc. We then show how the patterns of Ft-Ds bond polarization and Dachs localization arise in such a run. Finally, we examine the effects of a stationary, rather than moving, front of Fj and Ds expression on patterning in the wing pouch, and compare these results to those from the moving front. This demonstrates that the movement of the front is responsible for the polarization of the cells in the wing pouch.

Chapter 5 presents results related to cell proliferation. We examine the results of the simulation in terms of the final size of the disc for a number of phenotypes involving underexpression and overexpression of the morphogen, Ft, Ds, and Fj, and compare these results to those of corresponding experiments. We also induce elevated morphogen signaling, Ds expression, and Fj expression in regions of the disc, and analyze the effects of steep discontinuities of expression at the boundaries of these regions. Again, we compare these

results to those of analogous experiments that altered gene expression within a single clone. We also compare the spatial patterns of cell growth and proliferation when the Fj/Ds expression front is moving and when it is stationary.

In Chapter 6, we summarize the points that the model has addressed. We review assumptions made for the sake of the model, and examine their possible effects on our results. Finally, we make suggestions for future experiments and examine what topics have not been satisfactorily addressed by the model.

Chapter 2: Motivation for the model

In this chapter, we introduce the related problems of tissue patterning in the face of spatially uniform signals and uniform cell proliferation due to nonuniform signals. We examine these problems in the context of our chosen model system, the *Drosophila* wing imaginal disc, and describe our approach to the problems.

2.1 Polarization from uniform signals

Cells in developing tissues typically become polarized along a body axis as they proliferate. The wing imaginal disc of the fruit fly *Drosophila melanogaster*, the structure in the larval fly that later becomes the adult wing, is a widely used model system for studying the growth and patterning of a developing tissue. In the central portion of the wing disc, known as the wing pouch or wing primordium, cells exhibit a radial polarization in which the unconventional myosin Dachs consistently localizes to the side of the cell facing the center of the wing pouch [9, 95]. Dachs localization reflects the distribution of bonds between the protocadherins Fat (Ft) and Dachsous (Ds) that a cell forms with its neighboring cells. In wild-type discs, cells bind more of their Ft on the side facing the edge of the disc (the proximal side) and more of their Ds on the side facing the center of the disc (the distal side) [10, 11]. Dachs, then, localizes on the side of the cell with the least amount of bound Ft [9, 95]. However, Ft, Ds, and Four-jointed (Fj), which affects the binding affinities of Ft and Ds [55, 56], are present in fairly uniform concentrations (compared to the width of a cell) throughout the wing pouch [12–19, 58]. How, then, do cells establish a pattern of polarization in these proteins that they retain over multiple cell cycles?

2.2 Uniform growth from graded signals

Signaling via Ft, Ds, and Fj is also associated with cell proliferation. Wing discs that are mutant for Ft, Ds, or both overgrow [86], while discs that uniformly express Ds, Fj, or both undergrow [9]. However, this is not the only mechanism affecting the growth or patterning of the disc. The growth factor Decapentaplegic (Dpp) is also necessary for normal wing development, since discs lacking Dpp severely undergrow [23]. However, the profiles of Dpp concentration and proliferation rate do not match. Cell proliferation in the disc is fairly uniform [2, 20, 22], while the Dpp concentration is graded. This is a long-standing question regarding the development of the disc: how does a nonuniform signal give rise to comparatively uniform proliferation?

2.3 The Dpp and Wg profiles

Dpp [33] and Wingless (Wg) [72] are examples of morphogens, signaling molecules that are produced in one part of a tissue and move through it to form a graded concentration profile [26]. In the wing pouch, Dpp and Wg are expressed along the anterior-posterior and dorsal-ventral boundaries (Figure 1.5) respectively, and form graded concentration profiles along these axes [46, 102]. Together, Dpp and Wg have the highest concentrations in the center of the wing pouch, and their total concentration decreases with distance to the center. Dpp and Wg also affect patterning; the polarization (i.e., the Dachs localization) of cells in the disc roughly parallels the gradients of Dpp and Wg sketched in Figure 1.5 [9]. So the direction of the morphogen gradients may determine the direction of cell polarization. It has been suggested that the steepness of a morphogen gradient may also determine the growth rate [50]. Indeed, cells near spatial discontinuities of Dpp signaling tend to proliferate faster, suggesting that the spatial gradient, not the local concentration, of Dpp

affects a cell's growth rate [9, 44]. These results might suggest that cells establish their growth rates and polarization based solely on the gradients of Dpp and Wg.

This idea is attractive because such a mechanism would allow both polarization and proliferation to be linked via these two proteins. Dpp and Wg are necessary for normal cell proliferation; discs mutant for Dpp or Wg undergrow [23, 73]. According to the French flag model of morphogenesis (Figure 2.1), cells respond to their local morphogen concentration [27], and this response may take the form of growth rate or differences in gene expression or cell fate. Under this model, the morphogens might have a permissive effect on growth, allowing proliferation to happen at a given rate as long as their concentrations are above a certain threshold. However, the proliferation rate is to some degree concentration-dependent, since ectopically elevated Dpp signaling leads to ectopic cell proliferation [23, 35]. So the gradient of Dpp is unlikely to determine the growth rate by itself; the Dpp concentration has some effect.

Other quantities in addition to the local concentration or gradient of a morphogen may also affect growth. Cells experience an increase in their amount of Dpp signaling over time, so the rate of increase of Dpp rather than its instantaneous value may control the growth rate [45]. Similarly, the position of a cell relative to the morphogen profile can change as the tissue grows. If the morphogen gradient is not spatially uniform, the local gradient that a cell senses can vary as the cell moves relative to the concentration profile. Furthermore, cells do not necessarily respond to an instantaneous signal, but can integrate the signal over a period of time, e.g., through integral feedback [103]. Other models suggest that a second quantity, such as mechanical compression, may build up over time, counteracting the effects of morphogen signaling [41–43]. As a result, the history of the local signal in the vicinity of a cell can affect its growth, not just the instantaneous signal or its gradient.

In any case, even measuring the local morphogen gradient poses a challenge for a cell. Suppose the local steepness of Dpp is measured by comparing the Dpp concentrations on either side of a cell. By the start of the third larval instar, the characteristic length of the

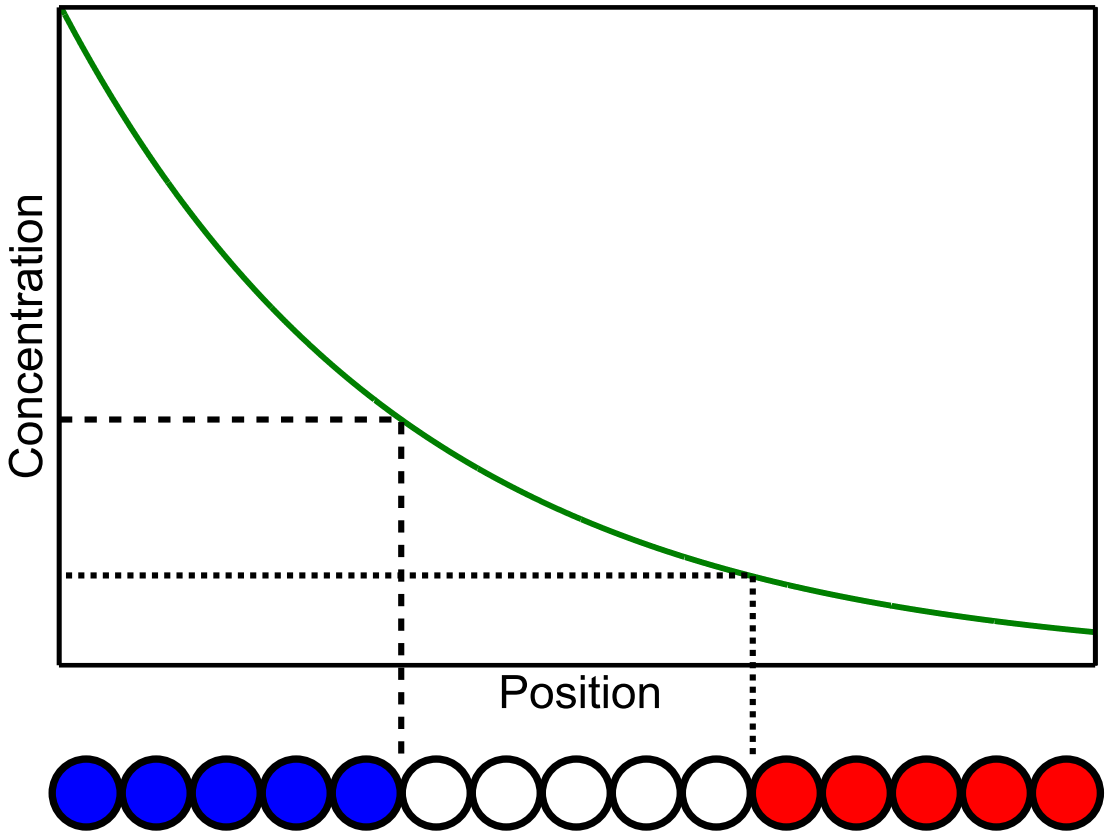

Figure 2.1: The French flag model of morphogen signaling. A signaling molecule called a morphogen is produced in one part of a tissue (here, the left side) and spreads throughout the tissue, perhaps via diffusion through the spaces between cells. The result is a graded concentration profile that is greatest near the source and decreases with distance. A cell can use its local concentration of morphogen as an indirect measure of its position. If the morphogen concentration (green) varies spatially, then cells (circles below graph) may have qualitatively different reactions depending on whether their local morphogen concentration is above or below some threshold level (shown by dashed and dotted lines). In this example, cells with a high morphogen concentration express a "blue" gene, cells with a morphogen concentration between the two thresholds express a "white" gene, and cells whose morphogen concentration falls below both thresholds express the "red" gene. In two dimensions, this system would give rise to a pattern of parallel blue, white, and red stripes, giving the French flag model its name.

exponential decay of the Dpp concentration is about 20 μm [31, 45]. This is much larger than the typical diameter of a columnar cell in the wing pouch, which is 2-3 μm [1]. We would then expect the Dpp concentrations on either side of a single cell to differ by only 10-15%. Variations in cell shape and size lead to an uncertainty on the order of 1-2 cell diameters in both Dpp concentration and Dpp signaling levels [32]. So the Dpp gradient cannot be measured with great precision on the scale of a single cell. However, cells might effectively sample a larger area by receiving input from their neighboring cells. The Ft pathway, which acts downstream of Dpp signaling [9], is one mechanism that allows cells to do this.

2.4 The Fat pathway

The Ft pathway is a likely intermediate step linking Dpp and Wg signaling to cell growth and polarization. Clones of cells with altered expression levels of Ft pathway components exhibit altered polarization patterns and proliferation rates [9, 95], even though the Dpp and Wg profiles are unchanged from wild-type. This pathway includes the protocadherins Ft [51] and Ds [12] and the Golgi kinase Four-jointed (Fj) [52]. The expression rates of Fj and Ds are affected by Dpp; increased Dpp signaling is associated with more Fj expression and less Ds expression [9]. However, the Fj and Ds profiles do not directly parallel that of Dpp. Rather, cells in the wing pouch express Fj at (fairly uniform) high levels and express Ds at (fairly uniform) low levels [12–19, 58] (Figure 1.5). Outside the wing pouch, the reverse is true; Fj is expressed at low levels and Ds at high levels. Both Fj and Ds are most steeply graded at the boundary of the wing pouch. (Ft is expressed comparatively uniformly throughout the disc [19].) Thus the Fj and Ds profiles do not appear to be a simple readout of the Dpp concentration, or of its steepness.

The localization of Ft and Ds within individual cells has a consistent pattern in the wing pouch. A Ft protein on the membrane of one cell can bind to a Ds protein on

the membrane of an adjacent cell [54, 104] and the phosphorylation of Ft and Ds by Fj affects their binding affinities [55, 56]. Cells throughout the wing pouch typically have more Ds on their distal side (i.e., the side facing the disc's center) and more Ft on their proximal side (i.e., the side facing the disc's edge) [10, 11]. The arrangement of Ft-Ds bonds also affects the distribution of the unconventional myosin (motor protein) Dachs, which localizes toward the side of the cell with the least amount of bound Ft [9, 10, 95]. For example, clones of cells that are mutant for Ft have Dachs all around the periphery of each cell [9]. In discs where one compartment overexpresses Fj or Ds, cells outside that compartment exhibit Dachs localization on the side facing away from the Ds-expressing cells and toward the side facing the Fj-expressing cells [10]. Greater asymmetry in the distribution of Ft-Ds bonds is associated with both stronger Dachs localization and a higher proliferation rate [9, 57]. Discs mutant for Dachs undergrow, much like discs in which Fj or Ds are expressed uniformly [57, 95], suggesting that Dachs localization is an intermediate step between Ft-Ds binding and cell proliferation. Since proliferation is roughly uniform in the wing pouch [2, 20, 22], this would suggest that all cells in the wing pouch have a similar degree of polarization in the arrangement of their Ft-Ds bonds and in their Dachs localization. However, the mechanism by which this occurs is not obvious.

2.5 The common model of Ft-Ds bond asymmetry

A common conceptual model [56, 81, 95, 105, 106] of Ft-Ds bond arrangement supposes that the Fj and Ds profiles have a uniform slope throughout the disc, causing adjacent cells to have slightly different amounts of Ft and Ds available for binding (Figure 1.4). These consistent differences in Ft and Ds availability lead to asymmetrically distributed Ft-Ds bonds in every cell, since a cell will bind more of its Ft to neighboring cells with more available Ds, and vice versa. Recent mathematical models [107] have also demonstrated that this is plausible. Similarly, if Ft-Ds bonds are equally asymmetrically distributed

in all cells and their asymmetry determines a cell's growth rate, then we would expect proliferation to be roughly uniform throughout the disc.

However, evidence suggests that Fj and Ds are *not* evenly graded. As described above, Fj is expressed primarily in the wing pouch and Ds is expressed primarily in the periphery of the disc, with a region of steep transition at the border of the wing pouch [12–19, 58]. Rather than varying linearly with position, Ds is expressed at high levels outside the wing pouch and much lower, nearly uniform, levels within it.

Under these conditions, the conceptual model would predict that Ft-Ds bonds will be asymmetrically distributed only near the edge of the wing pouch, rather than throughout the wing primordium as observed experimentally [10, 11]. Similarly, cell proliferation in the wing pouch would be nonuniform; it would be significantly faster at the edge of the wing pouch. How, then, can polarization (and the associated growth rate) be roughly uniform throughout the tissue when Fj and Ds are only steeply graded in a small fraction of it?

A recent model [108] suggests that cells might preferentially form new Ft-Ds bonds with the same polarity as existing bonds. This feature could amplify the effects of Fj and Ds gradients, allowing the bonds to be asymmetrically distributed even when the local Ds gradient is very shallow. However, there is no known mechanism by which Ft-Ds binding exhibits this kind of cooperativity.

Experiments have shown that spatial discontinuities of Ft and Ds availability (similar to the Fj/Ds expression boundary at the border of the wing pouch) can alter the arrangement of Ft-Ds bonds over a distance of several cell diameters [10]. However, the disc has a radius on the order of 100 cell diameters at the end of the larval phase, so this effect alone is not sufficient to explain the polarization of Ft-Ds bonds throughout the entire wing pouch. It may be the case that cells establish their polarization early in the development of the disc, when they are relatively near the edge of the wing pouch, then retain it throughout the larval phase. However, it is unclear how cells might retain this polarization over multiple cell cycles.

Another possible explanation for why the Ft-Ds bonds on cells throughout the wing pouch are polarized when Fj and Ds are not steeply graded in the wing pouch involves changes in the Fj and Ds expression profiles over time. Ds-expressing cells in the periphery of the disc gradually become part of the Fj-expressing wing pouch, so the wing pouch grows as a fraction of the overall disc [58]. This movement of the wing pouch boundary may be caused by the active recruitment of cells by their neighbors [58], changes in mechanical compression [109], or some combination of mechanisms. In any case, the transition region where the Fj and Ds gradients are steep expands outward, sweeping over a large fraction of the disc. This means that most cells in the interior of the wing pouch, or their progenitors, have been near the transition region at some point in the past. If the Ft-Ds bonds on a cell become asymmetrically distributed when the cell is near the transition region and remain so after the transition region has swept over them, most of the wing pouch can have asymmetrically distributed bonds.

None of the mechanisms described above address how cells might retain the distribution of their Ft-Ds bonds over the course of multiple cell cycles. Cells in the disc divide several times during the larval phase, forming new cell-cell interfaces. Since Ft pathway activity depends on the arrangement of Ft-Ds bonds between adjacent cells, cell divisions could potentially affect polarization (and consequently proliferation) in the disc. Therefore, a realistic model of Ft-Ds binding in the wing disc needs to address the behavior of Ft-Ds bonds when cells divide.

2.6 The model

We have developed a model of growth and polarization in the wing disc in which cells form Ft-Ds bonds with their neighbors and proliferate. In this model, the Fj and Ds concentration profiles are steep sigmoid curves rather than straight, graded lines, consistent with observations of the disc. The border of the wing pouch, where Fj and Ds are most

steeply graded, sweeps outward through the disc over time. The changing expression rates of Fj and Ds are determined by a growing morphogen concentration (corresponding roughly to Dpp and Wg) that has a maximum at the center of the disc and decays exponentially in the radial direction. The fundamental elements of the model are cells that grow and divide in response to the level of the morphogen concentration as well as the asymmetry of the distribution of Ft-Ds bonds around their periphery. The steeper the Fj and Ds gradients are, the more asymmetric the bond distribution and the greater the cell growth.

When the disc is small, nearly all of the cells are in the vicinity of the steep gradients of the transition region. As the disc grows, the transition region sweeps over many cells, adding them to the Fj-expressing wing pouch. However, cells continue to have polarized Ft-Ds bonds and grow because they retain a memory of their previous environment. Only a small fraction of the Ft-Ds bonds are broken and formed at each simulation time step, corresponding to one minute of real time. This means that the bond distribution on a cell changes over the course of hours, comparable to the time scale of the front's movement or of cell proliferation. (We refer to the moving transition region as the "front". In the simulation the front is an expanding circle.) By defining cell polarization in terms of the side with the least amount of bound Ft, since that is the side where Dachs is observed to localize, we find that our model reproduces the observed proximal-distal cell polarization.

We tested the validity of our model by showing that it reproduces not only the relatively uniform growth seen in wild-type discs, but also the observed growth under disc-wide overexpression or underexpression of Dpp, Ft, Ds, and Fj [9, 13, 15, 16, 18, 51, 84–86, 94]. Similarly, it reproduces the nonautonomous growth observed around the boundaries of clones that overexpress Ds or Fj, or that have artificially high morphogen signaling [9, 44]. It also reproduces the phenotypes produced by mutants that just express the intracellular or extracellular domains of Ft [86].

Our model yields two major results: first, that the movement of this transition region alone is sufficient to induce proximal-distal polarization in the cells that it passes over;

second, that this polarization can be retained over multiple cell cycles. Together, these results mean that cells throughout the wing pouch have similar degrees of Ft-Ds bond asymmetry, and therefore similar polarizations and growth rates, as seen experimentally.

Chapter 3: Methods

In this chapter, we describe the model itself. We begin by reviewing the problems we wish to address, giving an overall direction for the model. We then explain how the cells in our model form a single layer without substantial gaps or overlaps while also growing and dividing. Next, we describe how the model keeps track of which cells are adjacent, and how it updates this information efficiently when a cell divides. We explain how cells in the model keep track of their amounts of morphogen, Ft, Ds, and Fj, and how those proteins interact. We describe the few stochastic aspects of the model. We give an expression for the growth rate of each cell and show how it is determined from morphogen signaling and Ft-Ds binding. We describe our metric for cell polarity based on Dachs localization. Finally, we summarize the information that the model uses as input and output.

3.1 Overview

While there has been speculation regarding the effects of Ft-Ds bond asymmetry on cell proliferation [9, 56, 81, 105, 106], there is a dearth of quantitative models that explicitly incorporate the formation and dissolution of Ft-Ds bonds. Here, we outline a model for individual cells that grow, proliferate, and form Ft-Ds bonds with their neighbors. This model needs to allow us to investigate how the Ft-Ds bond arrangement around a cell is affected by changes in Fj and Ds expression and in the cell's set of neighbors. Because the disc epithelium consists of a single layer of cells, and Ft-Ds binding occurs in roughly a single plane, our model is two-dimensional, representing a cross-section of every cell in the disc. Because a cell's set of neighbors changes over time due to cell division, and because Ft-Ds binding must by necessity involve pairs of adjacent cells, the model needs to track each cell's set of neighbors and update these sets as the cells grow and divide. The model should also allow us to alter the expression patterns and the effects of morphogen, Ft, Ds,

and Fj, either throughout the disc or in one part of it, so that we can replicate various experiments on the wing disc.

Our model is a C++ simulation of cells that can interact, grow, and divide. Its main feature is that it tracks individual Ft-Ds bonds between adjacent cells, and keeps this information updated as the cells proliferate and rearrange. To this end, each cell in the simulation tracks both a set of several neighboring cells and a set of bonds with each of those neighbors. Because cells track their neighbors, they can stay in a single contiguous group without substantial gaps or overlaps between neighbors, much like a cross-section of the actual disc. Since cells in the wing disc generally do not retain the same set of neighbors as they grow and proliferate, our model also needs to allow for changes in a cell's neighbor set over time. These neighbor sets are vital for our simulation of Ft-Ds binding. Because Ft-Ds bonds are formed between adjacent cells, and the arrangement of these bonds affects a cell's growth rate, we cannot form these bonds or accurately model growth without knowing which cells are adjacent. This model, then, will allow for realistic changes in a cell's set of neighbors, the arrangement of its Ft-Ds bonds, and its growth rate.

3.2 Bulk interactions

Cells in the wing disc adhere to their neighbors and form a single layer without substantial gaps or overlaps between adjacent cells. The cells in our model, then, should behave similarly: they should exert forces on their neighbors and arrange themselves such that adjacent cells are just touching. Since the cells in the disc are roughly cylindrical, each cell in the simulation is represented by a circle: a radius and a center with a given position. The simulation then represents a cross-section of the disc.

3.2.1 Intercellular forces

One subroutine in the simulation is responsible for updating the acceleration of a cell given its location with respect to its neighbors. It steps through each neighbor of the given cell, calculating the distance between the center of the cell and the center of the neighbor. Thus, for two cells whose centers are at (x_1, y_1) and (x_2, y_2), the distance d between the centers is:

$$d = \sqrt{(x_2 - x_1)^2 + (y_2 - y_1)^2} \tag{3.1}$$

If two neighboring cells are separated by a gap, they will attract; if they are overlapping, they will repel (Figure 3.1). The equilibrium distance from a cell's center to the edge it shares with a given neighbor is equal to the cell's radius. Thus, the equilibrium separation d_{eq} between the centers of two neighboring cells is

$$d_{eq} = r_1 + r_2 \tag{3.2}$$

where r_1 and r_2 are the radii of the two cells; in other words, the cells are at equilibrium if their edges are just touching. If the distance between these two cells is greater than d_{eq}, the two cells are separated by a gap and should attract. If the distance is less than d_{eq}, the cells are overlapping and should repel. The force between the cells should be zero if the cells are just touching at the edge—in other words, if $d = d_{eq}$.

For the sake of simplicity, we treat all the cells as having the same mass, so a cell's acceleration only depends on the sum of the forces on it. The base acceleration $\vec{a}$ is then calculated given the distance between the two cells. For adjacent cells with a gap between them (i.e., when $d > d_{eq}$), a Lennard-Jones-like force is used:

$$|\vec{a}| = -C_{gap}\left(\frac{d_{eq}^6}{d^7} - \frac{d_{eq}^{12}}{d^{13}}\right) \tag{3.3}$$

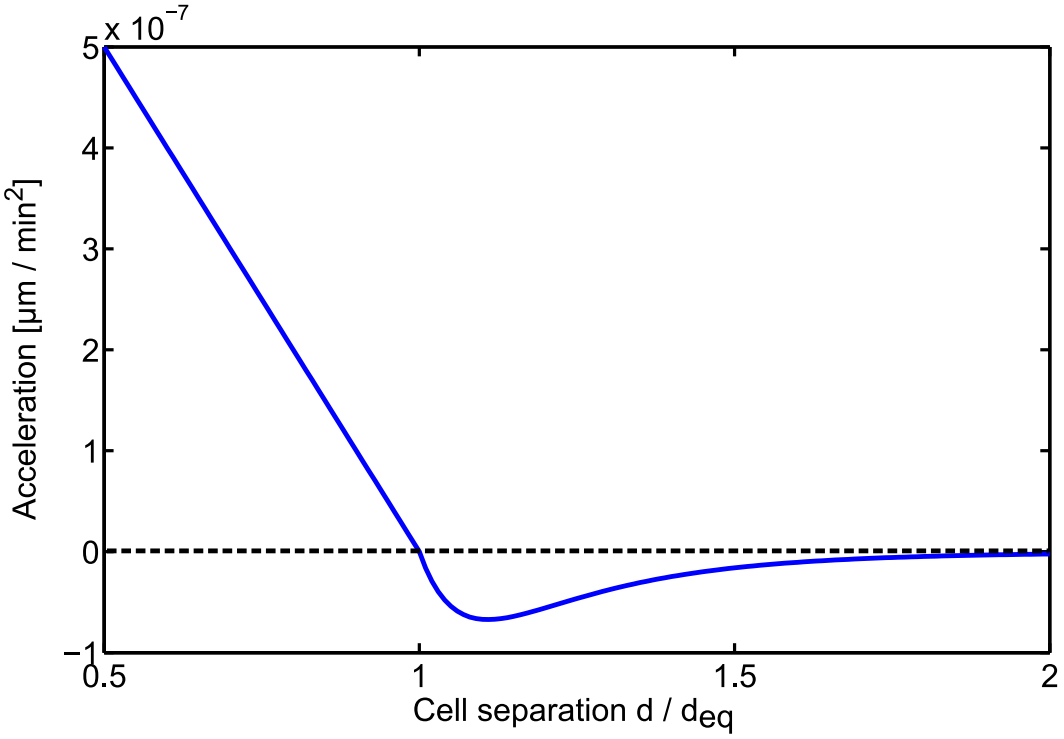

Figure 3.1: The acceleration of a cell as a function of its distance from its neighbor d/d_{eq}. Here, d is the distance between the centers of the cells and d_{eq} is the sum of the radii of the cells. Cells attract (negative acceleration) when they have a gap between them ($d > d_{eq}$) and repel (positive acceleration) when they overlap ($d < d_{eq}$). Note that the acceleration is zero when the cells are just touching ($d/d_{eq} = 1$) and when the cells are very far from one another ($d/d_{eq} \to \infty$).

Overlapping cells ($d < d_{eq}$) repel with a Hookean force:

$$|\vec{a}| = C_{over}(d_{eq} - d) \tag{3.4}$$

Here, C_{gap} and C_{over} are constants; C_{gap} is 3×10^{-7} μm^2 min^{-2}, and C_{over} is 1×10^{-6} min^{-2}. The overall acceleration is plotted in Figure 3.1. Note that in both cases, acceleration is zero when $d = d_{eq}$. We use a Hookean force rather than a Lennard-Jones force for overlapping cells because the springlike force does not approach infinity for small distances between cells. Because cells proliferate and the simulation uses discrete time steps, there is a small chance that cells will suddenly substantially overlap without the opportunity to

repel one another first. Furthermore, cells in the wing disc can deform when compressed, allowing adjacent cells to be closer than their equilibrium separation, so this approach is realistic.

The x and y components of this acceleration are calculated given the relative positions of the original cell and its neighbor. For example, if the cells are separated only in the x direction, then the acceleration will only have an x component. These components are then summed over all the cell's neighbors to yield the total acceleration of the cell at this time step.

This acceleration, $\vec{a}_{raw}$, is used by a second subroutine, which updates the cell's velocity and actually moves the cell. First, a drag term γ (equal to 2×10^{-3} min^{-1}) is applied to the newly calculated acceleration to damp out oscillations:

$$\vec{a}_{n+1} = \vec{a}_{raw} - \gamma \vec{v} \tag{3.5}$$

where $\vec{v}$ is the cell's current velocity. This new acceleration $\vec{a}_{n+1}$ is then used along with the acceleration $\vec{a}_n$ from the previous time step to find the new position and velocity using leapfrog integration [110]:

$$\vec{x}_{n+1} = \vec{x}_n + \vec{v}_n \Delta t + \frac{\vec{a}_n}{2}(\Delta t)^2 \tag{3.6}$$

$$\vec{v}_{n+1} = \vec{v}_n + \frac{\vec{a}_n + \vec{a}_{n+1}}{2}\Delta t \tag{3.7}$$

Here, $\vec{x}_{n+1}$ and $\vec{v}_{n+1}$ are the new values of position and velocity for step $n+1$, while $\vec{x}_n$ and $\vec{v}_n$ are the values of position and velocity at step n. The time step Δt is 1 minute. The cell is then updated with this new position and velocity.

3.2.2 Cell division

A cell grows by increasing its equilibrium size, pushing its neighbors back. A cell's probability of dividing during any given time step is determined by its area:

$$P(\text{division}) = \frac{1}{1 + \left(\frac{\pi r^2}{A_c}\right)^n} \tag{3.8}$$

where r is the cell's radius, A_c is a critical area of 4π μm^2, and the exponent n is 100. Thus, a cell becomes increasingly likely to divide as its area approaches A_c.

To find the angle at which a cell divides, we find the cell's single closest neighbor (in terms of distance between centers) and its angular position (i.e., the angle associated with a vector drawn from the dividing cell's center to the center of the nearest neighboring cell), then set the division plane at that angle. Thus, cells with an elongated shape will tend not to divide lengthwise, consistent with observed results [99]. When the cell divides, the neighbor lists of the daughter cells are rebuilt. The radii of the daughter cells are chosen such that each one has half the area that its progenitor did when it divided. These radii are then each adjusted by a small amount (randomly chosen between -1% and +1%) so that the areas are slightly different. This prevents entire clones of cells from dividing at nearly the same time.

3.3 Building the neighbor list

When the simulation is launched, the full neighbor list must be determined. The neighbor list does not need to be entirely rebuilt at every time step, since the cells in the simulation do not rearrange substantially except to accommodate their neighbors' growth and proliferation. (This also appears to be the case experimentally, as suggested by the distribution of the neighbor counts of cells in a tissue [59, 111]). However, cells do move with respect to one another fast enough that the neighbor list must be rebuilt occasionally.

The main loop of the program keeps track of how fast its cells are moving as well as the number of time steps since the neighbor list was last rebuilt. Whenever enough time steps have passed that a cell can have moved a distance equal to 0.2 times the average cell radius at that time step, or if 10 time steps have passed since the list was rebuilt, then the entire neighbor list will be rebuilt.

Furthermore, a cell's set of neighbors can change when it or an adjacent cell divides. So a cell that divides will need to partition its neighbors between the two daughter cells. Thus, the simulation is also written to handle rebuilding the neighbor list for a small subset of the disc's cells (i.e., those adjacent to a cell that has just divided), and then reintegrating the results into the main neighbor list. This improves the running time by avoiding rebuilding the full list every time a cell divides, which can happen many times per time step when the disc is large.

3.3.1 Delaunay triangulation

The neighbor list is built by a separate routine that constructs a Delaunay triangulation given a set of points in two dimensions. A Delaunay triangulation is a mesh of triangles drawn on a set of vertices such that no triangle's circumscribed circle contains any other vertex besides the three used to construct it (Figure 3.2). Here, each point represents the center of a cell, and only pairs of points (i.e., cells) connected by an edge are considered neighbors. When the neighbor list must be rebuilt, the program steps through the list of cells and stores the coordinates and label of each one together. The resulting data structure then passed to a separate function, which builds a triangulation recursively [112]. The algorithm works as follows:

- If there is only one vertex, no edges need to be constructed. If there are exactly two vertices, draw an edge between them. If there are three vertices, draw three edges to form a triangle. This is the base case.

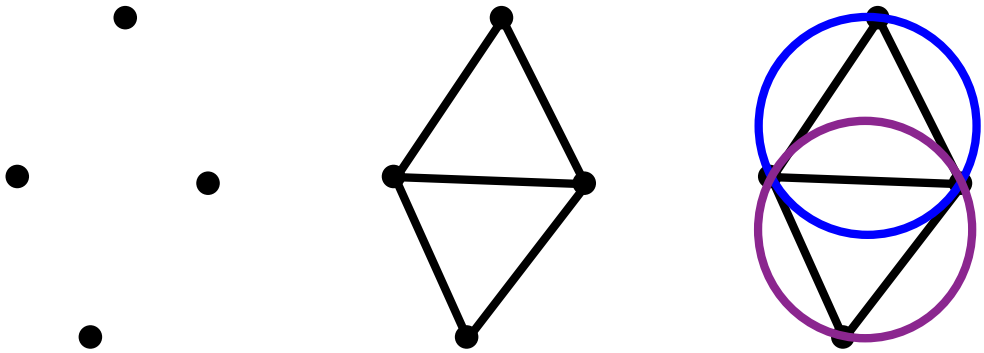

Figure 3.2: An example of a Delaunay triangulation. The four points are connected by edges (line segments) to form a mesh of triangles. Note that the circumscribed circle of each triangle contains no points besides the three used to construct the triangle: the blue circle does not contain the bottom point, and the purple circle does not contain the top point. Only pairs of points connected by edges are added to the neighbor list. In this example, the top and bottom points would not be considered neighbors, but every other pair of points would be.

- If there are more than three vertices, separate the vertices evenly into two sets by x-coordinate, leaving a left and a right half. (If there is an odd number of vertices, we allow the right half to have one more vertex than the left half.) Recursively, i.e., using this algorithm, build a triangulation from each half.

- To merge the left and right halves, first draw the bottom-most edge connecting the halves that lies on the overall convex hull of all the points. (The convex hull is the convex polygon made by connecting all of the outermost points; it contains all of the points.) In other words, all points on both halves of the triangulation should lie on only one side of this edge. We call this the "base edge" and its vertices A and B (Figure 3.3, panel 1).

- The next edge connecting the two triangulations will connect one vertex of the base edge with a vertex that is adjacent to the base edge's other vertex. In other words, if the vertices of the current base edge are labeled A and B, the next edge will either connect A with a neighbor of B, or connect B with a neighbor of A. This edge must not intersect any existing edges. In addition, the triangle formed by A, B, and this

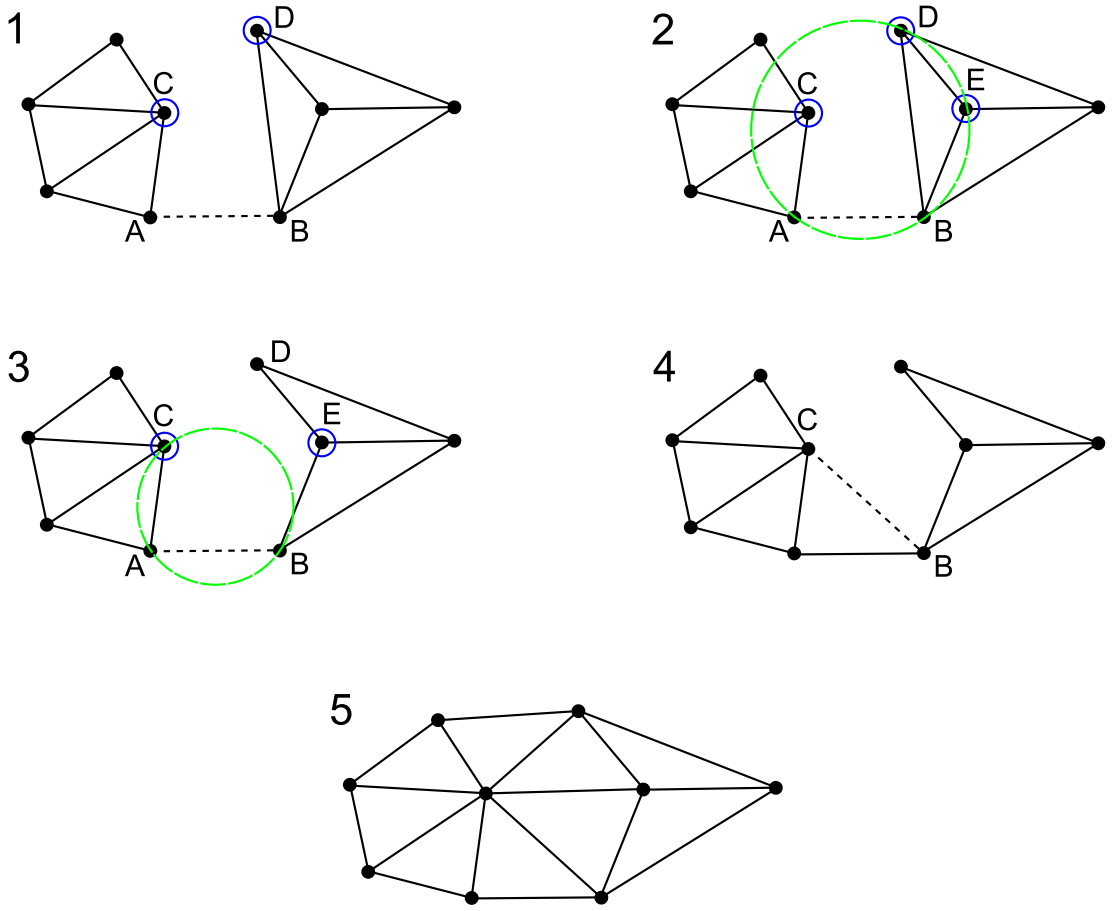

Figure 3.3: The Delaunay triangulation divide-and-conquer algorithm, based on [112]. (1) The base edge $\overline{AB}$ is chosen (dotted line). Note that all other vertices lie to one side of (in this case, above) this edge. (2) Candidate vertices C and D are chosen (circled in blue). C is the next neighbor of A going counterclockwise from the base edge, and D is the next neighbor of B going clockwise from the base edge. However, the next right-side candidate E lies within the circle (green) circumscribing the triangle $\triangle ABD$. (3) The edge $\overline{BD}$ is deleted and E becomes the new right-side candidate. The circle circumscribing the triangle $\triangle ABC$ does not contain the candidate E (while the circle circumscribing $\triangle ABE$ would contain C). (4) The candidate C is then chosen, $\overline{BC}$ is drawn and becomes the new base edge, and the process is repeated until neither side returns a suitable candidate. (5) The completed triangulation.

chosen vertex must contain no other vertices within its circumscribed circle (i.e., it must satisfy the main Delaunay condition). There should be no more than one vertex that fulfills all these conditions; there may be none.

- Find candidate vertices for this next edge. Check each neighbor of A and B, in ascending order of angle made with the base edge. Exclude any neighbors that lie below the base edge. If the triangle formed by the base edge and the current candidate contains the next candidate within its circumscribed circle, delete the edge between the candidate and its base vertex, then move on to the next candidate (Figure 3.3, panel 2). Otherwise, choose this candidate and move on. Do this for both the left and right sides. It is possible for a side to have no candidates.

- Choose the next step depending on whether two, one, or zero candidates have been selected:

  - If each side chooses a candidate, say C and E, look at the triangles formed by each candidate and the base edge. If the circumscribed circle of triangle ABC does not contain E, choose C; otherwise, choose E (Figure 3.3, panel 3). Draw an edge between the chosen candidate and the vertex of the base edge lying on the other side of the triangulation. This edge becomes the new base edge and the process is repeated (Figure 3.3, panel 4).
  - If only one side chooses a candidate, an edge is drawn from it to the vertex of the base edge that lies on the other side of the triangulation. This edge becomes the new base edge and the process is repeated.
  - If no candidate is found from either side, the two triangulations are now fully merged (Figure 3.3, panel 5).

- The process continues recursively, building and merging triangulations. Once all merges are finished, the resulting triangulation represents the complete neighbor list.

3.3.2 Building a subset of the list

Whenever a cell divides, the two daughter cells will likely have different sets of neighbors. To update the neighbor list efficiently, the main program sends the locations of the daughter cells as well as those of all the mother cell's original neighbors to the triangulation subroutine. The resulting neighbors are then integrated into the main neighbor list. Because cell divisions happen frequently, building only a small subset of the neighbor list then splicing this subset into the main list greatly lowers the running time compared to rebuilding the full list every time a cell divides.

A dividing cell will generally not retain the same set of neighbors that it had before division. The mother cell's neighbors are either shared between the two daughter cells or are retained by only one of the two daughter cells (Figure 3.4). Because each pair of neighboring cells is associated with a number of Ft-Ds bonds, these bonds must be accounted for each time a cell divides. When a cell divides, it becomes one of the two daughter cells (retaining its old numerical index) and a new daughter cell with a new index is created. Thus, several scenarios are possible for each neighbor of a dividing cell:

- If a neighbor stays with the original mother cell and is not shared with the newly created daughter, no action is necessary. Its bound Ft and Ds are retained.

- If a neighbor of the mother cell is now a neighbor of both daughters, its bound Ft and Ds are split evenly between the two. In other words, half the Ft-Ds bonds that this cell had with the mother cell are transferred to the new daughter cell. The other half are retained by the mother cell.

- If a neighbor of the mother cell is now only a neighbor of the newly created daughter, the Ft-Ds bonds between the mother and that neighbor are all transferred to the daughter.

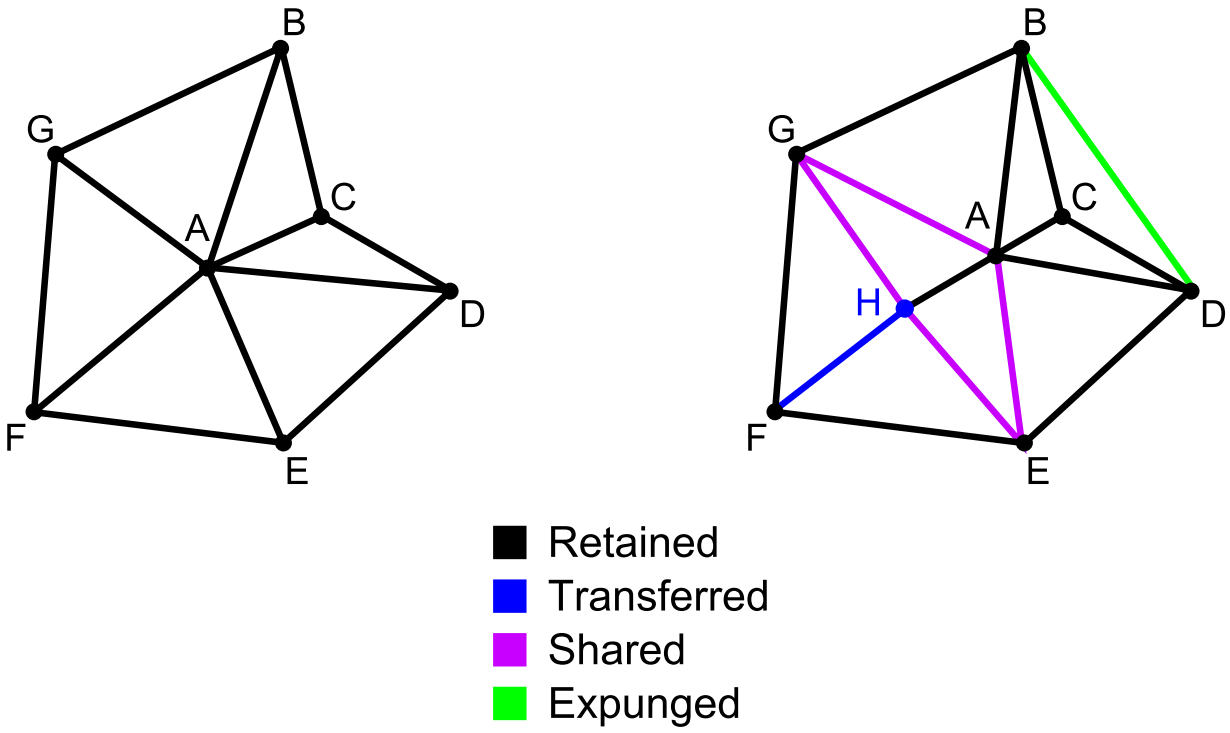

Figure 3.4: Partitioning the neighbors of a newly divided cell. Here, each of the labeled vertices represents the center of a cell, and the line segments correspond to neighbor pairs in the triangulation. Cell A has six neighbors, labeled B through G (left diagram). A divides and gives rise to H. The positions of these two cells, along with those of A's neighbors, are passed to the triangulation algorithm. The resulting neighbors may correspond to the preexisting set of neighbors and be retained (shown in black), or they may represent one of the mother cell's neighbors being transferred to the daughter cell (F, blue) or shared between the two daughter cells (E and G, violet). In addition, there is a chance that the algorithm will consider two non-adjacent neighbors of the mother (B and D) to be neighbors of one another (green), even though they are not adjacent in the context of the entire disc. Such neighbor pairs will be expunged before this set of neighbors is reintegrated into the main neighbor list.

- If a neighbor pair is formed between cells that are neither the mother nor daughter (and this pair is not already part of the main neighbor list), it is expunged, as these two cells are not actually adjacent. No action involving Ft and Ds is necessary, since the neighbor list has not changed.

3.4 Ft-Ds-Fj kinetics

Here, we discuss the expression of Ft, Ds, and Fj, as well as the formation and dissolution of Ft-Ds bonds between adjacent cells. The asymmetry of the distribution of these bonds around a cell contributes to the cell's growth rate and polarity.

3.4.1 Initial conditions

In the model, Dpp and Wg are conflated into a single quantity that we call the morphogen. When the simulation starts, each cell is given values for its starting amounts of morphogen, Ft, Ds, and Fj. The morphogen concentration decays exponentially with radial distance r from the center of the wing disc; it is greatest in the center of the disc. The most important feature of the morphogen profile in this model is that the amount of morphogen signaling in any given cell increases over time. We see similar results regardless of whether the decay length remains constant or scales with the size of the disc. The amplitude of the profile increases over time, and the decay length is fixed at 20 μm. The morphogen concentration as a function of time and position is given by

$$[M(x,t)] = C_0 e^{\left(\frac{t}{t_0} - \frac{Ar}{R}\right)} \tag{3.9}$$

Here, $[M(x,t)]$ is the morphogen concentration, and $C_0 = 1.5$ is the starting morphogen amplitude. t is the number of the current time step (starting with 0) and $t_0 = 1200$ time steps (1200 minutes) represents the length of time over which the morphogen concentration

increases by a factor of e at a given point. r is the distance from the disc's center in μm, R is the radius of the disc in μm, and A is a constant, set to 4. This means that the decay length of the morphogen (i.e., the distance over which the morphogen concentration decreases by a factor of e) is 1/4 the radius of the disc, and scales as the disc grows.

Each cell is also given a starting pool of $\mathrm{Ft}_{max} = 1 \times 10^3$ Ft. The starting amounts of Ds and Fj are based on the cell's amount of morphogen:

$$\mathrm{Ds}_{initial} = A_{Ds,initial}\left(\mathrm{Ds}_{min} + \mathrm{Ds}_{range}\left(\frac{1}{1+\left(\frac{[M]}{[M]_c}\right)^n}\right)\right) \tag{3.10}$$

Here, $\mathrm{Ds}_{initial}$ is the number of Ds proteins that the cell initially has. $A_{Ds,initial}$ is a constant coefficient of 1×10^3, Ds_{min} is 0.2, and Ds_{range} is 0.8. $[M]$ is as calculated in Equation (3.9), $[M]_c$ is a constant critical morphogen concentration of 0.5, and the exponent n is 10. This causes cells with higher concentrations of morphogen (those near the disc's center) to have less Ds and cells with less morphogen (those near the disc's edge) to have more Ds. The reverse is true of Fj:

$$\mathrm{Fj}_{initial} = \mathrm{Fj}_{max} - (\mathrm{Fj}_{range})\left(\frac{1}{1+\left(\frac{[M]}{[M]_c}\right)^n}\right) \tag{3.11}$$

where $\mathrm{Fj}_{initial}$ is the initial Fj concentration. Here, Fj_{max} is 0.8 and the Fj range is 0.6. Under normal circumstances, then, cells in the disc will have starting Fj values between 0.2 and 0.8. This allows us to introduce values of Fj that are outside the normal range, such as for cells that are missing Fj or that overexpress it. In the case of discs or clones that express no Fj, $\mathrm{Fj}_{initial}$ is directly set to 0. Discs or clones that overexpress Fj have $\mathrm{Fj}_{initial}$ set to 1.

The overall result for a wild-type disc is an exponential morphogen profile, and two sigmoid profiles of Fj and Ds. Fj is expressed at high levels in the wing pouch and low levels in the wing periphery. The Ds profile is complementary to that of Fj. Both profiles

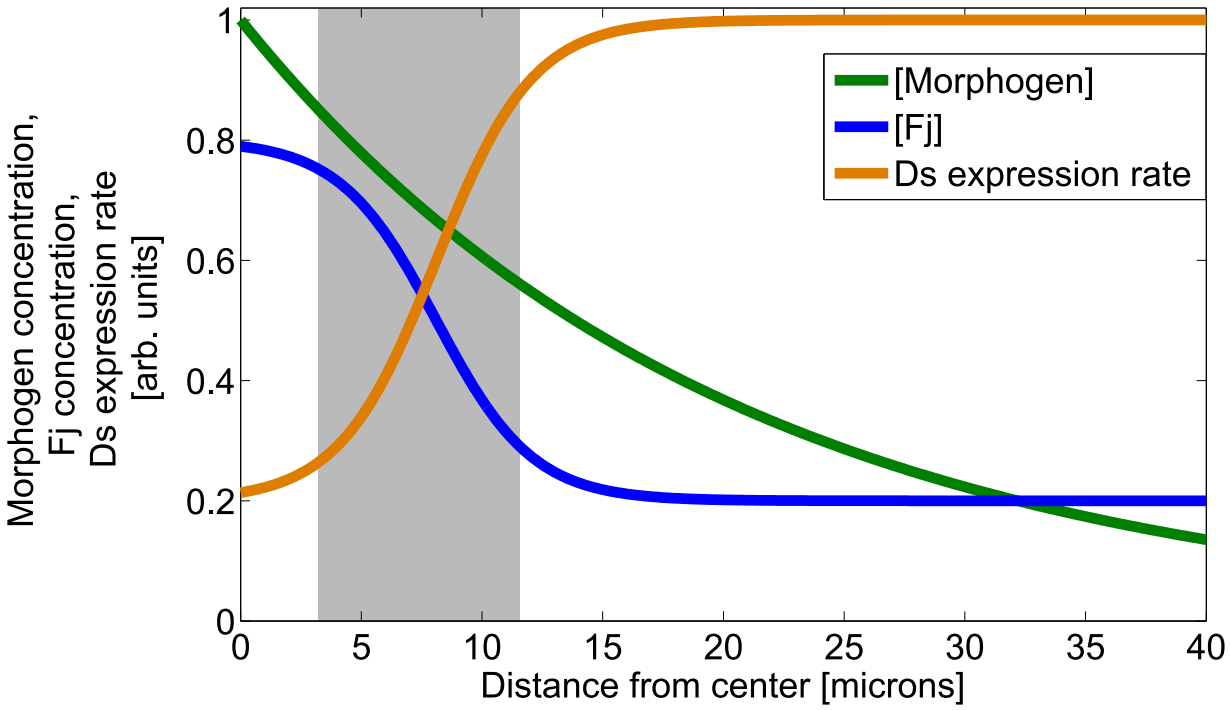

Figure 3.5: Sample morphogen and Fj amounts and Ds production rate as a function of distance from the disc's center. The morphogen concentration decays exponentially with radial distance. The Fj and Ds expression levels are functions of the local morphogen concentration, with Fj mostly near the disc's center (where the morphogen concentration is high) and Ds mostly near the disc's edge (where the morphogen concentration is low). Note that the Fj and Ds profiles are most steeply graded in a narrow transition region (shaded area) partway between the disc's center and its edge, corresponding to the boundary of the prospective wing blade. The initial radius of the disc is about 40 μmin our simulations.

are fairly flat in the wing pouch and the periphery, with a steep transition region at the edge of the wing pouch (Figure 3.5).

Not all of a cell's Ft and Ds proteins will necessarily form Ft-Ds bonds. The pools of free Ft and Ds associated with each cell are further divided into "bindable" and "unbindable" pools. Because phosphorylation by Fj makes Ft more likely and Ds less likely to bind [55,56], the bindable Ft pool and the unbindable Ds pool will be larger at higher concentrations of Fj, and vice versa. The fraction of starting bindable Ft is:

$$\frac{\text{initial bindable Ft}}{\text{initial total Ft}} = C_1(1 - P_{\text{base}}) + P_{\text{offset}} \tag{3.12}$$

Similarly, the fraction of starting bindable Ds is:

$$\frac{\text{initial bindable Ds}}{\text{initial total Ds}} = C_2 P_{\text{base}} + P_{\text{offset}} \tag{3.13}$$

Here, C_1 and C_2 are both set to 0.8. P_{offset}, set to 0.1, represents the fraction of bindable Ft or unbindable Ds in the absence of Fj. Thus, the bindable fractions range from P_{offset} to $C_1 + P_{\text{offset}}$ (for Ds), or from P_{offset} to $C_2 + P_{\text{offset}}$ (for Ft). In other words, both fractions range from 0.1 to 0.9. The base probability P_{base} is lower at high Fj concentrations:

$$P_{\text{base}} = \frac{1}{1 + \left(\frac{\text{Fj}}{\text{Fj}_c}\right)^n} \tag{3.14}$$

Here, Fj is the cell's amount of Four-jointed, Fj_c is a critical quantity of Four-jointed (set to 0.3), and the exponent $n = 2$ determines the steepness of the dependence.

Once amounts of Fj and bindable and unbindable Ft and Ds are established for each cell, the Ft-Ds binding algorithm is run once, so each cell begins the simulation proper with a set of Ft-Ds bonds. As the simulation continues, the number and distribution of these bonds can change.

3.4.2 Updating Ft, Ds, and Fj

During each time step, new Fj and free Ft and Ds can be expressed and degrade, Ft-Ds bonds can form and dissolve, and free Ft and Ds can become phosphorylated or unphosphorylated, depending on the local Fj concentration. Only phosphorylated Ft and unphosphorylated Ds can form bonds in the model. The Fj and Ds expression rates remain dependent on the amount of morphogen in a cell.

At each time step, a cell's concentration of morphogen is updated based on its radial position within the disc and the number of the current time step using Equation (3.9). All cells have the same constant production and degradation rates of free Ft, since Ft is

uniformly expressed in the wing disc compared to Ds and Fj [17, 19]. Ft can also bind and unbind with Ds. The rate of change of free Ft is given by:

$$\frac{\partial(\text{free Ft})}{\partial t} = R_{Ft} - k_{d,Ft}(\text{free Ft}) - \frac{\partial(\text{bound Ft})}{\partial t} \tag{3.15}$$

R_{Ft} is the rate of Ft expression, 20 molecules per time step (i.e., molecules per minute); the degradation rate $k_{d,Ft}$ is 0.08 min^{-1}. The process of Ft-Ds binding and unbinding is described in the next section.

The production rate of free Ds is based on a cell's amount of morphogen such that Ds expression is highest near the edge of the disc. Ds can bind and unbind, and free Ds can degrade:

$$\frac{\partial(\text{free Ds})}{\partial t} = R_{Ds,max}\left(\text{Ds}_{min} + \text{Ds}_{range}\left(\frac{1}{1+\left(\frac{[M]}{[M]_c}\right)^n}\right)\right) - k_{d,Ds}(\text{free Ds}) - \frac{\partial(\text{bound Ds})}{\partial t} \tag{3.16}$$

$R_{Ds,max}$ is the maximum rate of Ds production; it is set to 20 molecules per time step. Ds_{min}, Ds_{range}, $[M]$, $[M]_c$, and n are as in Equation (3.10). Thus, cells near the center of the disc will have a high amount of morphogen and their rate of Ds production will be low, while cells closer to the edge will have less morphogen and express Ds faster. Free Ds also degrades at a rate $k_{d,Ds}$ is 0.08 per time step, like Ft. Ds, like Ft, can also be bound or unbound.

The production rate of Fj depends on a cell's amount of morphogen, giving rise to a plateau of high expression in the center of the disc and a plateau of low expression at the edge:

$$\frac{\partial(\text{Fj})}{\partial t} = R_{Fj,max}\left(\text{Fj}_{max} - \text{Fj}_{range}\left(\frac{1}{1+\left(\frac{[M]}{[M]_c}\right)^n}\right)\right) - k_{d,Fj}(\text{Fj}) \tag{3.17}$$

Again, $[M]$, $[M]_c$ and n are as in Equations (3.10) and (3.11). The constants Fj_{max} and Fj_{range} are as in Equation (3.11). $R_{Fj,max}$ is the maximum rate of Fj production, set to

1.05 min^{-1}. The degradation rate $k_{d,Fj}$ is 0.05 min^{-1}. Unlike Ft and Ds, the amount of Fj is not an integer in our model; it is normally between 0 and 1.

As in the initial conditions, newly expressed free Ft and Ds are immediately divided into bindable and unbindable pools using the same ratios as in Equations (3.12) and (3.13), with "new bindable Ft/Ds ÷ total new Ft/Ds" in place of "initial bindable Ft/Ds ÷ initial total Ft/Ds". The same degradation rate applies to both bindable and unbindable free Ft and Ds each time step. Ft and Ds proteins that are newly freed (i.e., from a bond that was just dissolved) are all considered bindable and move to their respective bindable pools. As a separate mechanism, Ft and Ds can also move between the bindable and unbindable pools depending on Fj activity:

$$\frac{\partial(\text{bindable Ft})}{\partial t} = A[(C_1(1 - P_{\text{base}}) + P_{\text{offset}})(\text{unbindable Ft}) - D(\text{bindable Ft})] \quad (3.18)$$

Note that this only describes the phosphorylation and dephosphorylation of existing Ft, and is handled separately from Ft expression and degradation. Here, A is the fraction of bindable or unbindable Ft that can change pools in a single time step, set to 0.016 min^{-1}. C_1, P_{base}, and P_{offset} are as in Equations (3.12) and (3.14). D is a dephosphorylation rate for bindable Ft, set to 0.08 min^{-1}. Recall that P_{base} is low when the Fj concentration is high, and vice versa. This means that unbindable (unphosphorylated) Ft becomes bindable (phosphorylated) Ft at a rate that increases with the Fj concentration. The rate of change of unbindable Ft is simply the negative of this equation.

Ds behaves similarly, but now unphosphorylated Ds is bindable:

$$\frac{\partial(\text{bindable Ds})}{\partial t} = A[D(\text{unbindable Ds}) - (1 - (C_2 P_{\text{base}} + P_{\text{offset}}))\,(\text{bindable Ds})] \quad (3.19)$$

C_2, P_{base} and P_{offset} are again as in Equations (3.12), (3.14), and (3.13). The greater the Fj concentration, the lower the P_{base}, and the faster the decrease in bindable Ds due to

phosphorylation. A, the fraction of bindable or unbindable Ds that can change pools, and D, the dephosphorylation rate, are the same as in Equation (3.18). Again, this equation only applies to existing Ds and does not include Ds expression and degradation. The rate of change of unbindable Ds is the negative of this equation.

3.4.3 Binding algorithm

We now describe the algorithm by which Ft, Ds and Fj interact to form bonds. The following process is run for all cells during each time step:

- Unbind a certain fraction of all bound Ft and bound Ds, specifically 0.08. If either number (0.08 times the number of bound Ft or Ds) is less than 1, use it instead as the probability of undoing a single bond.

- Degrade a certain fraction of all free Ft and Ds, specifically $k_{d,Ft} = k_{d,Ds} = 0.08$. If this number (0.08 times the number of free Ft or Ds) is less than 1, use it instead as the probability of degrading one Ft or Ds.

- Handle phosphorylation and dephosphorylation of free Ft and Ds by Fj based on Equations (3.18) and (3.19) above. If less than 1 free Ft or Ds is to be phosphorylated or dephosphorylated, use this number instead as the probability of phosphorylating or dephosphorylating a free Ft or Ds.

- Degrade a certain fraction, specifically $k_{d,Fj} = 0.05$, of the cell's Fj.

- Update the morphogen concentration based on the cell's position within the disc and the current time step, using Equation (3.9).

- Produce new (free) Ft and Ds, as well as new Fj. The Ft production rate is constant, and the Ds and Fj production rates depend on the morphogen level, as shown in Equations (3.16) and (3.17).

- Separate the newly expressed free Ft and Ds into bindable and unbindable pools. $(1 - P_{\text{base}}) + P_{\text{offset}}$ of the free Ft pool becomes bindable (i.e., phosphorylated), and $P_{\text{base}} + P_{\text{offset}}$ of the free Ds pool becomes bindable (i.e., unphosphorylated). P_{base} is given in Equation (3.14). If the amount of Ft or Ds entering either pool is less than 1, use this number instead as the probability of moving a single Ft or Ds into this pool.

- Now iterate over each neighbor on each cell:

  - If the cells are too far apart, do not count them as adjacent for purposes of Ft-Ds binding. (In certain cases, the Delaunay triangulation algorithm can make cells near the disc's edge neighbors even when they are not touching.) In particular, if the edges of the cells are separated by a gap of at least 0.8 μm, skip this neighbor pair and move on.

  - Note the current number of available (i.e., bindable) free Ft and Ds on this cell and its neighbor.

  - Make sure this neighbor pair has not already been dealt with on the current pass. If it has, move to the next neighbor.

  - Determine how much of the available Ft and Ds on this cell to allot to this neighbor and how much of the available Ds and Ft on the neighbor to allot to this cell. Each cell divides its number of bindable Ft and Ds by its number of neighbors to determine the number to allot to each neighbor. Thus, a cell will not risk binding more Ft or Ds than it has. When this quantity is calculated for a cell's Ft, a complementary quantity is calculated for the neighboring cell's Ds and vice versa.

  - Form as many new bonds as possible. The number of Ft that becomes bound is the lesser of the bindable Ft on this cell allotted to this neighbor and the bindable Ds on the neighbor allotted to this cell. Similarly, the number of Ds

that becomes bound is the lesser of the cell's bindable Ds allotment and the neighbor's bindable Ft allotment.

- The newly bound Ft and Ds are then moved from the free to the bound pool on their corresponding cells.

Since this process is run for every cell at every time step, cells quickly bind as many of their Ft and Ds as possible. Note that the formation of new bonds at each time step is independent of the arrangement of existing bonds. In other words, a cell that already has many bound Ft with one neighbor does not show any special preference for that neighbor when binding additional Ft. Only the number of bindable Ft and Ds on each cell, along with the neighbor list, determines where new bonds are formed.

3.5 Nondeterministic aspects

Only a few minor aspects of the model are nondeterministic. The size at which a cell divides is not fixed; a cell's probability of dividing in a given time step is given by a Hill function that rises very steeply as the cell reaches a certain size. As mentioned earlier, the relative areas of the two daughter cells are distributed slightly unevenly to prevent their possible simultaneous division later. Ft-Ds kinetics (binding, unbinding, phosphorylation by Fj, expression, and degradation) are also handled stochastically when the number of proteins expected to change in a single time step is less than one. These aspects have little effect on the overall growth rate of the simulated disc, so the eventual size of the disc typically varies by less than 1% between runs.

3.6 Growth rate and adaptation

Here, we describe in detail the model for the growth rate of a cell, as well as the integral feedback mechanism that allows cells in our model to adapt to consistent signals.

The growth rate of a cell in our model depends on three factors: the distribution of its Ft-Ds bonds, its amount of morphogen signaling, and its number of leftover free Ft and Ds. The more asymmetrically distributed a cell's Ft-Ds bonds, the faster it grows. This asymmetry arises as a result of the spatially graded expression of Dachsous and Four-jointed. Experimentally, discs that express Ds or Fj uniformly are observed to undergrow, while discs with a single clone that overexpresses Ds or Fj show growth around the edge of the clone [9]. Thus, a cell whose bound Ft is distributed very nonuniformly among its neighbors should grow faster than a cell whose bonds are distributed evenly. Also, discs mutant for both Ft and Ds overgrow faster than discs mutant for only one or the other [86], suggesting that the number of free Ft and Ds should also affect the growth rate to some degree. In experiments, the disc also appears to adapt to consistently strong signaling both in and near a clone of cells with elevated Dpp signaling after multiple days [44]. This result suggests that the cells in the disc may use some form of integral feedback [103] to adapt to unchanging signaling, both from the morphogen and from Ft-Ds bond asymmetry. Here, then, is a model for cell growth that reflects all of these results.

At every time step, a cell grows by a certain ratio; that is, its new radius $r(t+1)$ becomes a certain multiple of its radius $r(t)$ at the previous time step:

$$\frac{r(t+1)}{r(t)} = 1 + G_0 \frac{(1 + C_M x_M(t))\,(1 + C_{Ft} x_{Ft}(t))\,(1 + C_{Ds} x_{Ds}(t))}{1 + U(t)} \tag{3.20}$$

G_0 is a unitless base growth rate of 4.4×10^{-4}. C_M, C_{Ft}, and C_{Ds} are unitless coefficients representing the relative strengths of the responses to morphogen signaling and to asymmetric bound Ft and Ds; they are equal to 40, 3000, and 3000, respectively. $x_M(t)$, $x_{Ft}(t)$, and $x_{Ds}(t)$ represent the disc's responses to morphogen signaling and asymmetry in Ft and Ds bonds, respectively, after applying integral feedback to represent adaptation (explained below). $U(t)$ is proportional to the number of leftover free (i.e., unbound) Ft and Ds; it is 3×10^{-5} times their sum.

In experiments, cells in the disc exhibit growth that is autonomously dependent on their amount of Dpp [23, 44]. Thus, the growth rate should be partially dependent on the morphogen concentration in each cell. Similarly, the growth rate should depend on the degree of asymmetry in a cell's Ft-Ds bonds. However, the autonomously elevated growth within clones of cells with artificially high Dpp signaling wanes over time, as does the nonautonomous effect near steep spatial gradients of Fj or Ds [9, 44]. Our model of growth, then, also allows for adaptation to a constant signal via integral feedback [103]. To do this, we consider a cell's "response" to morphogen signaling as separate from its instantaneous morphogen concentration. This response depends both on the local morphogen concentration and on its own time integral from the start of the simulation to the current time step.

We use $x_M(t+1)$ to represent the disc's response to morphogen signaling at time step $t+1$; it is given by

$$x_M(t+1) = G_M \left([M(t+1)] - \int_0^t x_M(\tau)\ d\tau \right) \tag{3.21}$$

where G_M is a constant parameter and $[M(t+1)]$ is the morphogen concentration given by Equation (3.9) at time step $t+1$. Note that if the morphogen concentration is constant, then x_M will decrease such that $\int x_M(\tau)\ d\tau$ will approach the same constant, and the instantaneous value of x_M will approach zero. The coefficient G_M, representing the speed with which the disc adapts to consistent morphogen signaling, is 2.8×10^{-2} min^{-1}. We choose this value so that the adaptation has a short characteristic time scale (less than an hour), meaning the growth rate is roughly proportional to the rate of change of morphogen concentration, as experimental evidence suggests [45].

Similarly, the simulated disc adapts to the degree of asymmetry in its bound Ft:

$$\text{Ft asymmetry} = 1 - S_F \tag{3.22}$$

$$x_{Ft}(t+1) = G_{Ft}\left(\text{Ft asymmetry}(t+1) - \int_0^t x_{Ft}(\tau)\ d\tau\right) \tag{3.23}$$

The same mechanism applies to the asymmetry of bound Ds:

$$\text{Ds asymmetry} = 1 - S_D \tag{3.24}$$

$$x_{Ds}(t+1) = G_{Ds}\left(\text{Ds asymmetry}(t+1) - \int_0^t x_{Ds}(\tau)\ d\tau\right) \tag{3.25}$$

The coefficients G_{Ft} and G_{Ds}, representing the speed with which the disc adapts to consistent asymmetry signaling, are both equal to 6×10^{-4} min^{-1}. Experimentally, the nonautonomously elevated growth around clones of cells with activated Tkv decreases with a characteristic time scale on the order of tens of hours [44], so we choose smaller values for G_{Ft} and G_{Ds} than for G_M. S_F and S_D are dependent on how symmetrically the cell's protocadherins are distributed, which we describe next.

3.7 The minimum fraction metric for symmetry

The quantities S_F and S_D are proportional to a cell's minimum fractions of bound Ft and Ds. To find the minimum fraction of bound Ft for S_F, for example, the cell checks each of its neighbors to find the minimum number of Ft proteins bound to any neighbor, then divides this amount by its total number of bound Ft. (In the event that the cell has no bound Ft whatsoever, it simply sets this fraction to zero to avoid dividing by zero.) It then multiplies this fraction by its number of neighbors to compensate for the fact that cells have different numbers of neighbors. For example, in Figure 3.6, the central cell has a total of 12 Ds bonds with its six neighbors. The smallest number of bonds it has with any single neighbor is the one Ds bond with the bottom cell. The minimum fraction is then 1/12. If we then multiply by 6 (the number of neighbors), we obtain 6/12 or 1/2, a quantity we refer to as the adjusted minimum fraction. Thus, a cell that divides its bound

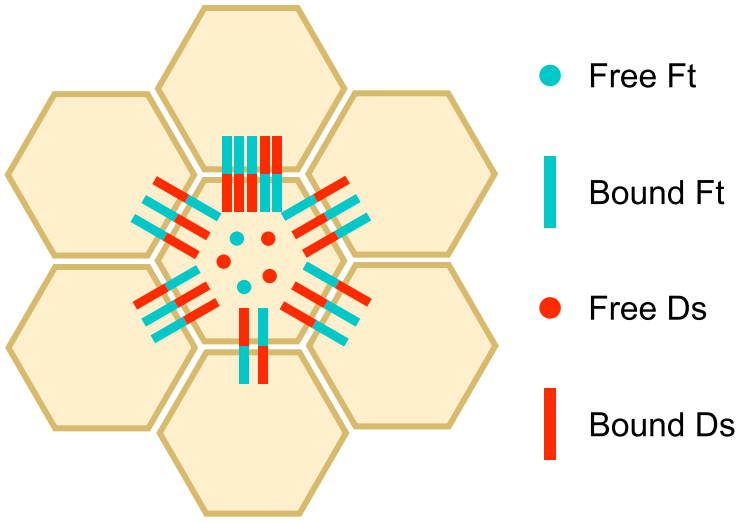

Figure 3.6: Ft-Ds bonds on adjacent cells. The more uneven the arrangement of these bonds, the faster the cell will grow. To calculate the minimum fraction of bound Ds on the central cell, we divide the smallest number of bound Ds shared with any of the neighbors by the total number of bound Ds. In this case, the central cell has one bound Ds (orange) with the bottom cell, the fewest of all its neighbors. Because the cell has a total of 12 bound Ds, the minimum fraction would then be 1/12. We then multiply by the number of neighbors to give an adjusted minimum fraction of 6/12 or 1/2. Similarly, the minimum fraction of bound Ft would be 6/7. Note that in the case of perfectly evenly distributed bonds (for this cell, 2 on each neighbor), this quantity would be equal to 1. Similarly, if the cell lacks bonds with at least one of its neighbors, the adjusted minimum fraction would be 0.

Ft or Ds evenly among all its neighbors will have this quantity equal to 1, and a cell with a more asymmetric distribution of bonds will have a smaller number. If a cell has no bonds with at least one of its neighbors, its adjusted minimum fraction will be zero.

These measures for bond symmetry, then, are given by:

$$S_F = \text{min. bound Ft fraction} \times \#\text{neighbors} \tag{3.26}$$

$$S_D = \text{min. bound Ds fraction} \times \#\text{neighbors} \tag{3.27}$$

Thus, from Equation (3.20), cells with uniformly distributed bound Ft and Ds (i.e., higher minimum fractions) grow more slowly than cells whose Ft-Ds bonds are more asymmetrically

distributed (i.e., lower minimum fractions). In the case of a disc that is mutant for either Ft or Ds (or both), both S_F and S_D will be set to zero, since no cell has any bound protocadherins. If this case were not treated specially, the minimum fraction would be undefined, since its denominator is the total number of bound Ft or Ds on a cell. Note that this special case only applies if a cell has no bonds with one or more of its neighbors. In our simulations, this situation only occurs in discs that are completely missing Ft and/or Ds, or where Ft or Ds lack the ability to bind. In wild-type discs and most other cases, every cell will have enough Ft and Ds to form at least one bond with each of its neighbors.

We note that the asymmetry of Ft-Ds bonds around a cell may be defined in a number of ways. However, in order to relate bond asymmetry to Dachs localization on the side with the least bound Ft [9, 11, 95], we chose to measure the asymmetry of the bond distribution using only the neighbor with the fewest bonds. This was primarily so that a cell with no Ft-Ds bonds at all (e.g., a *ft-* or *ds-* cell) would exhibit the strong overgrowth seen experimentally [86]. Cells with no bonds in our model would be treated as having a minimum fraction of zero, and thus very high asymmetry. Note that this is a special case that only occurs when a cell completely lacks bonds with at least one neighbor, a situation that only occurs in our model when a disc is completely missing either Ft or Ds, or if Ft or Ds lacks the ability to form bonds. In wild-type discs, cells in the model will always have at least one bond with each of their neighbors. (Experimentally, both Ft and Ds are detected at all cell-cell interfaces in a wild-type disc [10].)

When a cell divides, the mother and daughter cells will initially have no Ft-Ds bonds between them, since their interface is newly formed. Similarly, cells may rearrange as a result of mechanical forces from their neighbors, forming new interfaces. However, neighbor pairs formed within the last 100 time steps are ignored for the purpose of calculating bond asymmetry in the model. Otherwise, any pair of cells resulting from a recent division would have very small minimum fractions because they have very few bonds with one another, and thus they would have a very high growth rate due to bond asymmetry. The daughter

cell inherits the mother cell's values of Ft and Ds asymmetry until this grace period has passed.

We also include a penalty to a cell's growth rate for having leftover Ft and Ds. In experiments, discs that are mutant for both Ft and Ds are observed to grow faster than either single mutant [86], even though both single mutants should be completely lacking in Ft-Ds bonds. Since the only difference between the single and double mutants is that the single mutant contains a large number of free Ft or Ds, we speculate that free Ft and Ds have a tendency to slow growth. Similarly, cells in a Ft mutant disc proliferate faster in the center (where little Ds is present) than at the edge (where the most Ds is present) [25], suggesting that excess unbound Ds may be associated with slower growth.

3.8 Dachs localization

Here, we describe our model for the magnitude and direction of Dachs localization within each cell. We can use Dachs localization as an indicator of Ft-Ds bond asymmetry, allowing us to see which cell-cell interfaces form bonds and what polarity those bonds have. We implement a model of Dachs localization as driven by Ft bond distribution asymmetry. Each cell has a vector representing its Dachs localization whose magnitude varies between 0 (isotropically distributed) and 1 (fully localized to one side), and whose direction gradually changes to point towards the side of the cell with the least bound Ft:

$$\frac{d}{dt}(\overrightarrow{\text{Dachs}}) = (1 - S_F)\hat{p} - \overrightarrow{\text{Dachs}} \tag{3.28}$$

Here S_F is the minimum fraction of bound Ft, adjusted for the number of neighbors, as in Equation (3.26). It varies from 1 (evenly distributed bonds) to 0 (at least one neighbor with no bonds). The quantity $(1 - S_F)$ is a measure of bond asymmetry, causing Dachs to become more strongly polarized the more asymmetrically the bonds are distributed. The quantity $\hat{p}$ is simply a unit vector pointing toward the neighbor with which the cell has the

least bound Ft. Thus, Dachs moves toward the side of a cell with the least bound Ft. Note that Dachs localization matches the magnitude and direction of Ft asymmetry at every time step. Because there is a "grace period" before newly formed neighbors can contribute to the minimum fraction of bound Ft, Dachs polarization is not instantaneously affected by changes in a cell's set of neighbors caused by cell division.

3.9 Input and output

Here we describe the information that the simulation needs to begin a run, as well as the information the simulation records for later analysis.

Starting conditions for the simulation, including the progenitors, spatial coordinates, sizes, and velocities of each cell, are read in from an existing text file when the simulation begins. The program then calculates disc-wide quantities, including the disc's starting radius and the location of its center of mass, and builds the neighbor list for all the cells. (For purposes of finding the disc's radius, it assumes a roughly circular cluster of cells; since cell divisions are oriented in all directions and cells stay in a single contiguous cluster, the disc remains roughly circular throughout a run.) Finally, it assigns starting quantities of morphogen, Ft, Ds, and Fj to all cells, assigns each cell's Ft and Ds to phosphorylated and unphosphorylated pools depending on the cell's starting amount of Fj, and creates a starting set of Ft-Ds bonds as described above.

At each time step, the simulation records information about all the cells, including their indices, spatial coordinates, and radii, and the indices of each cell's parent. If the simulation involves marking certain cells as part of a "clone" for later manipulation, it records which cells are in the clone, and the distance of each cell from the clone's edge (in terms of cells). The simulation also records each cell's growth rate and associated quantities, including its amounts of free and bound Ft and Ds; its amount of Fj; the minimum fractions of bound Ft and Ds as used in Equations (3.26) and (3.27); and x_M, x_{Ft}, and x_{Ds}, the contributions

of morphogen signaling and Ft and Ds bond asymmetry to the growth rate. It also records the angular position of Dachs localization (i.e., the direction of the neighbor with which the cell has the least bound Ft). Because it contains information on every cell at every time step, this file can become very large, especially for longer runs and runs involving larger discs.

We also need a more compact way to record general information about a single run. The overall size of the disc is fairly consistent from one run to another under the same conditions. However, the location, bond arrangement, and growth rate of any given cell will not be fixed between runs. To determine the overall pattern of bond asymmetry and growth, then, it can be useful to collect information over many runs. To do this, the simulation can record more general data intended to be averaged. Every 100 time steps, the simulation records the location of the front (i.e., the point where the Fj and Ds gradients are steepest), and then divides the disc into 50 evenly spaced concentric rings. For each of the rings, it calculates the average growth rate, the average contributions of morphogen signaling and bond distribution asymmetry to the growth rate, and the average Ft asymmetry (i.e., the minimum fraction of bound Ft, adjusted for the number of neighbors). Since the overall size of the disc typically varies by less than 1% between runs, the absolute size of each ring is fairly consistent from one run to another. If this information is appended to an existing file rather than written to a new file each time the program is run, we can examine the average spatial patterns of signaling and growth over many runs. Similarly, every time a cell divides, the location and time step of the division are also recorded in a separate file. Again, by appending this information to an existing file during each run, we can find an average pattern of cell proliferation over multiple runs.

The simulation can be set to run for either a certain number of time steps or until the disc has a certain number of cells. In either case, when the program finishes, the final state of all cells is recorded in the same format used for the input file, so a run can be stopped and then resumed in a later session. The records made during the run can be read by a set

of MATLAB scripts to generate graphs and movies. Using these scripts, we can show the spatial patterns of, for example, Dachs localization or cell proliferation.

Chapter 4: Results regarding cell polarization

Our results fall into two broad categories. In this chapter, we examine the effects of the movement of the Fj/Ds expression front on proximal-distal polarization in the wing pouch. In the next chapter, we will show that our model of cell growth reproduces many different experimental results, and examine how the movement of the front affects the pattern of proliferation in the wing pouch.

The arrangement of a cell's Ft-Ds bonds in our model—and, by extension, its growth rate—is dependent on its entire history rather than its instantaneous state. The expression patterns of Fj and Ds, which determine the availability of Ft and Ds for binding, change over time. These expression patterns take the form of complementary sigmoid curves with a steep transition region, or front, between their high and low plateaus. A radially symmetric morphogen concentration profile determines the patterns of Fj and Ds expression; the front is located where the morphogen has a certain critical concentration. As the morphogen profile increases in amplitude, this front moves radially outward. Because the front moves, it can affect the arrangement of the Ft-Ds bonds on all the cells that it has passed over, not just the cells near it at any one time. This mechanism has implications for both the growth and patterning of the disc because the Ft pathway is involved in both cell proliferation and polarity. We also show that the model gives results similar to experimental ones when Fj and Ds expression are altered in only one portion of the disc. Finally, we examine cell polarity in the form of Dachs localization and show that the movement of the front leads to realistic patterning.

4.1 Emergent behaviors in the wild-type disc

We first address our original question: how do Ft-Ds bonds on cells in the wing pouch become polarized when Ft, Ds, and Fj are all present in fairly spatially uniform

concentrations? The cells in our model respond to their history, not just their instantaneous state. The Ft-Ds bonds that each cell forms with its neighbors constitute a cell's "memory" in this context. The distribution of these bonds reflects not only current Ft and Ds availability, but the cell's entire history of Ft and Ds availability. This is because Ft-Ds bonds on a cell persist for some time after they are formed, rather than dissolving when local expression rates change. Because of this mechanism, changes in morphogen, Fj, and Ds expression are critical. Even if Fj and Ds expression are only steeply graded in one region of the disc (i.e., the transition region), the bond distribution can be polarized in a large fraction of the tissue, because the transition region moves with respect to individual cells. For this reason, growth rate and polarization can be much more spatially uniform than the instantaneous expression patterns might suggest.

4.1.1 Movement of the expression front

The one dynamic quantity that is directly specified in the model is the amplitude of the morphogen concentration in Equation (3.9) that increases exponentially in time (Figure 4.1A), driving the Fj/Ds transition region radially outward. As a result, each cell experiences a gradual increase in its morphogen concentration. Since the Fj and Ds expression rates depend on the local morphogen concentration, these rates change as a result of the changing morphogen profile. Experiments have shown that increased Dpp signaling is associated with higher Fj and lower Ds expression [9], that the amplitude of the Dpp profile increases over time [45], and that the Fj-expressing central region encompasses an increasing fraction of the disc as the third instar progresses [58]. Consequently, as the morphogen amplitude in our model increases, more cells express Ds at low rates and Fj at high rates (Figure 4.1B-C). Cells with a morphogen concentration above a certain constant threshold express primarily Fj, and cells whose morphogen concentration is below that threshold express more Ds (Figure 3.5).

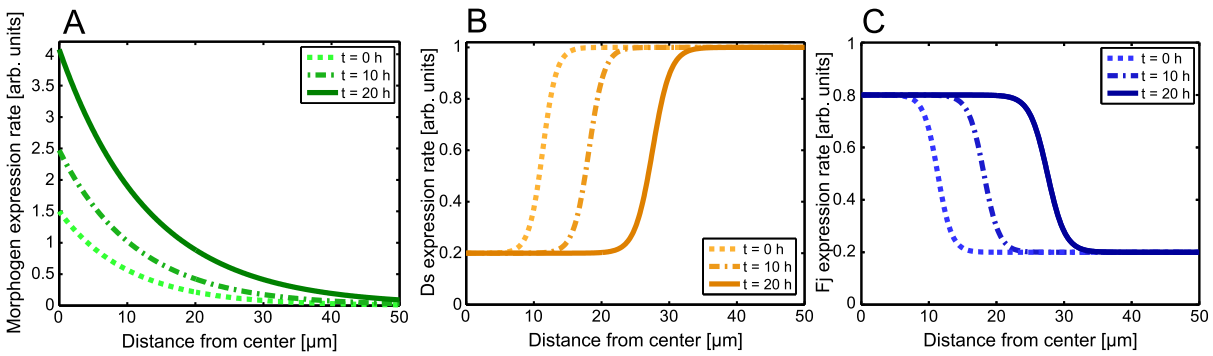

Figure 4.1: The increasing amplitude of the morphogen profile causes the Fj/Ds expression front to move outward over time. (A) The morphogen concentration as a function of radial position at 0 (dotted light green), 10 (dashed medium green), and 20 hours (solid dark green) from the beginning of the simulation. A radial position of 0 corresponds to the center of the disc. The amplitude (i.e., the concentration at the disc's center) increases with time. Consequently, the position at which the morphogen concentration equals a given value, in this case 0.5, moves radially outward, as indicated by the vertical dashed lines. Because the transition region corresponds to a morphogen concentration of 0.5 on this plot, this mechanism moves the Fj/Ds front outward as well. (B) The Ds expression profile as a function of position at 0 (dotted light orange), 10 (dashed medium orange), and 20 hours (solid dark orange) hours from the beginning of the simulation. Note that the region where the gradient is steepest moves outward over time. (C) The Fj expression profile as a function of position at 0 (dotted light blue), 10 (dashed medium blue), and 20 hours (solid dark blue) hours from the beginning of the simulation. Again, the region with the steepest slope moves outward over time.

Because the morphogen profile in the model is radially symmetric, there is a circular boundary or front separating the Fj-expressing central region and the Ds-expressing peripheral region. In the model, the gradients of the Ds and Fj expression rates are steepest near this front. The gradual increase in morphogen concentration causes this boundary to move outward. Cells near the boundary go from expressing more Ds to expressing more Fj when their morphogen concentration exceeds the threshold concentration (Figure 4.1). Furthermore, cells near this boundary have substantially different Fj and Ds expression rates from their neighbors, leading to differences in Ft and Ds availability for binding. These differences in turn lead to an uneven distribution of new Ft-Ds bonds, stronger Dachs localization, and a higher growth rate.

4.1.2 Recovery of polarization after mitosis

Note that all the processes described earlier (Ft/Ds/Fj expression and degradation, bond formation and dissolution, phosphorylation and dephosphorylation) happen at finite rates, with characteristic time scales on the order of hours. Because a cell cycle lasts several hours, this means that the number and distribution of bonds between a cell and its neighbors reflect the history of a cell and its neighbors, not just its instantaneous state. This mechanism allows cells to have a memory of past expression levels. In particular, the rate at which bound Ft and Ds are degraded goes as the product of the rate of dissolving existing bonds and the degradation rate of free Ft and Ds. In our model, this product is less than 1% which means that less than 1% of the bound Ft and Ds are degraded per time step, so it takes on the order of hundreds of time steps (i.e., several hours) to turn over all the bonds on a cell. This time scale is comparable to the time scales of the movement of the front and of the cell cycle. This means that the arrangement of bonds around a cell can persist well after the cell is no longer near the front. So even when a cell and its neighbors are in a region where Fj and Ds concentrations are spatially rather uniform, the cells can still have asymmetrically distributed bonds that were formed when the local Fj and Ds gradients were steep. In our model, this allows Ft-Ds bonds to be asymmetrically distributed on cells throughout the wing primordium, not just on cells near the front.

During this process, cells are constantly growing and dividing, forming new interfaces between adjacent cells. In our model, these new interfaces begin with no Ft-Ds bonds, so the polarization of recently divided cells may be disrupted. Figure 4.2 illustrates what happens to the arrangement of Ft-Ds bonds around a newly divided cell. Before division (Figure 4.2A), cells all have similarly polarized Ft-Ds bonds. These cells are assumed to be far from the transition region, and so express Ft, Ds, and Fj at similar rates. When a cell divides, it creates a new interface between the two daughter cells with no bonds on it, temporarily affecting the polarization of the daughter cells (Figure 4.2B). Over time,

however, new bonds of both polarities form at the interfaces, and the overall pattern of Ft-Ds bond polarization is recovered (Figure 4.2C). Cells recover their polarization so quickly because the number of bonds at a new interface can reach a steady state within only a few time steps. As described earlier, the Ft-Ds binding algorithm tends to form as many bonds as possible at each time step. This means that the daughter cells form new bonds with one another at a high rate after a cell division.

4.2 Ft-Ds bond polarization in the wing pouch

The outward movement of the front, combined with the ability of cells to recover their polarization after dividing, can polarize all the cells that the front passes over. Figure 4.3 shows the degree of bond asymmetry as a function of radial position at different times in the simulation. At the beginning of a run of the simulation, the concentration profiles of Fj and Ds will be steepest near the front and spatially flat far from the front. This means that initially, Ft-Ds bonds will be asymmetrically distributed only for cells near the front (Figure 4.3A). As the front moves outward, cells near the front's new position will form new bonds with an asymmetric distribution because their expression rates of Fj and Ds have a large spatial gradient. Cells inside the front (i.e., within the central plateau) will have expression rates that vary more slowly in space as the front moves away from them, but their asymmetric bond arrangement will persist after the front has passed. Over the course of the run, more and more cells will have asymmetrically distributed bonds because the front has passed over them (Figure 4.3B-C). Eventually, this region of higher bond asymmetry will encompass most of the wing primordium (Figure 4.3D). This result is consistent with experiments, which show that cells throughout the wing pouch, not only those near the edge of the primordium, exhibit an asymmetric distribution of Ft and Ds, as well as a localization of Dachs to the distal side [10, 11].

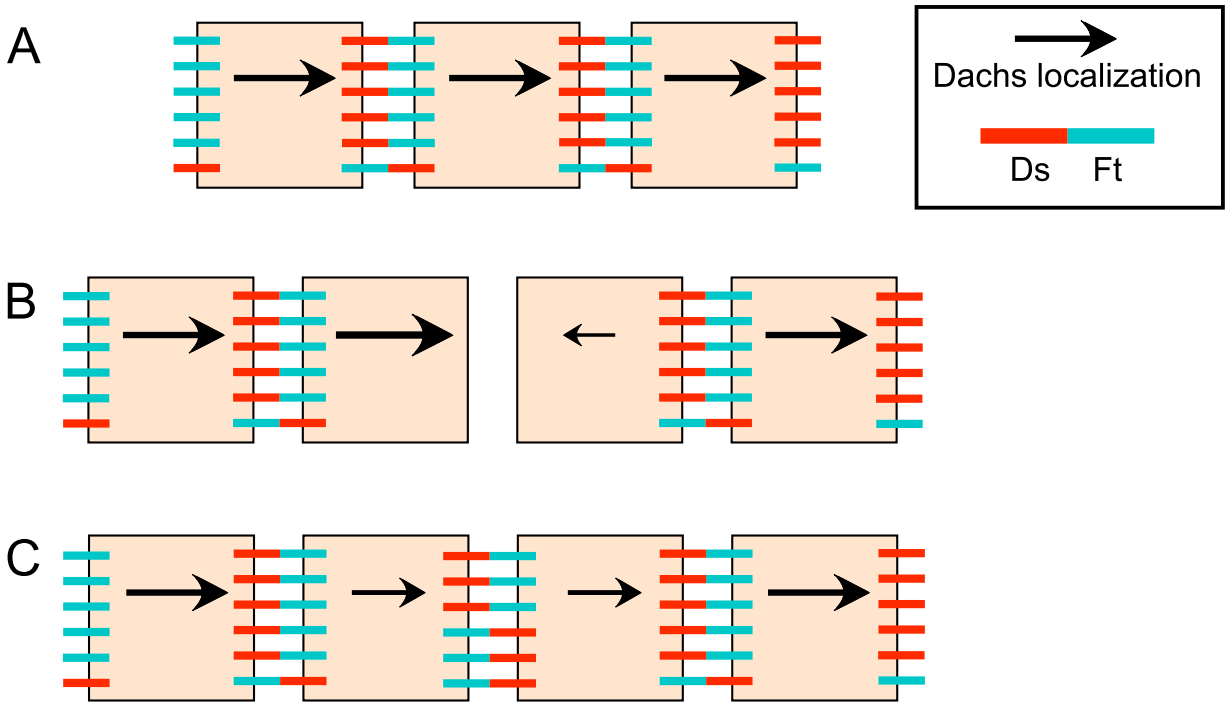

Figure 4.2: Cells far from the front can recover their polarization after dividing. (A) Three cells, assumed to have the same rates of Fj and Ds expression, have highly asymmetrically distributed bonds between Ft (red) and Ds (light blue). Dachs (black arrows) localizes to the side of each cell with the fewest bound Ft, the right side in this figure. (B) The central cell divides, forming two cells with a new interface between them. This newly formed interface has no Ft-Ds bonds; the changed bond distribution temporarily affects the Dachs localization in the two daughter cells. (C) Over time, Ft and Ds form bonds at the new interface. The two cells express Fj and Ds at equal rates and the formation of new bonds is independent of the polarity of existing bonds, so new Ft-Ds bonds are equally likely to form with either polarity at this interface. However, the overall pattern remains the same; both cells now have more bound Ft on their left interface, so Dachs localizes to the right side of each cell.

For the sake of comparison, we also show a simulated disc with a stationary Fj/Ds expression front that stays roughly two-thirds of the way between the disc's center and edge. Again, cells that begin near this front exhibit high bond asymmetry (Figure 4.3E), but now the front does not sweep over a large fraction of the disc. (The front does gradually move with respect to some individual cells due to growth of the wing disc and faster proliferation near the front, as shown in Figure 4.3F-G). At the end of the run (Figure 4.3H), the bump in bond asymmetry remains close to the starting point of the front, rather than encompassing the whole wing primordium. This indicates that movement of the front is necessary to induce bond asymmetry in the entire wing pouch.

4.3 Dachs localization with a moving front

As the Fj/Ds expression front moves outward through the disc, cells at the front make a transition from expressing mostly Fj to expressing mostly Ds. When a cell is near this boundary, its Ft-Ds bonds will become strongly polarized because the local gradients of Fj and Ds are very steep. Because the front moves, more cells will have their bonds become polarized over time. Since Ft-Ds bonds do not rearrange instantaneously, cells retain their bond polarization after the front has passed over them and Fj/Ds expression has again become locally flat. This mechanism constitutes a sort of "memory" of the moving front in the form of bond asymmetry, lasting on the order of hundreds of time steps, or hours of real time. The result of this moving front is bond asymmetry throughout the wing primordium (i.e., the area within the front), with the inner (distal) side of each cell having the least bound Ft.

Dachs localization in our model is used as an indicator of Ft-Ds bond asymmetry as given by the "minimum fraction" metric described in Section 3.6. At every time step, the vector of Dachs polarization points toward the side of a cell with the least bound Ft, as observed experimentally [9, 95, 96]. (Cells that have only recently become adjacent, i.e.,

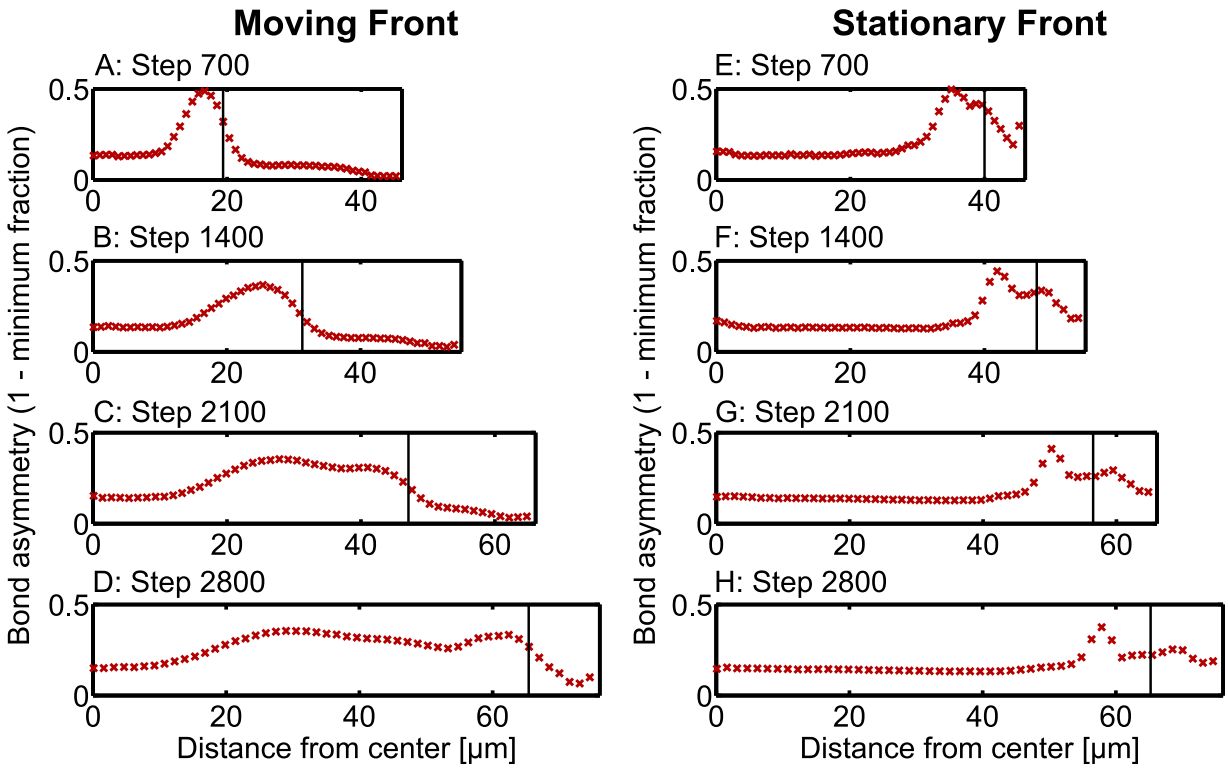

Figure 4.3: Ft-Ds bond asymmetry persists after the expression front has passed, so the movement of the front allows a large portion of the disc to be patterned. The asymmetry of bonds (vertical axis) is shown as a function of absolute radial position (horizontal axis) in the case of both a moving (panels A-D) and a stationary (panels E-H) front. Note that the bond asymmetry is simply 1 minus the minimum fraction, so an asymmetry of 0 corresponds to evenly distributed bonds. When the front (vertical black line) is moving, the cells that it has passed over have more asymmetrically distributed bonds. (A-D) As the front moves, the region of greater bond asymmetry grows to encompass a larger fraction of the disc. (E-H) Here, the front is fixed at roughly 85% of the distance from the disc's center to its edge, so that its ending position in panel H is the same as that in panel D. When the front is stationary in this manner, only cells near the front have asymmetrically distributed bonds, giving rise to a relatively narrow peak of bond asymmetry.

via cell division, do not count as neighbors as far as Dachs localization and the minimum fraction are concerned. Otherwise, newly adjacent cells would have very little bound Ft, and Dachs would simply tend to localize toward a cell's newest neighbor.) This Dachs polarization vector has a magnitude equal to the cell's bond asymmetry, a quantity between zero (evenly distributed bonds) and one (at least one neighbor with no bonds). Figure 4.4 shows the direction (panels A-D) and magnitude (panels E-H) of Dachs polarization at three different times during a run of the simulation. At the start of a run (Figure 4.4, A-B and E-F) only cells close to the front have strongly polarized Dachs, while cells outside the front have Dachs that is roughly randomly oriented. As the simulation continues and the front passes over more cells, an increasing fraction of the disc exhibits polarized Dachs (Figure 4.4, C and G). After 35 hours, nearly all of the cells have Dachs localized to their distal (i.e., center-facing) side (Figure 4.4, D and H), which is consistent with experiment [9–11,99]. Thus, we predict that Dachs polarization, like Ft-Ds bond asymmetry, follows the movement of the Fj/Ds expression front as the third instar progresses.

4.4 Dachs localization with a stationary front

For the sake of comparison, we also consider a disc whose Fj/Ds expression front is fixed in terms of relative position between the disc's center and edge, rather than being determined by a critical value of the morphogen concentration. In this case, individual cells primarily express either Fj or Ds for the entirety of the run without the front passing over them. (Note that individual cells can still move away from the front as they and their neighbors proliferate, but this effect is less pronounced when the front's location is fixed.) Even though the front is stationary, the morphogen profile remains the same as with the moving front; i.e., the amplitude of the morphogen profile still increases with time. The result is a peak of faster growth in the center of the disc due to morphogen signaling and an annulus of faster growth near the front.

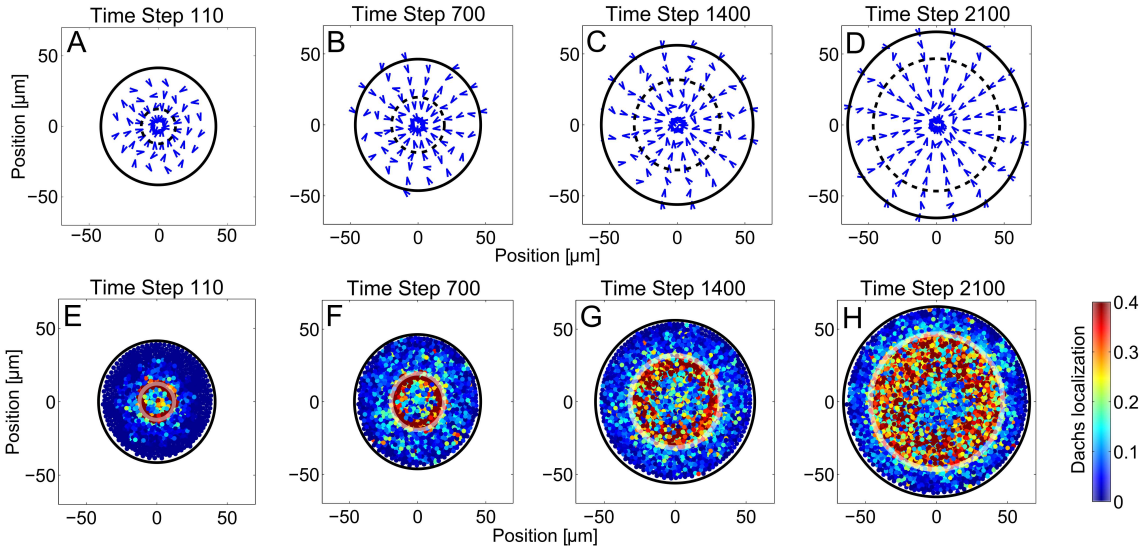

Figure 4.4: A moving front of Fj/Ds expression leads to bond asymmetry throughout the wing pouch. The direction (panels A-D) and magnitude (panels E-H) of Dachs polarization at 110 (A, E), 700 (B, F), 1400 (C, G) and 2100 (D, H) minutes after the beginning of a single run are shown. The arrows in panels A-D represent spatial averages of cell polarization; they point to the side of the cell with the least bound Ft. Panels E-H show the magnitude of Dachs polarization in the disc; blue represents weaker polarization, red stronger. The solid black circle is the approximate edge of the entire disc, while the dashed black circle (panels A-D) and solid white circle (panels E-H) represent the Fj/Ds expression front and the boundary of the prospective wing blade. This front moves radially outward over time, encompassing an increasing fraction of the whole disc. Cells that have had this front pass over them (i.e., those inside the front) retain their elevated bond asymmetry for some time, leading to elevated Dachs localization throughout the wing primordium compared to the hinge region. Note that cells within the Fj/Ds expression front strongly tend to have polarization pointing inward; i.e., their bound Ft is predominantly on the outer (proximal) side, consistent with the observed localization of Dachs. Cells outside the front have weaker and less consistent Dachs localization.

The cells near the stationary Fj/Ds boundary have very strongly polarized Ft-Ds bonds, and thus very polarized Dachs, because the local gradients of Fj and Ds remain relatively steep. In contrast, cells near the disc's center or edge consistently experience spatially uniform Fj and Ds concentrations, leading to more symmetric bond distribution and less polarized Dachs. Figure 4.5 shows the direction (panels A-D) and magnitude (panels E-H) of Dachs polarization in a disc with a stationary front. Again, cells near this front have less bound Ft on the side nearest the center of the disc (i.e., the proximal side), but this effect is much less pronounced in the disc's center, which is far from the front for the duration of the run. This annulus of increased polarization widens over time as the cells near the front proliferate, but does not encompass the entire wing primordium. Contrast this result with the moving front, which polarizes Dachs in all the cells that it sweeps over as shown in Figure 4.4.

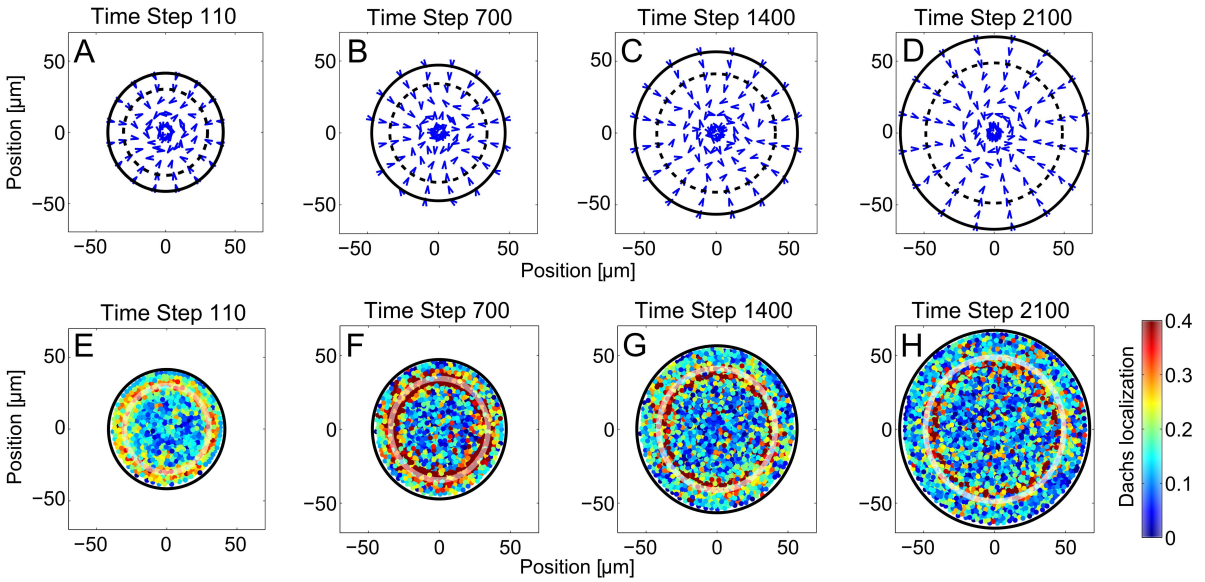

Figure 4.5: A stationary Fj/Ds expression front results in an annulus of Ft-Ds bond asymmetry. Again, the direction (panels A-D) and magnitude (panels E-H) of Dachs localization in the disc are pictured. Dachs localization is a vector that varies from zero, for an isotropic distribution of Dachs, to unity, if Dachs is all on one side. The arrows in panels A-D represent spatial averages of the direction of Dachs localization; the markers in panels E-H represent the magnitude of Dachs localization. Blue represents less asymmetry, red represents more. Images are taken at 110 (A and E), 700 (B and F), 1400 (C and G), and 2100 (D and H) minutes into the third instar. Because the same set of cells is near the Fj/Ds expression front (dashed black circle in A-D, white circle in E-H) throughout the run of the simulation, this set of cells experiences elevated Dachs localization (red ring in panels E-H). Dachs localization near the front points predominantly inward due to the steep local slopes of Fj and Ds, and is much weaker and less directed at the disc's center, far from the front (green/blue markers in panels E-H).

Chapter 5: Results regarding cell proliferation

Using only a few variables to determine a growth rate—morphogen signaling, bound Ft and Ds asymmetry, and leftover free Ft and Ds—we can replicate a large number of experimental results. We show that our model for growth gives disc sizes similar to those seen experimentally under a wide variety of conditions. The model also replicates results regarding clones of cells in which Fj, Ds, or morphogen signaling are increased. We also examine the spatial patterns of cell proliferation, showing that Ft-Ds bond asymmetry and morphogen signaling dominate in complementary parts of the disc, giving rise to more uniform growth and proliferation than either effect alone.

5.1 Size of the disc under different conditions

A number of experimental results on disc growth are given in terms of the eventual size of the wing disc. We show a summary of the results of our model in Figure 5.1, where the number of cells in the disc is given for various conditions. In some runs, we remove Ft, Ds, both Ft and Ds, or Fj. In other runs, we examine discs that express Fj, Ds, or both Fj and Ds at uniformly high levels. We simulate a disc that underexpresses Ft without lacking it entirely. We also simulate discs in which Ft is lacking its intra- or extracellular domain. Finally, we examine discs that either lack the morphogen or have uniformly high morphogen signaling. We compare each of these cases to the growth of a wild-type case as a control. All other parameters are fixed between runs. The results of our model are qualitatively consistent with a variety of experiments, as we describe in detail below.

5.1.1 Removing Ft and Ds

The dramatic overgrowth of *ft*- discs is widely observed experimentally [51,84–86]. Wing discs mutant for *ds* overgrow to a lesser degree [12,15,86], although the size of adult *ds*-

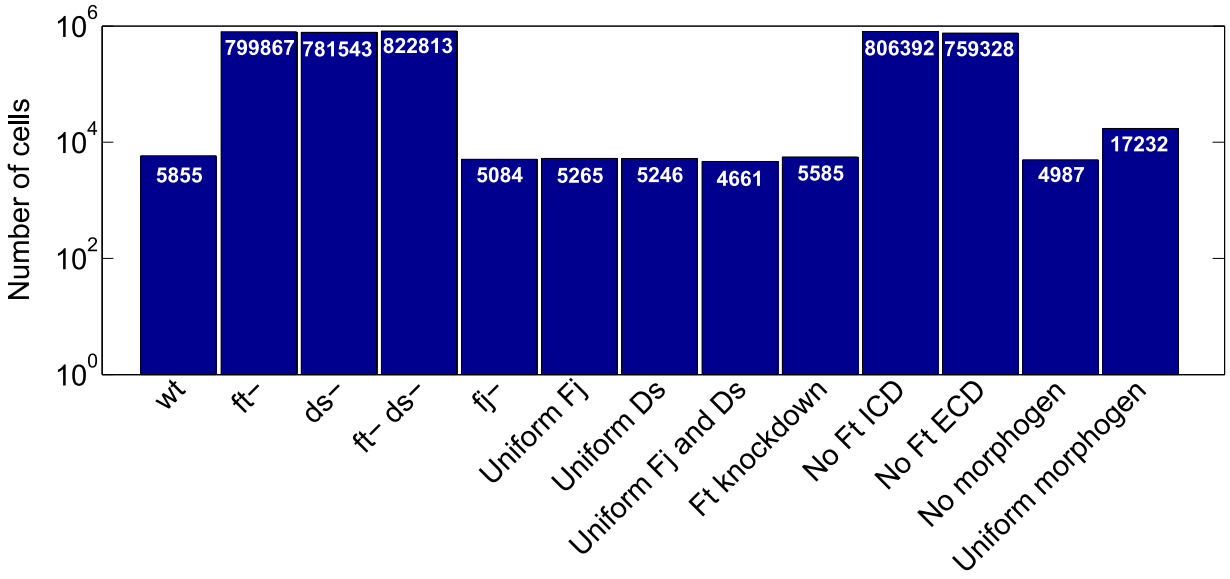

Figure 5.1: The number of cells in the wing disc under various conditions. In each case, the same starting set of 1000 cells was simulated for 1700 time steps. Each bar represents the average number of cells in the disc over 20 runs with the same conditions. (Because the size at which a cell divides and the rate at which it forms and dissolves Ft-Ds bonds are not completely deterministic, simulation runs under the same conditions are not identical.) Here, "ft-", "ds-", "ft- ds-", and "fj-" refer to discs missing Ft, Ds, both Ft and Ds, or Fj, respectively. "Uniform Fj", "uniform Ds", and "uniform Fj and Ds" are discs that uniformly express high levels of Fj, Ds, or both. "Ft knockdown" means that every cell starts with half as much Ft as wild-type and expresses Ft at half the normal rate. "No Ft ICD" means that the discs' Ft has no intracellular domain; it binds to Ds but the resulting bonds are not counted by their cells, and there is no penalty to the growth rate for free Ft. "No Ft ECD" means that the discs' Ft has no extracellular domain; it cannot bind to Ds and is consequently always treated as free. "No morphogen" and "Uniform morphogen" refer to discs with no morphogen and uniformly high morphogen levels, respectively. (In every case, the standard deviation of the number of cells in the disc was less than 1% of the mean, so error bars are not shown.) Other than the stated variations, each run used the same set of parameter values.

wings depends on the exact allele used. Furthermore, *ft- ds-* double mutants overgrow more than either single mutant [86].

In our model, discs that are mutant for Ft and/or Ds overgrow substantially compared to wild-type discs (Figure 5.1, *"ft-"*, *"ds-"*, and *"ft- ds-"*). When a cell lacks Ft-Ds bonds with at least one of its neighbors, then its minimum bond fraction will be zero, and its bond distribution will be considered completely asymmetric. Greater bond asymmetry is associated with faster growth in Equation (3.20), so these discs will overgrow. However, discs in our model that lack either Ft or Ds will have their growth rate penalized for having a substantial amount of free, or unbound, Ds or Ft (respectively) remaining. In particular, discs mutant for Ft grow slightly faster than discs mutant for Ds in our model simply because a disc normally contains more Ft than Ds. (Recall that Ft is expressed at high levels uniformly, while Ds is expressed at similarly high levels only outside the front.) In other words, a *ds-* disc will have more free Ft than a *ft-* disc will have free Ds, and free Ft and Ds tend to hinder growth. Double mutant discs, i.e., discs that express neither Ft nor Ds, will have no penalty for free Ft or Ds, and will grow faster than either single mutant.

5.1.2 Uniform Fj and Ds expression

Experimentally, discs that uniformly express Ds or Fj tend to undergrow compared to wild-type discs, and discs that uniformly express *both* Ds and Fj undergrow even more [9,16]. Our model is consistent with these results. The main drivers of Ft-Ds bond asymmetry in our model are the Ds and Fj gradients, which lead to a spatially nonuniform availability of Ds as well as nonuniform binding probabilities for Ft and Ds. (Recall that Fj affects the binding probabilities of Ft and Ds [55, 56].) Because the model's growth rate is heavily dependent on Ft-Ds bond distribution asymmetry, making the Ds or Fj concentrations spatially uniform will lead to slower growth and a smaller disc (Figure 5.1, "uniform Fj" and "uniform Ds"). In addition, in runs where the Fj or Ds profiles are uniform, the disc

expresses Fj or Ds at a level above the wild-type rate. In these cases, Fj is expressed at 25% more than its maximum wild-type rate and Ds is expressed at 10 times its maximum rate. If both Fj and Ds are expressed uniformly, the growth rate will be slower still (Figure 5.1, "uniform Fj and Ds"), because both the availability and the binding probabilities of Ft and Ds will be spatially uniform.

5.1.3 Removing Fj

Flies mutant for Fj tend to have smaller wings than wild-type flies [13,16,18,94]. In our model, discs that lack Fj grow more slowly than wild-type discs (Figure 5.1, "fj-"). This is because their Ft and Ds binding affinities do not vary spatially, leading to more uniform bond distributions on each cell.

5.1.4 Altering Ft expression

In a naïve view of disc growth, the growth rate is simply a function of the number of Ft-Ds bonds. According to this scenario, since discs mutant for Ft overgrow, one would expect discs with reduced Ft expression to slightly overgrow compared to wild-type discs—in other words, to have a milder version of the same phenotype. However, experimentally, discs with reduced Ft activity undergrow slightly compared to wild-type discs [108], suggesting that the growth rate is not simply a function of the number of Ft-Ds bonds. In our model, discs with reduced Ft (here, half the amount of starting Ft and half the expression rate of new Ft) undergrow compared to wild-type discs (Figure 5.1, "Ft knockdown"). This is because these cells have a surplus of free Ds because of their lack of bindable Ft, and the growth rate is penalized by the presence of free Ft and Ds.

5.1.5 Altering Ft activity

When we simulate different forms of Ft and their effects on the growth rate, we find results that are consistent with experiment. For example, discs that express FtΔICD, a form of Ft missing its intracellular domain (ICD), overgrow more than ft- discs and slightly less than ft- ds- double mutant discs [86]. In our model, this form of Ft still binds to Ds but is not counted by its cell as either bound or free. Similarly, the Ds bound to this form of Ft is also not recognized by its cell, possibly because the Ft side of the bond would not be tethered to the cytoskeleton. The result is a disc that grows very quickly, as each cell recognizes no bound Ft or Ds, experiences no growth penalty for having free Ft, and has only a small penalty for its free Ds ("no Ft ICD" in Figure 5.1). This type of disc, then, acts like a *ft- ds-* double mutant with free Ds. Simulated discs with this form of Ft overgrow more than *ft-* mutants but less than *ft- ds-* double mutants, consistent with experimental results.

Similarly, we can consider FtΔECD, a form of Ft that has its intracellular domain but is missing its extracellular domain (ECD), presumably preventing it from binding to Ds. Experimentally, discs that express this form of Ft rather than wild-type Ft grow slightly larger than wild-type discs [86], In our model, this version cannot form bonds with Ds (leading to a high effective bond distribution asymmetry), but all of its Ft and Ds will be free (resulting in a strong penalty for leftover Ft and Ds). Discs with this form of Ft, then, will overgrow due to the lack of Ft-Ds binding, but the large amounts of free Ft and Ds mean that they will grow more slowly than *ft-* discs ("no Ft ECD" in Figure 5.1).

5.1.6 Altering the morphogen profile

Experimentally, wing discs that are mutant for Dpp undergrow [24, 64]. In the model, the morphogen plays a dual role in the disc's growth rate. Cells grow in direct response to their level of morphogen signaling. In addition, morphogen signaling affects the expression

patterns of Fj and Ds, which in turn affect the degree of Ft-Ds bond asymmetry in a given cell. Discs with a dramatically decreased morphogen concentration, then, will tend to undergrow. The reason for this is twofold; first, the lack of autonomous morphogen signaling will lower the growth rate. Second, because morphogen signaling is low, these discs will express both Ds and Fj fairly uniformly (Ds at a high level and Fj at a low level), leading to highly symmetric bond distributions and thus dramatic undergrowth ("no morphogen" in Figure 5.1) in agreement with experiment [60].

Experimentally, discs with uniformly high Dpp signaling overgrow, suggesting that the autonomous effects of Dpp signaling dominate in this case [9, 24, 25]. In our model, a disc with uniformly high morphogen expression will experience more overall morphogen signaling, but it will also lack a spatial gradient in Fj and Ds expression, as it will express both Fj and Ds uniformly (Fj in large quantities and Ds in small quantities). We would expect the net effect on the disc's growth rate to be parameter-dependent, as the two effects oppose one another. For the set of parameters we use in the simulation, discs with uniform morphogen signaling overgrow slightly compared to the wild-type disc which is qualitatively consistent with experiment [24, 25] ("uniform morphogen" in Figure 5.1).

5.2 Artificial expression boundaries

We also examined how bond asymmetry and growth rate might be affected by artificial expression boundaries. To this end, we marked a circular cluster of cells in the simulation that was concentric with the whole disc, and altered either morphogen concentration or the Fj or Ds expression rate in the marked cells. We then examined the degree of bond asymmetry and the growth rate as functions of distance from the cluster's edge. Furthermore, we varied the radius of this "clone" and compared the results when the clone boundary lay inside versus outside the wing primordium boundary.

5.2.1 Fj overexpression

Clones of cells that overexpress Fj or Ds in an otherwise wild-type background exhibit nonautonomous proliferation near their edges [9]. This effect is most pronounced in the region of the disc that does not normally produce much of the protein that the clone is overexpressing. (For example, clones that overexpress Fj exhibit more nonautonomous growth when they are in the periphery of the disc, which normally expresses low levels of Fj.) We increased the rate of Fj expression in a circular cluster of cells concentric with the whole disc, i.e., a circle whose center coincides with the center of the disc. We then examined the degree of bond asymmetry (Figure 5.2) and the growth rate (Figure 5.3) as functions of distance from the circle's edge. By altering the radius of this "clone", we can examine how the position of the clone boundary changes the nonautonomous effects on growth. In our model, clusters of cells overexpressing Fj show the most nonautonomous growth in the outer (proximal) regions of the disc that express little endogenous Fj.

When elevated Fj expression is induced in a clone concentric with the disc, the resulting Ft-Ds bond asymmetry and cell growth are comparable to those in the wild-type disc when the clone's edge is within or near the Fj/Ds expression front. In this case, the cells in the clone do not have much more Fj than is expressed endogenously in this region, so the behavior is much like that in the wild-type disc (Figures 5.2 and 5.3, panels A and B). However, when the clone's boundary lies outside the usual Fj/Ds expression front, we see increased bond asymmetry and faster growth rates near the clone's boundary (Figures 5.2 and 5.3, panels C and D). In this case, the cells outside the clone's boundary have much less Fj than those within the clone, leading to an increase in bond asymmetry and an increase of growth rate among cells near the boundary, consistent with experimental results.

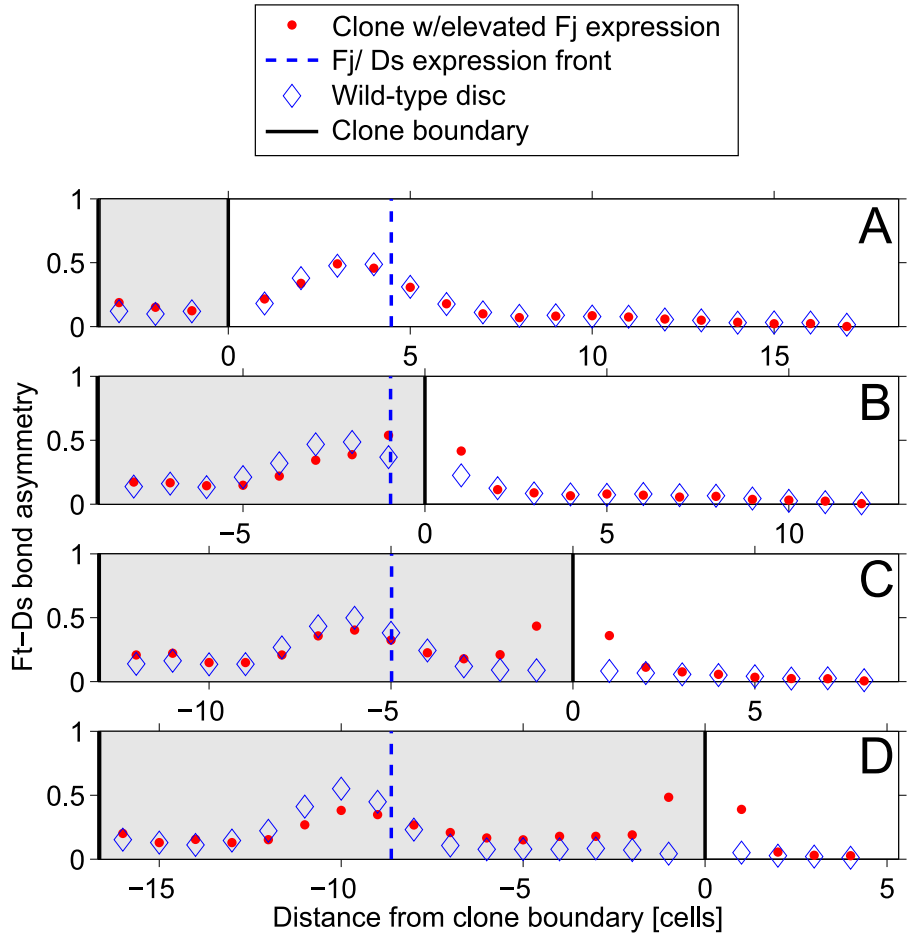

Figure 5.2: Bond asymmetry near a Fj-overexpressing clone 400 time steps (i.e., 400 minutes) after induction. In separate runs, circular clusters or "clones" of cells concentric with the disc were induced at time step 50 with different radii (0.2 times the disc's overall radius in A, 0.4 in B, 0.6 in C, and 0.8 in D). This allows the disc to be roughly radially symmetric in terms of morphogen, Ft, Ds, and Fj expression. The horizontal axis indicates the distance in cells from the clone's boundary (vertical black line); negative values are inside the clone (shaded background) and positive values are outside the clone (unshaded background). The vertical axis is the average degree of asymmetry in bound Ft among all cells with a given distance from the clone boundary, calculated via the adjusted minimum fraction metric. (A) Cells in a disc with a Fj-expressing clone (red dots) have similar amounts of bond asymmetry as those in a wild-type disc (blue diamonds) when the clone is within the Fj/Ds expression front (dashed vertical blue line), since this region of the disc already has a high Fj concentration. (B, C, D) When the clone boundary is outside the front, however, the steep discrepancy in Fj between adjacent cells leads to greater bond asymmetry both inside and outside the clone boundary.

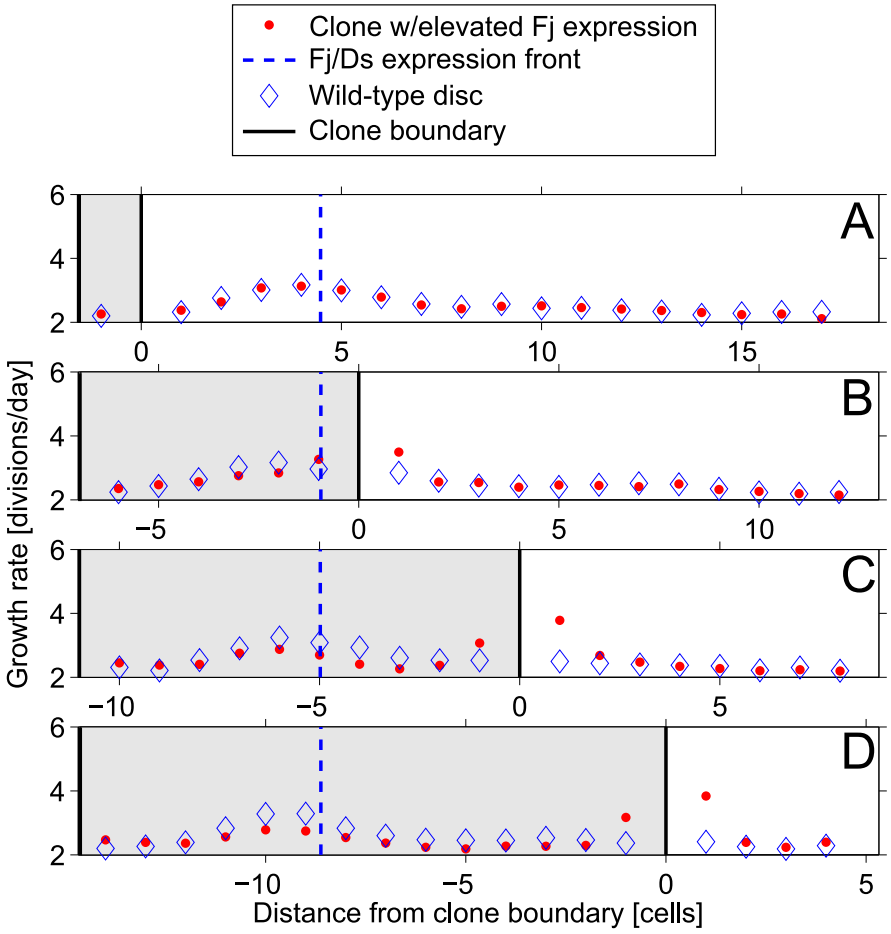

Figure 5.3: Cell growth rate in a disc with a Fj-overexpressing clone. Conditions are the same as in Figure 5.2, except that growth rate in divisions per day is plotted on the vertical axis. The growth rate here is expressed in terms of the ratio of a cell's radius at one time step to its radius at the previous time step. When the clone boundary (solid vertical black line) is outside the front (vertical dashed blue line), the growth rate is elevated near the clone's boundary on either side. This is because the Fj-overexpressing cells of the clone are next to the Ds-expressing cells of the disc's periphery.

5.2.2 Ds overexpression

In our model, a Ds-expressing clone concentric with the disc exhibits increased bond asymmetry (Figure 5.4) and increased growth (Figure 5.5) when the clone's boundary is within the Fj/Ds expression front. In this case, the cells just outside the clone's boundary express much less Ds than the cells inside the clone, leading to an increase in bond asymmetry near the boundary. Experimentally, cells near the edge of a Ds-expressing clone are observed to proliferate faster when they are near the disc's center [9]. Our simulations are consistent with this result; Ds clones whose boundaries are near the center of the disc exhibit more proliferation near their edges than Ds clones whose boundaries are near the disc's periphery.

5.2.3 Morphogen overexpression

Experimentally, when elevated Dpp signaling is induced in a clone of cells (e.g., via constitutively active Tkv), nonautonomous effects on cell proliferation are visible via BrdU incorporation [44]. Cells in the clone express both more Fj and less Ds than cells adjacent to the clone [9], presumably leading to elevated bond distribution asymmetry and thus faster proliferation near the clone boundary. To study this, we did simulations to compare a wild-type disc to a disc with a circular clone. The edge of the clone and the wing disc boundary are concentric circles. The clone has morphogen signaling at a level, constant in space and time, that is higher than that of wild-type (analogous to cells expressing activated Tkv). Outside the clone, the cells are wild-type and are subjected to an exponentially decaying morphogen profile. Figure 5.6 shows the degree of bond distribution asymmetry at different radial positions within the simulated discs. When the clone is large enough that its boundary lies outside where the Fj/Ds expression front would be in the wild-type disc, a dramatic increase in bond distribution asymmetry can be seen both inside and outside the vicinity of the clone's border. This is because the Fj-expressing cells of the

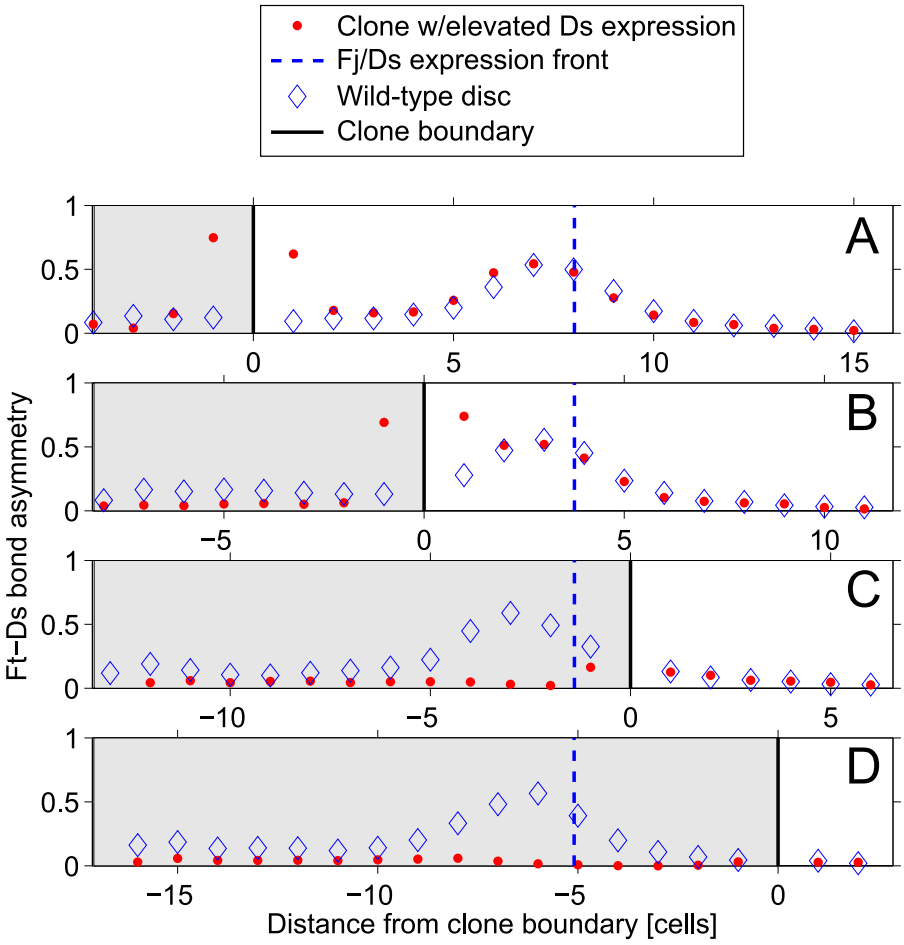

Figure 5.4: Bond asymmetry near a Ds-expressing clone (red dots) 400 time steps (i.e., 400 minutes) after induction compared to that in a wild-type disc (blue diamonds). Again, the clone's radius is 0.2, 0.4, 0.6, and 0.8 that of the disc in A, B, C, and D, respectively. (A, B) Note that the nonautonomous effect on growth is strongest when the clone boundary (vertical black line) is in the central region of the disc, where endogenous Ds expression is lowest. In the interior of the clone (negative numbers) far from the boundary, bond asymmetry is low, since Ds is available uniformly within the clone. (C) When the clone boundary nearly coincides with the location of the front (vertical dashed blue line), the peak of bond asymmetry is smaller because cell-cell differences in Ds expression are less pronounced. (D) When the boundary of the clone is near the Fj/Ds expression front, bond asymmetry is uniformly low, because the disc then has uniformly high Ds expression.

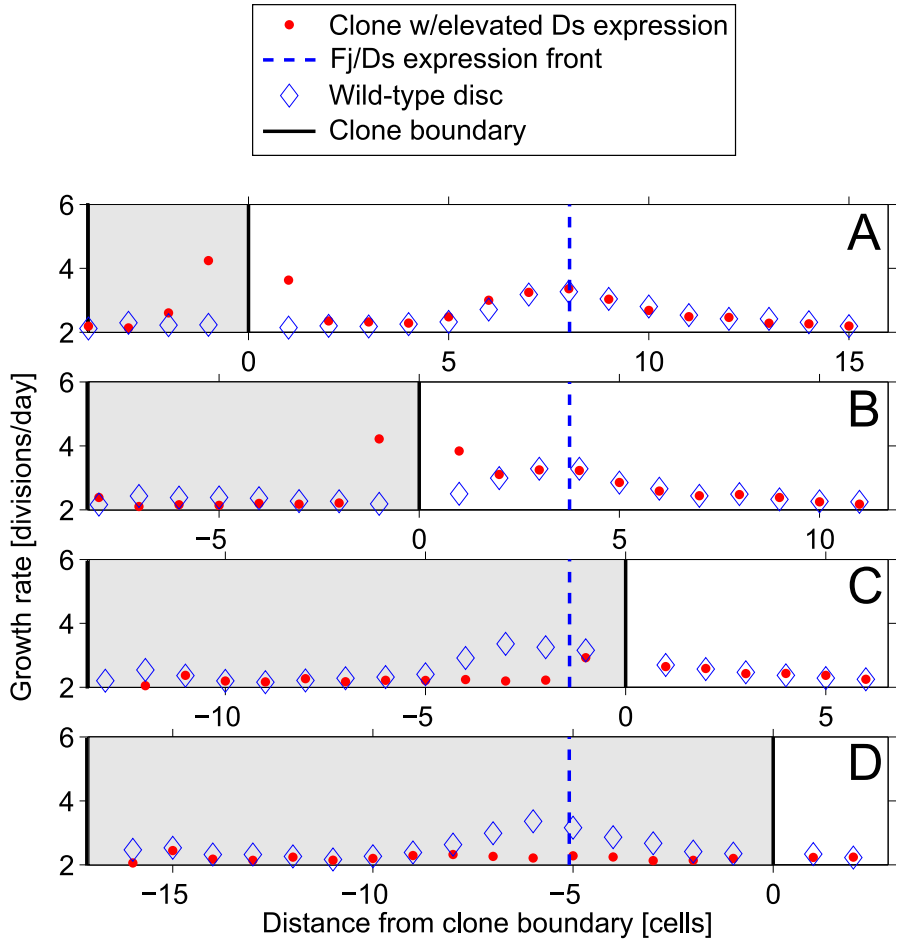

Figure 5.5: Growth rate near a Ds-expressing clone. Conditions are the same as in Figure 5.4, except that the vertical axis now represents growth rate in divisions per day. (A, B) The proliferation rate is fastest at the clone border when it lies within the wing primordium due to the increased bond asymmetry. (C) When the clone is large enough that its boundary is near the expression front, growth is slower because bonds are symmetric compared to those in a wild-type disc. (D) When the clone is large enough to span the entire wing pouch, Ds expression is uniformly high, leading to symmetrically distributed bonds and a low growth rate throughout the disc.

clone are juxtaposed next to the Ds-expressing cells of the disc's periphery, rather than the Fj-expressing cells in the wing primordium. Figure 5.7 shows the corresponding cell growth rates when a morphogen-overexpressing clone is induced; in addition to the increased growth seen due to the autonomous effects of morphogen signaling, regions with increased bond asymmetry also proliferate faster.

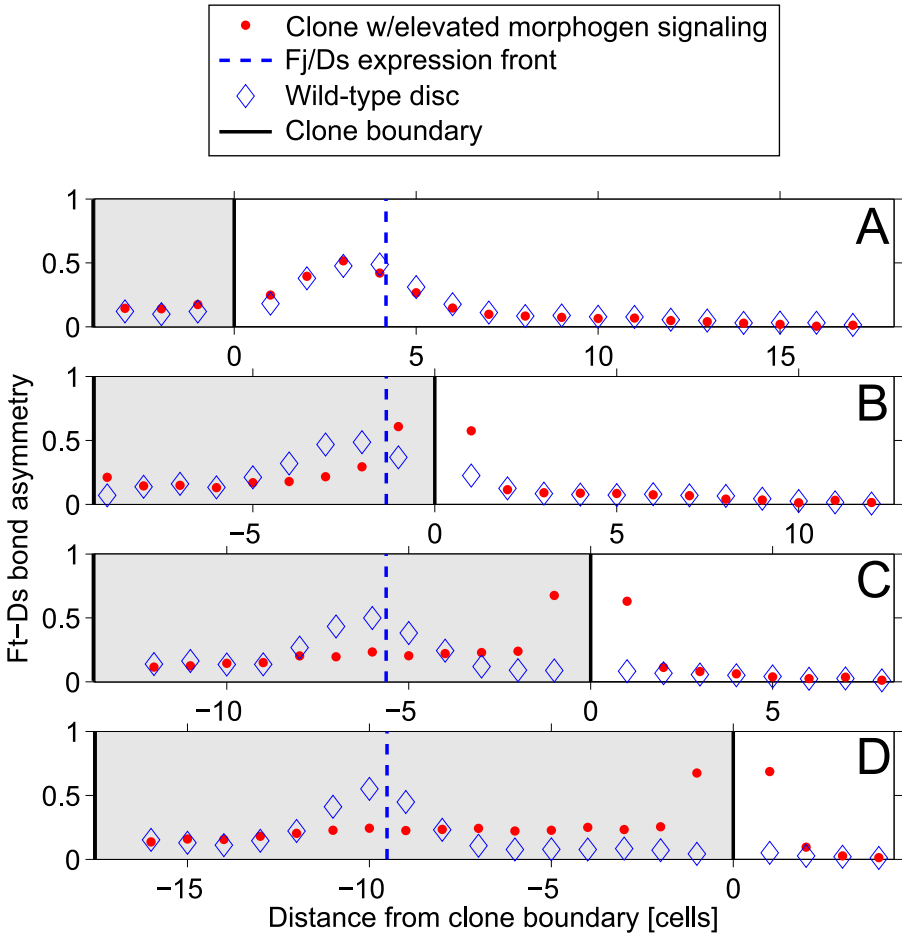

Figure 5.6: Bond asymmetry in a disc with a clone whose morphogen signaling is elevated (red dots), 400 time steps (i.e., 400 minutes) after induction, compared to bond asymmetry in a wild-type disc without a clone (blue diamonds). The clone's radius is 0.2, 0.4, 0.6, and 0.8 that of the disc in A, B, C, and D, respectively. The Fj/Ds expression front is indicated by the dashed vertical blue line. The horizontal axis indicates the distance in cells from the clone boundary (vertical black line); negative values are inside the clone (shaded area), and positive values are outside the clone (unshaded area). The center of the disc is at the left edge of each plot. The vertical axis is the average degree of asymmetry in bound Ft among all cells with a given distance from the clone boundary. We measure asymmetry as one minus the adjusted minimum fraction of bound Ft. An asymmetry of 0 indicates an even distribution of bound Ft (leading to slower growth), while an asymmetry of 1 indicates at least one neighbor with no bonds (leading to faster growth). Note that the nonautonomous effect on bond asymmetry is most pronounced when the boundary is outside the Fj/Ds expression front (B, C, and D), where morphogen concentration is lowest. Also note that the effect extends multiple cells from the boundary on both sides, particularly in D.

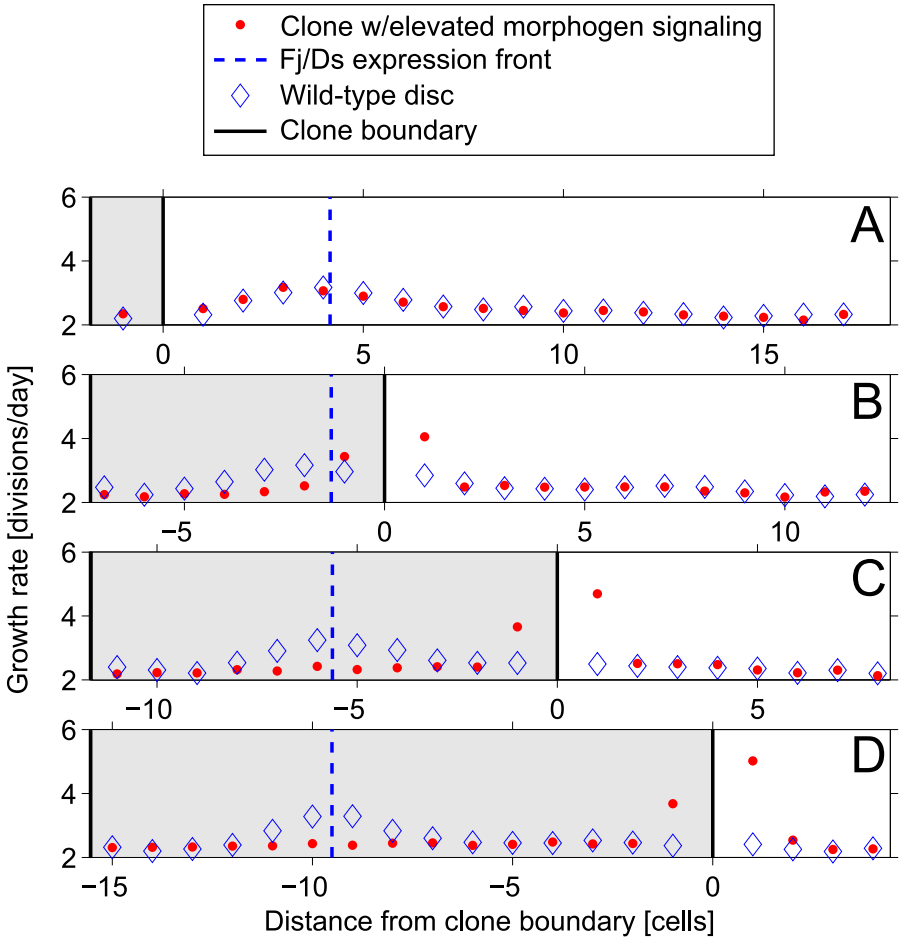

Figure 5.7: Cell growth rate in a disc with a clone whose morphogen signaling is elevated (red dots) compared to that in a wild-type disc (blue diamonds). The location of the Fj/Ds expression front (or the boundary of the wing primordium is marked by the vertical blue dashed line. We measure the growth rate in cell divisions per day (each time step corresponds to 1 minute of real time, so a day is 1440 time steps). Conditions are the same as in Figure 5.6. Again, the nonautonomous effect on growth is strongest when the clone boundary is near the disc's periphery (C and D), where the morphogen concentration is normally lowest. This effect spans the width of multiple cells near the clone's boundary. Note the autonomously increased growth within the clone compared to wild-type due to the increased morphogen signaling.

5.3 Spatial patterns of cell growth

To test the idea that morphogen signaling and bond asymmetry form complementary spatial patterns in the growth rate, we recorded the location of each cell division and the growth rate of each cell, along with the contributions of morphogen signaling and bond asymmetry to the overall growth rate, over many runs of the simulation. For the sake of comparison, we also did a set of runs where Fj and Ds expression were independent of morphogen signaling, and the expression front was stationary in terms of its relative position (i.e., its distance from the disc's center in terms of the disc's overall radius). In these runs, the front remained at roughly 85% of the disc's radius throughout the run. This distance was chosen because it is approximately the same as the final position of the front in a normal (i.e., wild-type) run. This set of runs allowed us to see whether the motion of the front with respect to the cells was necessary for the patterns of growth seen experimentally, or if instead the pattern of cell proliferation was robust to the front's movement.

5.3.1 Moving front

Figure 5.8 shows the overall growth rate (black) as well as the contribution to the growth rate due solely to morphogen signaling (green) or solely to bond asymmetry (blue) as a function of radial position within the disc. Cells near the Fj/Ds expression front (vertical black line) exhibit faster growth due to bond asymmetry, while cells near the center exhibit faster growth due to morphogen signaling. As the expression front moves outward, the wing primordium (i.e., the area of the disc lying inside the front) exhibits complementary patterns of growth signaling due to bond asymmetry and morphogen concentration. The net effect from these two signals is comparatively uniform growth throughout the wing primordium. Because these patterns counterbalance each other, the overall growth rate

should be more uniform throughout the wing pouch than the contributions from either morphogen signaling or bond asymmetry alone.

The profile of growth rate is not a direct reflection of the spatial profile of the morphogen concentration or of the bond asymmetry because the growth rate is subject to integral feedback (see Section 3.6). As a result the growth rate gradually adapts to a constant signal. So cells that have had asymmetric bonds for most of the run will grow more slowly than cells that have recently undergone an increase in bond asymmetry. This means that the cells in the center (the distal cells) will respond less to their bond distribution asymmetry than the cells at the front (the proximal cells). The overall effect is a signaling gradient; growth due to bond asymmetry will be stronger near the front and weaker at the center of the disc.

Morphogen signaling in our model is strongest at the center of the disc and weakest at the edge, and its amplitude increases over time. The growth rate used in the simulation is affected by the integral feedback adaptation mechanism described above. This means that regions where the morphogen concentration increases rapidly (i.e., the center of the disc) experience more growth due to morphogen signaling than regions where the concentration increases slowly (i.e., the disc's periphery). The result is a profile of morphogen-driven growth that is still fastest in the center and slowest at the edge. This pattern is roughly complementary to the pattern of growth induced by bond asymmetry. The overall growth rate, which is essentially the superposition of these two effects, is more uniform throughout the wing pouch than the contributions from either morphogen signaling or bond asymmetry alone. It may be this superposition that leads to the roughly uniform cell proliferation observed experimentally.

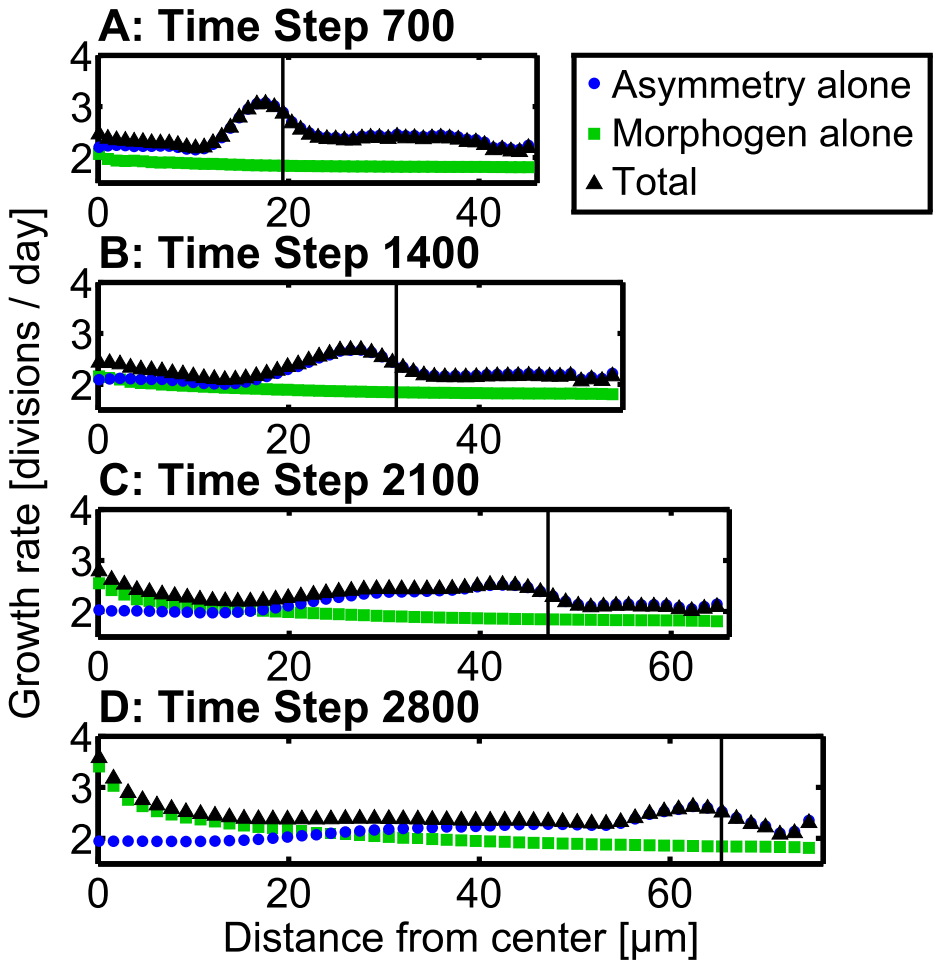

Figure 5.8: Growth rates due to morphogen signaling and Ft-Ds bond asymmetry form complementary patterns. The horizontal axis is the absolute position of cells within the disc, measured from the center (left) to the edge (right). The vertical axis shows the actual growth rate in divisions per day (black), along with the value of the growth rate due only to bond asymmetry (blue) or morphogen signaling (green), averaged over 20 runs of the simulation. The transition region (vertical black line), which corresponds to the border of the prospective wing blade, moves radially outward over time, so that the wing primordium takes up an increasing fraction of the disc. Cells that have had this front pass over them recently (i.e., cells near the front) have the highest growth rate due to bond asymmetry. Cells near the disc's center experience the most morphogen signaling and the highest associated growth rate. The two patterns are complementary, such that their product (essentially, the overall growth rate) is more uniform throughout the wing pouch than either profile alone.

5.3.2 Stationary front

Next, we consider a disc in which the Fj and Ds expression rates are unaffected by the changing morphogen concentration. In this case, the morphogen profile is the same as with the moving front; its amplitude increases exponentially in time and its decay length scales with the disc's radius. However, the Fj/Ds expression front in this case does not sweep over cells; its position is fixed at about 85% of the disc's radius. When the Fj/Ds expression front does not move, only the cells near this front (and their descendants) will ever experience substantial spatial gradients of Fj and Ds. The only relative motion between the cells and the front in this case is due to cell proliferation; cells can push their neighbors aside as they grow and divide. Most cells in this disc, then, will express roughly constant amounts of Fj and Ds for the duration of the run. In this case, only an annulus of cells near the front experience elevated bond asymmetry and the resulting growth. This growth is further reduced due to the adaptation mechanism, since bond asymmetry is consistently high in these cells. Since the morphogen profile is unchanged from wild-type, however, morphogen signaling will continue to drive cell growth near the disc's center. The result is a pattern of cell proliferation that is dominated by morphogen signaling with relatively little contribution from bond asymmetry (Figure 5.9).

5.4 Patterns of cell proliferation

We now compare the effects of the stationary and moving fronts on the pattern of actual cell divisions within the model. Figure 5.10 shows the spatial distribution of cell divisions in discs with moving and stationary fronts. With a moving front (panel A), the complementary, counterbalancing effects of morphogen signaling and bond asymmetry lead to proliferation throughout the wing pouch, i.e., the region inside the front. When the front is stationary in terms of its relative location between the disc's center and edge (panel B), cells near the front adapt to the consistently high bond asymmetry and the

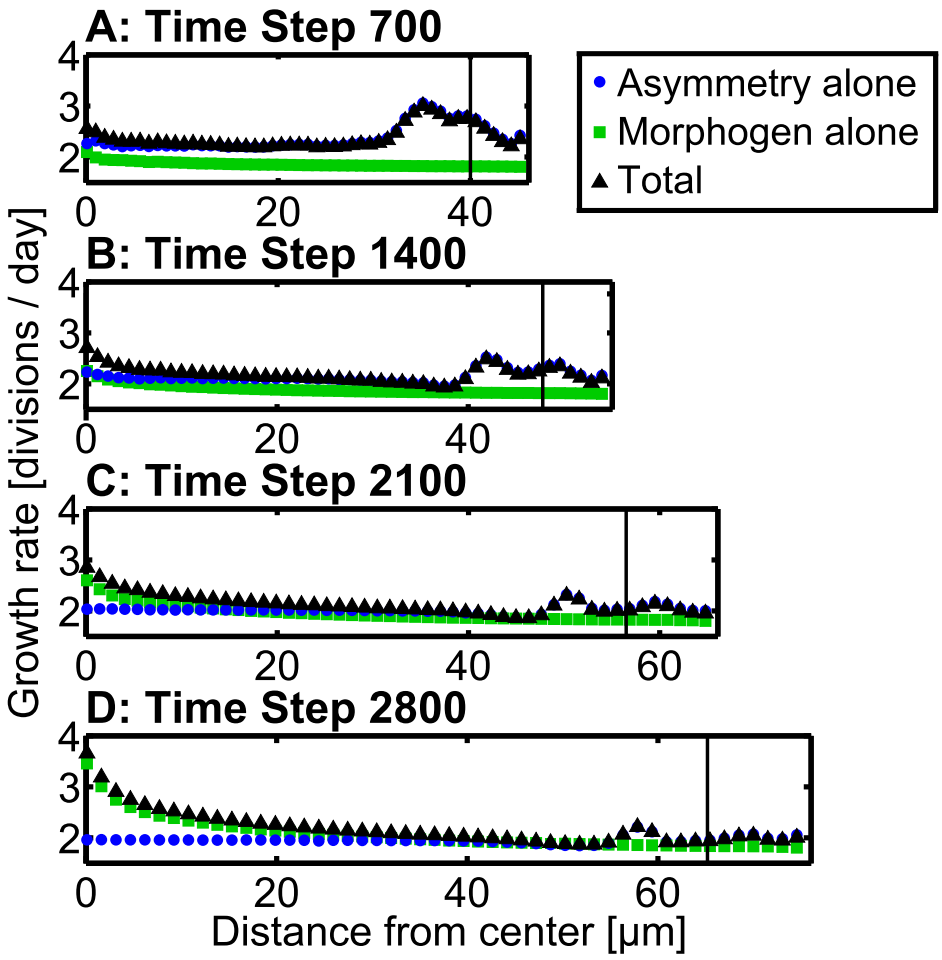

Figure 5.9: A stationary Fj/Ds expression front leads to a diminished effect on growth rate due to bond asymmetry. Again, the horizontal axis is the relative position of cells within the disc, with the disc's center on the left and the edge on the right. The vertical axis represents the overall growth rate in divisions per day (black), and the growth rates due solely to bond asymmetry (blue) and morphogen signaling (green), averaged over 20 runs. When the Fj/Ds expression front (vertical black line) is stationary, in terms of its relative position between the cell's center and edge, the effect of bond asymmetry is most prominent near the front, forming a small peak (seen at approximately 85% of the disc's overall radius). This effect fades over time due to the adaptation mechanism, since the cells near the front are experiencing a fairly constant amount of bond asymmetry. The resulting pattern of cell growth is then dominated by morphogen signaling, rather than by counterbalancing patterns of morphogen signaling and bond asymmetry.

effect on growth rate near the expression front is lessened with time, so that the effect of morphogen signaling dominates. The result is a narrower peak of cell proliferation at the disc's center corresponding to the region of highest morphogen signaling. This region does not encompass the majority of the wing pouch. Again, this result suggests that the expansion of the Fj expression domain seen experimentally results in a more uniform pattern of cell proliferation. Note that in both panels, the front has approximately the same location; it is roughly two-thirds of the way between the disc's center and edge. The two cases, then, differ in their history but not in their instantaneous states.

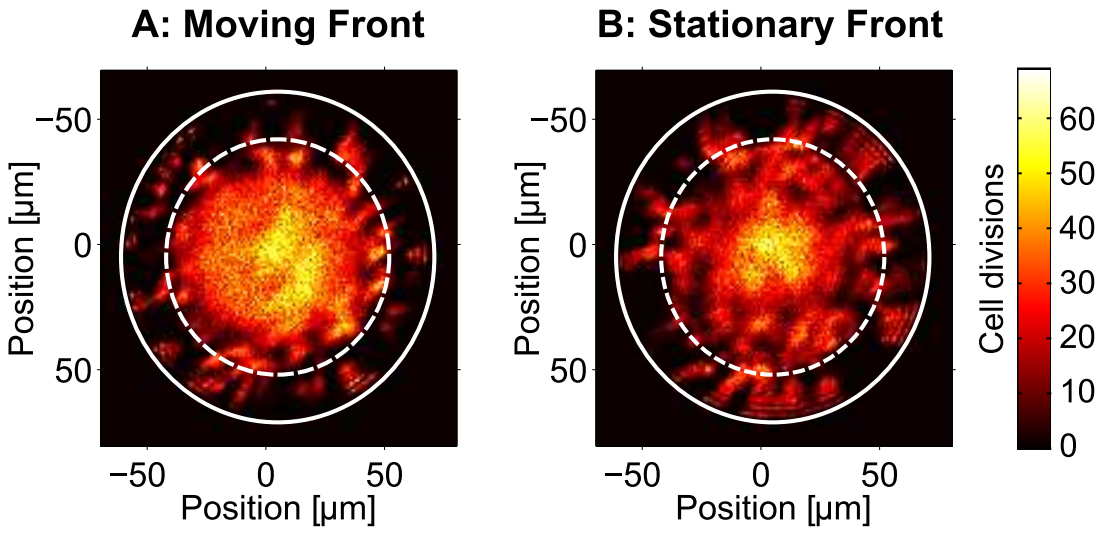

Figure 5.10: A moving front of Fj/Ds expression leads to more uniform proliferation within the wing pouch than a stationary front. The figure shows the total number of cell divisions in each 1 μm $\times$ 1 μm square in a 60-minute period (time steps 2040 to 2100) summed over the course of 350 runs of the simulation is plotted as a function of two-dimensional position. The outer edge of the whole disc is indicated by a solid circle; the approximate location of the Fj/Ds expression front is a dashed circle. This expression front roughly corresponds to the boundary of the wing pouch. Note that the location of the front is roughly the same in both panels, indicating that the instantaneous Fj and Ds expression patterns are also the same in both panels. When the front is moving (A), the interior of the wing pouch shows a wide plateau of fast cell proliferation. In the case of a stationary front (B), however, there is a narrow peak of proliferation in the very center of the pouch resulting from autonomous morphogen signaling, surrounded by a faint ring of slightly elevated proliferation due to steep local gradients in Fj and Ds expression. Thus, the pattern of cell proliferation in the disc is dependent upon the movement of the Fj/Ds expression front, even when the instantaneous Fj and Ds expression rates are the same.

Chapter 6: Discussion

6.1 Overview

The cells of the *Drosophila* wing imaginal disc proliferate roughly uniformly in space [2, 20,22], despite the nonuniform concentrations of signaling molecules such as the morphogens Dpp and Wg that are necessary for normal growth. These cells are also polarized in the plane of the tissue, even though Ft, Ds, and Fj (all proteins involved in cell polarization) have a fairly flat spatial concentration profile in most of the tissue. However, these concentration profiles are not static. Rather, the amplitude of the Dpp profile increases with time [45] and the boundary between the Fj-expressing and Ds-expressing regions of the tissue expands outward over time, sweeping over a large fraction of the disc [58]. Our model describes both how these dynamics produce uniform cell proliferation from nonuniform signals and how cells with spatially uniform signaling levels become polarized.

A cell's growth rate and polarization in our model are determined in part by the spatial distribution of the Ft-Ds bonds that the cell forms with its neighbors. The concentrations of bindable Ft and Ds have a steep slope in a small region of the disc (referred to as the "transition region") and are relatively uniform in the rest of the tissue. If the arrangement of Ft-Ds bonds on each cell were determined only by the instantaneous spatial concentration profiles of bindable Ft and Ds, we would expect bonds to be asymmetrically distributed only on cells in the proximity of the transition region. This is because adjacent cells in this region would have substantially different amounts of bindable Ft and Ds. Similarly, we would expect bonds to be symmetrically distributed on cells far from the transition region, where all cells have similar amounts of available Ft and Ds. However, the concentration profiles of available Ft and Ds change over time as the transition region sweeps radially outward. We find that cells retain a "memory" of the steep Fj and Ds gradients in the form of their bond arrangement. If the transition region passes over many cells, then it

can pattern a large portion of the disc. In other words, a cell's Ft-Ds bonds start with a symmetric arrangement, become more asymmetrically arranged when it is within the transition region, and then remain asymmetric after the transition region has passed over it. This bond asymmetry can even persist after a cell divides, since cells can quickly form new Ft-Ds bonds at the new interface between the two daughter cells. These mechanisms allow cells in the entire wing primordium (i.e., the area inside the transition region) to have asymmetric Ft-Ds bonds, consistent with the polarization seen experimentally [10].

6.2 Model design choices

Not every aspect of our model corresponds to a specific experimental result. Here, we motivate a variety of choices we made when designing the model.

6.2.1 Minimum fraction metric

We note that the asymmetry of Ft-Ds bonds around a cell may be defined in a number of ways. However, in order to relate bond asymmetry to Dachs localization on the side with the least bound Ft [9, 11, 95], we chose to measure the asymmetry of the bond distribution using only the neighbor with the fewest bonds. This was primarily so that a cell with no Ft-Ds bonds at all (e.g., a *ft-* or *ds-* cell) would exhibit the strong overgrowth seen experimentally [86]. Cells with no bonds in our model would be treated as having a minimum fraction of zero, and thus very high asymmetry.

One could also argue that such cells have very low asymmetry, since they have the same number of bonds (i.e., zero) with each of their neighbors. However, other factors also make this mechanism a plausible one. In particular, the myosin Dachs is observed to localize to the side of each cell with the least bound Ft [9], suggesting that Ft signaling may involve mechanotransduction. Ft signaling is also known to affect microtubule orientation and mitotic angle [39], indicating a link with cytoskeletal organization. In addition, Yorkie,

which is downstream of Dachs in the Ft pathway, is homologous to YAP (Yes-associated protein). YAP is a transcriptional coactivator associated with cell-ECM interactions and mechanotransduction [100]. We speculate that the Ft pathway may be involved in sensing the mechanical stresses that a cell experiences from its neighbors, and in how cells proliferate in response to these stresses. However, our model does not address these effects directly. Rather, it is primarily the asymmetry in the distribution of Ft-Ds bonds around a cell that affects growth. We speculate that this asymmetry may be sensed via mechanical tension in the cytoskeleton from the Ft-Ds bonds. This is a separate mechanism from the bulk mechanical forces in our model that only prevent adjacent cells from overlapping or separating. In our model, these mechanical forces do not directly affect a cell's growth rate.

6.2.2 Morphogen profile

In our model, the movement of the front of Fj/Ds expression is driven solely by the increasing amplitude of the morphogen profile. We chose this mechanism largely for its simplicity; it makes few assumptions about other signaling pathways. However, recent studies have shown that discs with spatially uniform Dpp signaling still exhibit a pattern of Fj and Ds expression roughly resembling that in wild-type discs, with Fj expressing dominating in the center and Ds at the edge [25]. In our model, a disc with uniform morphogen expression would uniformly express Fj at a high rate and Ds at a low rate and not have a transition region. Other mechanisms besides morphogen signaling may underlie Fj and Ds expression, such as the recruitment of cells from the Ds-expressing periphery into the Fj-expressing wing primordium [58]. Fj expression is also affected by the levels of Ft, Dachs, and Ds, suggesting mechanisms for movement of the front. In particular, Fj expression is upregulated in Ft mutant clones [95] so that the front could be accelerated by decreasing Ft expression. Fj is downregulated in Dachs mutant clones [95] so that the front could be slowed by reducing Dachs expression. Clones that overexpress Ds reveal elevated

levels of nonautonomous Fj on both sides of their boundaries [57], suggesting that the front could be accelerated by increasing the Ds gradient at the front. Other models have also suggested that mechanical compression affects Fj and Ds activity [109]. The exact relationship between morphogen signaling and Fj and Ds expression merits further study.

For the sake of simplicity, our model conflates Dpp (which is expressed along the anterior-posterior compartment boundary) and Wg (which is expressed between the dorsal and ventral halves) into a single quantity with radial symmetry. If we were to use two separate profiles corresponding to Dpp and Wg and use their sum to drive Fj and Ds expression, our results would be qualitatively similar, but with a lozenge shape rather than radially symmetric. However, no particular evidence exists that Wg signaling affects Fj and Ds expression in a similar way to Dpp.

6.2.3 Ft/Ds kinetics

Several features of this model are dependent upon parameter values. The degree to which cells retain their polarization after the Fj/Ds expression front has passed over them, for example, is fairly parameter-dependent. The rate at which Ft-Ds bonds turn over (i.e., dissolve and are possibly replaced with different bonds) is on the order of 1% per time step. This figure is dependent on several parameters, but depends most strongly on the degradation rate of free Ft and Ds and the rate of dissociation of Ft-Ds bonds. (Note that only free, not bound, Ft or Ds can be degraded in our model since endocytosis is usually involved in the degradation of receptors.) Under normal conditions, these rates are both 8% per time step. If one of these rates is too low, say halved to 4% per time step, a cell's bond distribution will be insensitive to changes in the Fj and Ds expression rates, thus limiting the ability of a moving front of Fj and Ds expression to increase the degree of bond asymmetry in nearby cells. In other words, each cell's pool of bindable Ft and Ds would change too slowly to reflect the changes in Fj and Ds expression caused by the

movement of the front. However, if one of the rates of bond dissociation or free Ft/Ds degradation is high, the steady-state amounts of Ft and Ds will be lower. (Note that only free, not bound, Ft or Ds can be degraded in our model.) For example, if the degradation or dissociation rate is increased to 16% per time step, cells will exhaust the Ft and Ds available to form bonds. (Under normal conditions, cells in our model express 20 new Ft molecules per time step, and between 4-20 new Ds molecules per time step; however, not all of these will ultimately form bonds.) So in the case of a high degradation or dissociation rate, a substantial number of cells will have no bonds, causing the simulation to treat them like *ft* or *ds* mutant cells. This will lead to overgrowth in areas of the disc that are far from the transition region, since these parts of the disc have the least bindable Ft or Ds.

6.3 Future work

Our results both address and raise questions about the relationships between cell-cell signaling, tissue growth, and patterning. Here, we suggest directions for future work, both theoretical and experimental, based on the model.

6.3.1 Experiments on Ft/Ds/Fj kinetics

The model relies on the idea that the Fj and Ds expression domains change over time; that is, individual cells will go from expressing primarily Ds to expressing primarily Fj as the boundary of the wing primordium expands. In the model, cells retain their bond distribution for some time after the front has passed over them, allowing the bonds to be asymmetric even when the Fj and Ds concentrations are locally flat and the cells have divided several times. This effect is to some extent dependent on some parameters of Ft-Ds interaction, particularly the rates of bond dissolution and degradation of free Ft and Ds, as described above. It may be possible to measure these parameters experimentally.

For example, to measure the rate of bond dissolution and investigate the relationship between bond asymmetry and growth rate, one could halt the expression of either Ft or Ds in part of an otherwise wild-type disc. The expression of a gene can be induced in a single clone via, for example, treatment with a drug [44]. If this gene coded for an RNA that inhibited Ft or Ds expression (similar to those used in [10]), the resulting clone would have its Ft or Ds expression rates dramatically lowered after delivery of the drug. Consider a clone of cells in which Ft expression is suddenly stopped. In our model, this would drastically slow the formation of new Ft-Ds bonds, since no new Ft will be expressed and existing Ft would continue to degrade. Eventually all the existing bonds would dissolve, leading to cells with no bonds. We would then expect the overall number (but not the distribution asymmetry) of bonds to decline over time. Both the quantity and distribution of bonds could in principle be observed by measuring the intensity of fluorescently labeled Ft near cell interfaces (as in [10]) at different times after Ft expression is inhibited. Measuring the time scale over which Ft localization changes occurs would offer some insight into the dissociation rate of Ft-Ds bonds. According to our model, such an experiment would cause the clone's growth rate to stay fairly constant (or even decrease due to the new excess of free Ds), until suddenly the growth rate would increase when cells lose all of their bonds. A similar reversal in growth rate is seen experimentally; discs with reduced Ft expression undergrow [108] but discs mutant for Ft overgrow [51, 84–86].

An experiment of this kind could also give more insight into the relationships between Ft-Ds binding, Dachs localization, and growth. For example, in a clone that suddenly stopped expressing Ft, it would be interesting to determine the overall pattern of Ft and Ds localization by adopting the techniques used to observe Ft and Ds localization in a wild-type disc [10]. In particular, one could investigate whether the Ft and Ds distributions in individual cells change with time, or if the bonds retain their distribution pattern as they dissolve. We predict that the total number of bonds will decay exponentially with a characteristic time scale on the order of hours while retaining a similar degree of

asymmetry. Since Dachs localizes preferentially but not exclusively to the distal side of cells in wild-type discs [9, 11, 95, 99], it would be worthwhile to measure Dachs localization at cell membranes as a function of time in this clone. Such an experiment would determine whether Dachs localization responds to the (presumably stable) distribution pattern of Ft-Ds bonds, the (presumably decreasing) overall number of bonds, or some combination. In addition, watching how the number of cells in this clone changes over time would show whether the clone acts as a Ft mutant and overgrows once all its Ft has degraded, and (if so) the time scale over which this happens, giving us a better picture of the dissolution rate of Ft-Ds bonds.

We can imagine a similar experiment to measure the degradation rate of free Ft and Ds. Suppose a *ft* single mutant disc suddenly has its Ds expression halted in a clone as well. By measuring the overall amount of Ds in the clone, perhaps by measuring the intensity of fluorescently labeled Ds as a function of time [10], we can find the rate at which free Ds degrades, since all the Ds in the disc should be free. A corresponding experiment–halting Ft expression in a Ds mutant disc–would yield the degradation rate of free Ft.

6.3.2 Experiments involving twin clones

If mitotic recombination is induced in a cell (i.e., if portions of two chromosomes in a homologous pair switch places), the two daughter cells can inherit different sets of genes. This technique allows for adjacent "twin spot" clones with different phenotypes from one another and potentially different from their background [113]. Experiments of this kind, then, can create three different types of cell-cell interfaces: one between the two clones, and one between each clone and the background.

This feature may make twin spots particularly useful for studying the Ft pathway, since Ft signaling involves the interaction between adjacent cells (S. Fraser, personal communication, 2012). Altering Ft, Ds, or Fj expression in twin clones could offer new

insight into how Ft, Ds, and Fj interact. In particular, we would expect twin clones where one clone underexpresses Fj and the other overexpresses Fj to have different Ft-Ds binding affinities [55, 56], differing both from one another and from the wild-type background. In our model, the phosphorylation rates of Ft and Ds in a cell increase monotonically with the amount of Fj in that cell. In experiments, phosphorylated Ft and unphosphorylated Ds appear to have greater binding affinities [55, 56]. In our model, bonds only form between phosphorylated Ft and unphosphorylated Ds. Thus we would expect to see the greatest number of Ft-Ds bonds at the interface between these two clones, because the clone overexpressing Fj would have the most available Ft and the clone underexpressing Fj would have the most available Ds. This prediction assumes that the Ft and Ds binding affinities depend roughly linearly on the amount of Fj. If, instead, the dependence of these binding affinities on the Fj concentration is described by (for example) a steep Hill function, we would find that one of the two clones behaves similarly to the surrounding wild-type cells since the wild-type cells would be in the regime of low or high Fj. In this case, there would be as many Ft-Ds bonds at the interface between the two clones as there would be at the interface between the other clone (the one with altered binding affinities) and the wild-type background.

In our model, cells form new Ft-Ds bonds independently of existing bonds; they simply try to form as many new bonds as possible with each neighbor at each time step. However, another model [108] has suggested that Ft-Ds binding exhibits cooperativity; i.e., cells are more likely to form new bonds in the same configuration as existing ones. In other words, if a bond involves the Ft in cell A binding to the Ds in cell B, additional bonds between the cells will be more likely to involve Ft molecules from A and Ds molecules from B. Twin spot experiments could provide insight into how cells form Ft-Ds bonds with their neighbors. For example, consider two adjacent clones: one overexpressing Ft compared to the background, and one underexpressing Ft. At the interface between these two clones, we would expect the majority of the bonds to involve a Ft from the Ft-overexpressing clone and a Ds from

the Ft-underexpressing clone. However, both clones (and the background) have the same amounts of Ds available to bind. So if the formation of new bonds is independent of the existing bond arrangement, we would expect the Ft-underexpressing clone to bind its Ft in similar quantities at all interfaces since all interfaces have the same amount of Ds. If, however, formation of ft-Ds bonds at an interface tends to inhibit the formation of Ds-Ft bonds at the same interface, we would expect the Ft-underexpressing clone to bind much less of its Ft at the interface with the Ft-overexpressing clone. Twin-spot experiments, then, may be able to tell us whether existing bonds can inhibit the formation of bonds with the opposite polarity.

6.4 Omissions

Several phenomena remain unexplained by our model. For example, the model shows that complementary patterns of morphogen and Ft signaling can lead to fairly uniform growth in the wing pouch (i.e., within the wake of the expression front). It does not address what causes the cells outside the wing primordium (the cells that have never been near the front) to proliferate. Since these cells experience little morphogen signaling and consistently have high Ds and low Fj expression rates, our model would predict that cells outside the wing primordium would grow more slowly than cells within it. However, studies of the uniformity of cell proliferation in the disc have focused largely on the cells within the wing pouch, not those in the hinge region. Further exploration is necessary to determine what signaling pathways control growth in the periphery of the disc.

Experimentally, nonautonomous proliferation around clones with altered Dpp, Fj, or Ds signaling have been shown to decrease after about 50 hours [9, 44]. While our model includes a form of integral feedback that gradually attenuates the effects of consistent bond asymmetry and morphogen signaling, the exact reason why these effects diminish with time remains unknown. The model also does not address the mechanism underlying

the autonomous effects of Dpp signaling on cell proliferation [23, 44]; it only relates the growth rate to the morphogen concentration. Similarly the model does not address how the arrangement of Ft-Ds bonds may couple to mechanical forces within the cytoskeleton, or how these forces in turn regulate growth [114]; rather, it directly relates the Ft-Ds bond distribution to the growth rate.

Our model does not explain what causes the disc to stop growing. We incorporate the adaptation mechanism described above, which causes cells to stop responding to steady morphogen signaling or asymmetric bond distribution. However, this mechanism alone cannot cause the cells in our model to stop growing entirely. Because the morphogen concentration continuously increases, each cell's amount of morphogen (and, by extension, its rates of Fj and Ds expression) constantly changes, so our adaptation mechanism will not eliminate all growth. Even if the simulation runs long enough to allow the front to pass the edge of the disc, cells will continue to proliferate because of their increasing autonomous morphogen signaling. However, it may be the case that the Dpp profile eventually ceases to scale with the growing disc. This would cause individual cells to stop experiencing a continuous increase in their amount of Dpp signaling, and instead experience a decrease in Dpp signaling. (Indeed, evidence suggests that the amplitude of the Dpp profile may decrease near the end of the larval phase [45].) In our model, a decrease in morphogen signaling in a given cell would tend to lower its growth rate, counteracting the effects of Ft-Ds bond asymmetry. In principle, a fast enough decrease in morphogen signaling would stop growth altogether in the model. Other mechanisms, possibly including mechanical feedback [41–43, 109], or external hormonal signals [115], may also be involved in controlling the final size of the disc.

Our aim was to create a model of polarization propagation and cell proliferation that relied on a minimal number of assumptions to show that the movement of the Fj/Ds expression front was sufficient to produce realistic results. This means that other possible mechanisms of including cell polarization are not addressed by the model. For example,

contrary to our model, discs and adult wings mutant for Ft or Ds are observed to exhibit some polarization [86, 89, 116]. It is likely that multiple mechanisms are responsible for inducing polarization, and that the Fj and Ds gradients constitute only one type of cue that is further refined by other signaling pathways [116]. Another recent model [108] showed that polarization can arise from relatively shallow gradients of bindable Ft and Ds. In this model, the formation of Ft-Ds bonds of one orientation facilitated the formation of bonds of the same orientation and repressed the formation of bonds of the other orientation. This allowed cells across the tissue to polarize cooperatively given very small cell-cell differences in available Ft and Ds. For the sake of parsimony, our model considers the formation of Ft-Ds bonds independently of other mechanisms, such as additional signaling pathways that induce polarity or cooperativity in Ft-Ds bond formation. However, a more realistic picture of cell polarity likely involves multiple interacting systems like these.

For the sake of simplicity, we treat all cells in the disc as having a comparable equilibrium size. However, this does not necessarily mean that the cells are evenly spaced. In our model, the cells near the disc's edge tend to be further apart than cells near the disc's center. This is an effect of compression; the cells are treated as "soft" and permit some degree of overlap (Equation 3.4), and cells in the center experience more compression than those at the edge. This effect is also observed experimentally; images of the disc show that cells in the peripheral regions of the disc tend to be larger than cells in the central region [1].

However, in our model, each cell's growth rate is affected by its distribution of Ft-Ds bonds, which is determined by differences in Ft and Ds availability between the cell and its neighbors, which in turn is determined by differences in morphogen concentration between adjacent cells. This means that cells measure the Fj and Ds gradients not in absolute terms, but in terms of the width of a cell. Thus, we would expect closely spaced (i.e., strongly overlapping) neighboring cells to have more symmetrically distributed bonds than more widely-spaced (i.e., non-overlapping) adjacent cells for this reason. Closely-spaced

cells would have similar amounts of morphogen, similar rates of Fj and Ds expression, and therefore more symmetrically arranged bonds. In contrast, non-compressed cells would have larger cell-cell differences in morphogen concentration and Fj and Ds expression rates, and less symmetrically arranged bonds. It may be the case, then, that systematic variations in cell size due to compression may cause systematic variations in growth rate.

This effect is parameter-dependent. If the cells were "harder", they would be less likely to overlap even when compressed, leading to a more even spacing of cells throughout the disc. Since our model relates cell separation (in the sense of center-to-center distance) to growth rate, it may be worthwhile to study the relationship between these quantities in further detail. In particular, past models have suggested that mechanical compression and cell growth rate form a negative feedback loop, such that cells that are more compressed tend to grow more slowly [41, 43]. However, the exact mechanism by which cells sense their compression or spacing is unclear. It may be worthwhile to study the relationship between cell spacing and growth rate in further detail, given that the growth rate calculation in our model involves comparing the gradients of various signaling proteins to cell size.

6.5 Conclusion

The Ft pathway is involved in both growth and polarization in the *Drosophila* wing disc. Although Ft-Ds bonds are asymmetrically distributed on cells throughout the wing pouch (the central region of the disc), the proteins Ft, Fj, and Ds are present in fairly uniform concentrations there. However, Fj and Ds are steeply graded at the edge of the wing pouch, and this region sweeps over a large portion of the disc during the larval phase. We propose that cells establish their Ft-Ds bond asymmetry when this front moves over them, and retain this asymmetry after the front has passed. Thus, the history of gene expression, not just the instantaneous protein concentrations, can induce cell polarization and control growth.

In our model, cells in the wake of the expanding front are more strongly polarized than cells that have never had the front pass over them. Cells can also retain this polarization after dividing by replenishing Ft-Ds bonds at the newly formed cell-cell interface. It is the movement of the front in our model that allows cells throughout the wing primordium to experience relatively uniform growth and patterning in the presence of dynamic, nonuniform signals. By integrating this mechanism into a simple model for proliferation, we obtain results consistent with a number of experiments on disc size and patterning.

We have proposed that the wing disc is an example of a biological system that depends not only on the instantaneous state of gene expression, but also on its history. There are other examples of this; e.g., somites, or body segments, of vertebrates are formed by a propagating wave front that passes over cells undergoing oscillatory changes in their gene expression [117]. The fate of each cell depends on its state when the front reaches it, with the result being a periodic spatial pattern that persists after the front has passed. Thus, the history of changes in tissue size, cell number, signaling levels, and expression patterns are an important mechanism in development.

Bibliography

[1] Fristrom D, Fristrom JW (1993) The metamorphic development of the adult epidermis. In: The Development of *Drosophila melanogaster*, Cold Spring Harbor: Cold Spring Harbor Laboratory Press. pp. 843–897.

[2] García-Bellido A, Merriam J (1971) Parameters of the wing imaginal disc development of *Drosophila melanogaster*. Developmental Biology 24: 61–87.

[3] Wu J, Cohen SM (2002) Repression of Teashirt marks the initiation of wing development. Development 129: 2411–2418.

[4] Williams JA, Paddock SW, Vorwerk K, Carroll SB (1994) Organization of wing formation and induction of a wing-patterning gene at the dorsal/ventral compartment boundary. Nature 368: 299–305.

[5] Bryant PJ, Levinson P (1985) Intrinsic growth control in the imaginal primordia of *Drosophila*, and the autonomous action of a lethal mutation causing overgrowth. Developmental Biology 107: 355-363.

[6] Fain MJ, Stevens B (1985) Alterations in the cell cycle of *Drosophila* imaginal disc cells precede metamorphosis. Developmental Biology 92: 247–258.

[7] González-Gaitán M, Capdevila MP, García-Bellido A (1994) Cell proliferation patterns in the wing imaginal disc of *Drosophila*. Mechanisms of Development 40: 183–200.

[8] Poodry CA, Schneiderman HA (1970) The ultrastructure of the developing leg of *Drosophila melanogaster*. Wilhelm Roux' Archiv für Entwicklungsmechanik der Organismen 166: 1–44.

[9] Rogulja D, Rauskolb C, Irvine KD (2008) Morphogen control of wing growth through the Fat signaling pathway. Developmental Cell 15: 309–321.

[10] Ambegaonkar AA, Pan G, Mani M, Feng Y, Irvine KD (2012) Propagation of dachsous-fat planar cell polarity. Current Biology 22: 1302–1308.

[11] Brittle A, Thomas C, Strutt D (2012) Planar polarity specification through asymmetric subcellular localization of Fat and Dachsous. Current Biology 22: 108.

[12] Clark HF, Brentrup D, Schneitz K, Bieber A, Goodman C, et al. (1995) *Dachsous* encodes a member of the cadherin superfamily that controls imaginal disc morphogenesis in *Drosophila*. Genes & Development 9: 1530–1542.

[13] Brodsky MH, Steller H (1996) Positional information along the dorsal-ventral axis of the *Drosophila* eye: graded expression of the *four-jointed* gene. Developmental Biology 173: 428–446.

[14] Cho E, Irvine KD (2004) Action of *fat*, *four-jointed*, *dachsous* and *dachs* in distal-to-proximal wing signaling. Development 131: 4489–4500.

[15] Rodríguez I (2004) The *dachsous* gene, a member of the cadherin family, is required for Wg-dependent pattern formation in the *Drosophila* wing disc. Development 131: 3195–3206.

[16] Strutt H, Mundy J, Hofstra K, Strutt D (2004) Cleavage and secretion is not required for Four-jointed function in *Drosophila* patterning. Development 131: 881–890.

[17] Strutt H, Strutt D (2002) Nonautonomous planar polarity patterning in *Drosophila*: Dishevelled-independent functions of Frizzled. Developmental Cell 3: 851–863.

[18] Villano JL, Katz FN (1995) Four-jointed is required for intermediate growth in the proximal-distal axis in *Drosophila*. Development 121: 2767–2777.

[19] Mao Y, Kucuk B, Irvine KD (2009) *Drosophila* lowfat, a novel modulator of Fat signaling. Development 136: 3223–3233.

[20] Milán M, Campuzano S, García-Bellido A (1996) Cell cycling and patterned cell proliferation in the wing primordium of *Drosophila*. Proceedings of the National Academy of Sciences 93: 640–645.

[21] Milán M, Campuzano S, García-Bellido A (1997) Developmental parameters of cell death in the wing disc of *Drosophila*. Proceedings of the National Academy of Sciences 94: 5691–5696.

[22] Resino J, Salama-Cohen P, García-Bellido A (2002) Determining the role of patterned cell proliferation in the shape and size of the *Drosophila* wing. Proceedings of the National Academy of Sciences 99: 7502–7507.

[23] Burke R, Basler K (1996) Dpp receptors are autonomously required for cell proliferation in the entire developing *Drosophila* wing. Development 122: 2261–2269.

[24] Schwank G, Restrepo S, Basler K (2008) Growth regulation by Dpp: an essential role for Brinker and a non-essential role for graded signaling levels. Development 135: 4003–4013.

[25] Schwank G, Tauriello G, Yagi R, Kranz E, Koumoutsakos P, et al. (2011) Antagonistic growth regulation by Dpp and Fat drives uniform cell proliferation. Developmental Cell 20: 123–130.

[26] Turing A (1952) The chemical basis of morphogenesis. Philosophical Transactions of the Royal Society of London 237: 37-72.

[27] Wolpert L (1969) Positional information and the spatial pattern of cellular differentiation. Journal of Theoretical Biology 25: 1–47.

[28] Basler K, Struhl G (1994) Compartment boundaries and the control of *Drosophila* limb pattern by *hedgehog* protein. Nature 368: 208–214.

[29] Zecca M, Basler K, Struhl G (1995) Sequential organizing activities of engrailed, hedgehog and decapentaplegic in the *Drosophila* wing. Development 121: 2265–2278.

[30] Entchev EV, Schwabedissen A, González-Gáitan M (2000) Gradient formation of the TGF-β homolog Dpp. Cell 103: 981–991.

[31] Kicheva A, Pantazis P, Bollenbach T, Kalaidzidis Y, Bittig T, et al. (2007) Kinetics of morphogen gradient formation. Science 315: 521–525.

[32] Bollenbach T, Pantazis P, Kicheva A, Bökel C, González-Gaitán M, et al. (2008) Precision of the Dpp gradient. Development 135: 1137–1146.

[33] Nellen D, Burke R, Struhl G, Basler K (1996) Direct and long-range action of a DPP morphogen gradient. Cell 85: 357–368.

[34] Capdevila J, Guerrero I (1994) Targeted expression of the signaling molecule decapentaplegic induces pattern duplications and growth alterations in *Drosophila* wings. The EMBO Journal 13: 4459–4468.

[35] Martin-Castellanos C, Edgar BA (2002) A characterization of the effects of Dpp signaling on cell growth and proliferation in the *Drosophila* wing. Development 129: 1003–1013.

[36] Bryant PJ (1975) Pattern formation in the imaginal wing disc of *Drosophila melanogaster*: fate map, regeneration and duplication. Journal of Experimental Zoology 193: 49-78.

[37] Nienhaus U, Aegerter-Wilmsen T, Aegerter CM (2009) Determination of mechanical stress distribution in *Drosophila* wing discs using photoelasticity. Mechanisms of Development 126: 942–949.

[38] Schluck T, Aegerter C (2010) Photo-elastic properties of the wing imaginal disc of *Drosophila*. European Physical Journal E 33: 111–115.

[39] Baena-López LA, Baonza A, García-Bellido A (2005) The orientation of cell divisions determines the shape of *Drosophila* organs. Current Biology 15: 1640–1644.

[40] Théry M, Jiménez-Dalmaroni A, Racine V, Bornens M, Jülicher F (2007) Experimental and theoretical study of mitotic spindle orientation. Nature 447: 493–496.

[41] Shraiman BI (2005) Mechanical feedback as a possible regulator of tissue growth. Proceedings of the National Academy of Sciences 102: 3318–3323.

[42] Hufnagel L, Teleman AA, Rouault H, Cohen SM, Shraiman BI (2007) On the mechanism of wing size determination in fly development. Proceedings of the National Academy of Sciences 104: 3835–3840.

[43] Aegerter-Wilmsen T, Aegerter CM, Hafen E, Basler K (2007) Model for the regulation of size in the wing imaginal disc of *Drosophila*. Mechanisms of Development 124: 318–326.

[44] Rogulja D, Irvine KD (2005) Regulation of cell proliferation by a morphogen gradient. Cell 123: 449–461.

[45] Wartlick O, Mumcu P, Kicheva A, Bittig T, Seum C, et al. (2011) Dynamics of Dpp signaling and proliferation control. Science 331: 1154–1159.

[46] Teleman AA, Cohen SM (2000) Dpp gradient formation in the *Drosophila* wing imaginal disc. Cell 103: 971–980.

[47] Lecuit T, Cohen SM (1998) Dpp receptor levels contribute to shaping the Dpp morphogen gradient in the Drosophila wing imaginal disc. Development 125: 4901–4907.

[48] Ben-Zvi D, Pyrowolakis G, Barkai N, Shilo BZ (2011) Expansion-repression mechanism for scaling the Dpp activation gradient in *Drosophila* wing imaginal discs. Current Biology 21: 1–6.

[49] Hamaratoglu F, de Lachapelle AM, Pyrowolakis G, Bergmann S, Affolter M (2011) Dpp signaling activity requires Pentagone to scale with tissue size in the growing *Drosophila* wing imaginal disc. PLoS Biology 9: e1001182.

[50] Day SJ, Lawrence PA (2000) Measuring dimensions: the regulation of size and shape. Development 127: 2977–2987.

[51] Mahoney PA, Weber U, Onofrechuk P, Biessmann H, Bryant PJ, et al. (1991) The *fat* tumor suppressor gene in *Drosophila* encodes a novel member of the cadherin gene superfamily. Cell 67: 853–868.

[52] Ishikawa HO, Takeuchi H, Haltiwanger RS, Irvine KD (2008) Four-jointed is a Golgi kinase that phosphorylates a subset of cadherin domains. Science 321: 401–404.

[53] Ma D, Yang CH, McNeill H, Simon MA, Axelrod JD (2003) Fidelity in planar cell polarity signaling. Nature 421: 543–547.

[54] Matakatsu H, Blair S (2004) Interactions between Fat and Dachsous and the regulations of planar cell polarity in the *Drosophila* wing. Development 131: 3785–3794.

[55] Brittle AL, Repiso A, Casal J, Lawrence PA, Strutt D (2010) Four-jointed modulates growth and planar polarity by reducing the affinity of Dachsous for Fat. Current Biology 20: 803–810.

[56] Simon MA, Xu A, Ishikawa HO, Irvine KD (2010) Modulation of Fat:Dachsous binding by the cadherin domain kinase Four-jointed. Current Biology 20: 811–817.

[57] Willecke M, Hamaratoglu F, Sansores-Garcia L, Tao C, Halder G (2008) Boundaries of Dachsous cadherin activity modulate the Hippo signaling pathway to induce cell proliferation. Proceedings of the National Academy of Sciences 105: 14897–14902.

[58] Zecca M, Struhl G (2010) A feed-forward circuit linking Wingless, Fat-Dachsous signaling, and the Warts-Hippo pathway to *Drosophila* wing growth. PLoS Biology 8: e1000386.

[59] Gibson MC, Patel AB, Nagpal R, Perrimon N (2006) The emergence of geometric order in proliferating metazoan epithelia. Nature 442: 1038–1041.

[60] Posakony LG, Raftery LA, Gelbart WM (1991) Wing formation in *Drosophila melanogaster* requires *decapentaplegic* gene function along the anterior-posterior compartment boundary. Mechanisms of Development 33: 69–82.

[61] Arias AM (1993) Development and patterning of the larval epidermis of *Drosophila*. In: The Development of *Drosophila melanogaster*, Cold Spring Harbor: Cold Spring Harbor Laboratory Press. pp. 517–608.

[62] Spencer FA, Hoffman FM, Gelbart WM (1982) Decapentaplegic: a gene complex affecting morphogenesis in *Drosophila melanogaster*. Cell 28: 451–461.

[63] Lecuit T, Brook WJ, Ng M, Calleja M, Sun H, et al. (1996) Two distinct mechanisms for long-range patterning by decapentaplegic in the *Drosophila* wing. Nature 381: 387–393.

[64] Campbell G, Tomlinson A (1999) Transducing the Dpp morphogen gradient in the wing of *Drosophila*: Regulation of dpp targets by *brinker*. Cell 96: 553–562.

[65] Gibson MC, Perrimon N (2005) Extrusion and death of dpp/bmp-compromised epithelial cells in the developing *Drosophila* wing. Science 307: 1785–1789.

[66] Shen J, Dahmann C (2005) Extrusion of cells with inappropriate Dpp signaling from *Drosophila* wing disc epithelia. Science 307: 1789–1790.

[67] Widmann TJ, Dahmann C (2009) Dpp signaling promotes the cuboidal-to-columnar shape transition of *Drosophila* wing disc epithelia by regulating Rho1. Journal of Cell Science 122: 1362–1373.

[68] Widmann TJ, Dahmann C (2009) Wingless signaling and the control of cell shape in *Drosophila* wing imaginal discs. Developmental Biology 334: 161–173.

[69] Martín FA, Pérez-Garijo A, Moreno E, Morata G (2004) The *brinker* gradient controls wing growth in *Drosophila*. Development 131: 4921–4930.

[70] Ben-Zvi D, Barkai N (2010) Scaling of morphogen gradients by an expansion-repression integral feedback control. Proceedings of the National Academy of Sciences 107: 6924–6929.

[71] Baena-López LA, Franch-Marro X, Vincent JP (2009) Wingless promotes proliferative growth in a gradient-independent manner. Science Signaling 2: ra60.

[72] Zecca M, Basler K, Struhl G (1996) Direct and long-range action of a Wingless morphogen gradient. Cell 87: 833–844.

[73] Neumann CJ, Cohen SM (1997) Long-range action of Wingless organizes the dorsal-ventral axis of the *Drosophila* wing. Development 124: 871–880.

[74] Zecca M, Struhl G (2007) Recruitment of cells into the *Drosophila* wing primordium by a feed-forward circuit of *vestigial* autoregulation. Development 134: 3001–3010.

[75] Alberts B, Johnson A, Lewis J, Raff M, Roberts K, et al. (2002) Molecular Biology of the Cell, Fourth Edition. Garland Science.

[76] Yagi T, Takeichi M (2000) Cadherin superfamily genes: functions, genomic organization, and neurologic diversity. Genes and Development 14: 1169–1180.

[77] Angst BD, Marcozzi C, Magee AI (2001) The cadherin superfamily: diversity in form and function. Journal of Cell Science 114: 629–641.

[78] Uemura T, Oda H, Kraut R, Hayashi S, Kataoka Y, et al. (1996) Zygotic *Drosophila* E-cadherin expression is required for processes of dynamic epithelial cell rearrangement in the *Drosophila* embryo. Genes and Development 10: 659–671.

[79] Adler PN, Charlton J, Liu J (1998) Mutations in the cadherin superfamily member gene *dachsous* cause a tissue polarity phenotype by altering *frizzled* signaling. Development 125: 959–968.

[80] Casal J, Struhl G, Lawrence PA (2002) Developmental compartments and planar polarity in *Drosophila*. Current Biology 12: 1189–1198.

[81] Casal J, Lawrence PA, Struhl G (2006) Two separate molecular systems, Dachsous/Fat and Starry night/Frizzled, act independently to confer planar cell polarity. Development 133: 4561–4572.

[82] Matakatsu H, Blair SS (2008) The DHHC palmitoyltransferase Approximated regulates Fat signaling and Dachs localization and activity. Current Biology 18: 1390–1395.

[83] Mohr OL (1923) Modifications of the sex-ratio through a sex-linked semi-lethal in *Drosophila melanogaster*. (besides notes on an autosomal section deficiency). In: Studia Mendeliana: Ad centesimum diem natalem Gregorii Mendelii a grata patria celebrandum, Brünn: Apud Typos. pp. 266–287.

[84] Bryant PJ, Huettner B, Held LI, Ryerse J, Szidonya J (1988) Mutations at the *fat* locus interfere with cell proliferation control and epithelial morphogenesis in *Drosophila*. Developmental Biology 129: 541-554.

[85] Garoia F, Guerra D, Pezzoli MC, López-Varea A, Cavicchi S, et al. (2000) Cell behaviour of *Drosophila fat* cadherin mutations in wing development. Mechanisms of Development 94: 95–109.

[86] Matakatsu H, Blair S (2006) Separating the adhesive and signaling functions of the Fat and Dachsous protocadherins. Development 133: 2315–2324.

[87] Stern C, Bridges CB (1926) The mutants of the extreme left end of the second chromosome of *Drosophila melanogaster*. Genetics 11: 503–530.

[88] Mohr OL (1929) Exaggeration and inhibition phenomena encountered in the analysis of an autosomal dominant. Zeitschrift für Induktive Abstammungs- und Vererbungslehre 50: 113–200.

[89] Matakatsu H, Blair SS (2012) Separating planar cell polarity and hippo pathway activities of the protocadherins Fat and Dachsous. Development 139: 1498–1508.

[90] Zhao X, Yang CH, Simon MA (2013) The *Drosophila* cadherin Fat regulates tissue size and planar cell polarity through different domains. PLoS One 8: e62998.

[91] Pan G, Feng Y, Ambegaonkar AA, Sun G, Huff M, et al. (2013) Signal transduction by the Fat cytoplasmic domain. Development 140: 831–842.

[92] Tyler DM, Baker NE (2007) Expanded and fat regulate growth and differentiation in the *Drosophila* eye through multiple signaling pathways. Developmental Biology 305: 187–201.

[93] Waddington C (1943) The development of some "leg genes" in *Drosophila*. Journal of Genetics 45: 29–43.

[94] Zeidler MP, Perrimon N, Strutt DI (2000) Multiple roles for *four-jointed* in planar polarity and limb patterning. Developmental Biology 228: 181–196.

[95] Mao Y, Rauskolb C, Cho E, Hu WL, Hayter H, et al. (2006) Dachs: an unconventional myosin that functions downstream of Fat to regulate growth, affinity and gene expression in *Drosophila*. Development 133: 2539–2551.

[96] Bosveld F, Bonnet I, Guirao B, Tlili S, Wang Z, et al. (2012) Mechanical control of morphogenesis by Fat/Dachsous/Four-jointed planar cell polarity pathway. Science 336: 724–727.

[97] Cho E, Feng Y, Rauskolb C, Maitra S, Fehon R, et al. (2006) Delineation of a Fat tumor suppressor pathway. Nature Genetics 38: 1142–1150.

[98] Willecke M, Hamaratoglu F, Kango-Singh M, Udan R, Chen CL, et al. (2006) The Fat cadherin acts through the Hippo tumor-suppressor pathway to regulate tissue size. Current Biology 16: 2090–2100.

[99] Mao Y, Tournier AL, Bates PA, Gale JE, Tapon N, et al. (2011) Planar polarization of the atypical myosin Dachs orients cell divisions in *Drosophila*. Genes and Development 25: 131–136.

[100] Dupont S, Morsut L, Aragona M, Enzo E, Giulitti S, et al. (2011) Role of YAP/TAZ in mechanotransduction. Nature 474: 179–183.

[101] Wada KI, Itoga K, Okano T, Yonemura S, Sasaki H (2011) Hippo pathway regulation by cell morphology and stress fibers. Development 138: 3907–3914.

[102] Strigini, Cohen (1999) Formation of morphogen gradients in the *Drosophila* wing. Seminars in Cell & Developmental Biology .

[103] Yi TM, Huang Y, Simon MI, Doyle J (2000) Robust perfect adaptation in bacterial chemotaxis through integral feedback control. Proceedings of the National Academy of Sciences 97: 4649–4653.

[104] Strutt H, Strutt D (2005) Long-range coordination of planar polarity in *Drosophila*. BioEssays 27: 1218–1227.

[105] Reddy B, Irvine KD (2008) The Fat and Warts signaling pathways: new insights into their regulation, mechanism and conservation. Development 135: 2827–2838.

[106] Lawrence PA, Struhl G, Casal J (2008) Do the protocadherins Fat and Dachsous link up to determine both planar cell polarity and the dimensions of organs? Nature Cell Biology 10: 1379–1382.

[107] Jolly MK, Rizvi MS, Kumar A, Sinha P (2014) Mathematical modeling of sub-cellular asymmetry of fat-dachsous heterodimer for generation of planar cell polarity. PLoS One 9: e97641.

[108] Mani M, Goyal S, Irvine KD, Shraiman BI (2013) Collective polarization model for gradient sensing via Dachsous-Fat intercellular signaling. Proceedings of the National Academy of Sciences 110: 20420–20425.

[109] Aegerter-Wilmsen T, Heimlicher MB, Smith AC, de Reuille PB, Smith RS, et al. (2012) Integrating force-sensing and signaling pathways in a model for the regulation of wing imaginal disc size. Development 139: 3221–3231.

[110] Rapaport D (1997) The Art of Molecular Dynamics Simulation. Cambridge: Cambridge University Press.

[111] Farhadifar R, Röper JC, Aigouy B, Eaton S, Jülicher F (2007) The influence of cell mechanics, cell-cell interactions, and proliferation on epithelial packing. Current Biology 17: 2095–2104.

[112] Guibas L, Stolfi J (1985) Primitives for the manipulation of general subdivisions and the computation of Voronoi diagrams. ACM Transactions on Graphics 4: 74-123.

[113] Griffin R, Binari R, Perrimon N (2014) Genetic odyssey to generate marked clones in *Drosophila* mosaics. Proceedings of the National Academy of Sciences 111: 4756–4763.

[114] Rauskolb C, Sun S, Sun G, Pan Y, Irvine KD (2014) Cytoskeletal tension inhibits Hippo signaling through an Ajuba-Warts complex. Cell 158: 143–156.

[115] Nijhout HF, Grunert LW (2010) The cellular and physiological mechanism of wing-body scaling in *Manduca sexta*. Science 330: 1693–1695.

[116] Sagner A, Merkel M, Aigouy B, Gaebel J, Brankatschk M, et al. (2012) Establishment of global patterns of planar polarity during growth of the *Drosophila* wing epithelium. Current Biology 22: 1296-1301.

[117] Palmeirim I, Henrique D, Ish-Horowicz D, Pourquie O (1997) Avian *hairy* gene expression identifies a molecular clock linked to vertebrate segmentation and somitogenesis. Cell 91: 639–648.

Appendix A: Parameters

These are the parameters used in the simulation, along with their values and the equations or sections in which they appear.

Name	Appears in	Description	Value
		Morphogen profile	
C_0	(3.9)	Beginning amplitude of the morphogen profile	1.5
t_0	(3.9)	Time over which the amplitude increases by a factor of e	1200 min
$[M]_c$	(3.10), (3.11)	Morphogen concentration at which the Fj and Ds gradients cross	0.5
A	(3.9)	Ratio of disc radius to morphogen decay length	4
n	(3.10)	Steepness of dependence of Fj/Ds expression on morphogen concentration	10
		Specific conditions	
–	§5.1.2	Overall multiplier for Ds expression when Ds is ubiquitous	10
–	§5.1.2	Fj expression level when Fj is ubiquitous	1
–	§5.3	Starting front location (radial distance) when the front is stationary	30 μm

Table A.1: Parameters used in the morphogen profile and for specific disc genotypes.

Name	Appears in	Description	Value
		Growth rate	
G_0	(3.20)	Overall multiplier to the growth rate	4.3×10^{-4}
C_{Ft}	(3.20)	Contribution of Ft asymmetry to the growth rate	3×10^3
C_{Ds}	(3.20)	Contribution of Ds asymmetry to the growth rate	3×10^3
C_M	(3.20)	Contribution of morphogen signaling to the growth rate	40
U	(3.20)	Penalty for leftover free Ft and Ds	3×10^{-5} proteins^{-1}
–	§3.6	Grace period before counting bonds with a new neighbor	100 min
		Cell division	
A_c	(3.8)	Critical area for cell division	4π μm^2
–	§3.2.2	Maximum amount by which the radii of daughter cells differ after division	1%
n	(3.8)	Steepness of division probability vs. radius	400
		Integral feedback	
G_{Ft}	(3.23)	Time scale for Ft asymmetry feedback	6×10^{-4} min^{-1}
G_{Ds}	(3.25)	Time scale for Ds asymmetry feedback	6×10^{-4} min^{-1}
G_M	(3.21)	Time scale for morphogen signaling feedback	2.8×10^{-2} min^{-1}
		Neighbor list	
–	§3.3	Fraction of a cell's radius a cell must move before a full neighbor rebuild is triggered	0.2 radii
–	§3.3	Time before a full neighbor rebuild is triggered, independent of cell motion	10 min
		Bulk interactions	
–	§3.4.3	Threshold membrane-membrane distance for interactions	0.8 μm
γ	(3.5)	Drag coefficient	2×10^{-3} min^{-1}
C_{gap}	(3.3)	Strength of attractive force	$3{\times}10^{-7}$ μm^2 min^{-2}
$C_{overlap}$	(3.4)	Strength of repulsive force	1×10^{-6} min^{-2}

Table A.2: Parameters used for cell growth, division, and interaction.

Name	Appears in	Description	Value
		Ft, Ds, and Fj expression	
Ft_{max}	§3.4.1	Starting Ft, overall Ft expression level	1×10^3 proteins
$A_{Ds,initial}$	(3.10)	Scaling coefficient for initial Ds	1×10^3 proteins
R_{Ft}	(3.15)	Ft expression rate	20 proteins/min
$R_{Ds,max}$	(3.16)	Base Ds expression rate	20 proteins/min
$R_{Fj,max}$	(3.17)	Base Fj expression rate	1.05 min^{-1}
Ds_{min}	(3.16)	Minimum level of Ds expression in terms of $R_{Ds,max}$	0.2
Ds_{range}	(3.16)	Range of Ds expression in terms of $R_{Ds,max}$	0.8
Fj_{max}	(3.11)	Maximum Fj expression rate in terms of $R_{Fj,max}$	0.8
Fj_{range}	(3.11)	Range of Fj expression in terms of $R_{Fj,max}$	0.6
		Ft-Ds binding	
C_1	(3.12), (3.18)	Maximum chance of Ft being bindable (before offset)	0.8
C_2	(3.13), (3.19)	Maximum chance of Ds being bindable (before offset)	0.8
Fj_c	(3.14)	Critical value of Fj (determines phosphorylation probabilities for Ft and Ds)	0.3
n	(3.14)	Steepness of dependence of phosphorylation rates on Fj	2
P_{offset}	(3.12)	Minimum probability of Ft/Ds being bindable	0.1
–	§3.4.3	Fraction of bonds unbound per step	0.08 min^{-1}
$k_{d,Ft}$	(3.15)	Fraction of free Ft degraded per time step	0.08 min^{-1}
$k_{d,Ds}$	(3.16)	Fraction of free Ds degraded per time step	0.08 min^{-1}
$k_{d,Fj}$	(3.17)	Fraction of Fj degraded per time step	0.05 min^{-1}
A	(3.18), (3.19)	Maximum fraction of free Ft/Ds to become phosphorylated/dephosphorylated per step	0.016 min^{-1}
D	(3.18), (3.19)	Dephosphorylation rate of free Ft and Ds	0.08 min^{-1}

Table A.3: Parameters used in the expression and binding of Ft, Ds, and Fj.